

Thesis for the Degree of Doctor of Philosophy

**Control of Mobile Manipulator
for Tracking Smooth 3D Curved
Welding Trajectory**

by

Thien Phuc Tran

Department of Mechatronics Engineering

The Graduate School

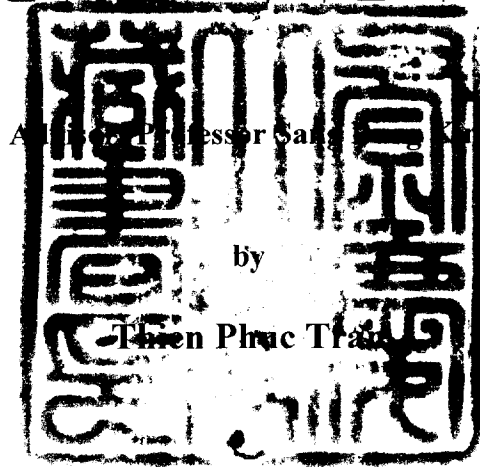
Pukyong National University

August 2005

Control of Mobile Manipulator for Tracking Smooth 3D Curved Welding Trajectory

매끄러운 3 차원 곡선 용접 궤도

추종을 위한 이동 매니퓰레이터의 제어



**A thesis submitted in partial fulfillment of the requirements
for the degree of**

Doctor of Philosophy

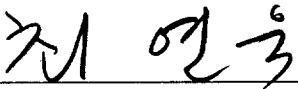
**In Department of Mechatronics Engineering, The Graduate School,
Pukyong National University**


August 2005


**Control of Mobile Manipulator
for Tracking Smooth 3D Curved Welding Trajectory**

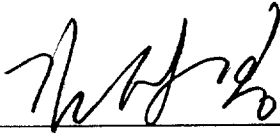
A Dissertation
by
Thien Phuc Tran

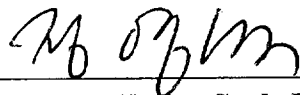
Approved of styles and contents by:


Chairman **Yeon Wook Choe**


Member **Hwan Seong Kim**


Member **Young Bok Kim**


Member **Sang Bong Kim**


Member **Young Seok Jung**

August 2005

Acknowledgements

*Where there is no counsel, plans are frustrated;
But in the multitude of counselors, they are established.
Proverbs 15:22.*

First and foremost, I would like to express my sincere thanks to my thesis advisor, Professor Sang Bong Kim, for his invaluable advice, guidance and motivation throughout the course of this research. Furthermore, he always gives me the best of mental and material conditions for the making of this research becomes possible.

I would like to show my gratitude to members of my thesis committee: Prof. Yeon-Wook Choe, Prof. Hwan-Seong Kim, Prof. Young-Bok Kim, and Prof. Young-Seok Jung for their many helpful comments and suggestions.

I would like to thank Prof. Myung Suk Lee in Department of Microbiology for her kindness and enthusiasm supports throughout the time that I live and study in Korea.

I greatly appreciate Dr. Tan Tien Nguyen from Ho Chi Minh City University of Technology for his essential assistances, and very special thanks to MSc. Tan Lam Chung for his cooperation for performing the experiments.

I would like to say thank you to all members of CIMEC Laboratory, especially Dr. Hak Kyeong Kim, Dr. Jin Ho Suh, MSc. Young Gyu Kim, Mr. Jae Sung Im, Mr. Sung Jin Ma, Dr. Trong Hieu Bui, MSc. Manh Dung Ngo, and Dr. Tan Tung Phan for all scientific discussions and helps when I studied in CIMEC Lab.

Thanks are due to all members of Vietnamese Student Community in Korea, especially MSc My Le Du and Missus Thuy Duong Nguyen for their vigorous support.

I am grateful to Assoc. Prof. Thanh Binh Phan, Assoc. Prof. Thanh Phong Ho, Dr. Thanh Son Nguyen, Assoc. Prof. Hoai Quoc Le, Assoc. Prof Dinh Chinh Vu, Dr. Van Ngo Dau, Dr. Huu Loc Nguyen, Dr. Khac Liem Lai, Dr. Tuan Kiet Nguyen and all colleagues in Vietnam National University - HCMC, HCMC International University, HCMC University of Technology, Research Center for Technology and Industrial Equipment for their advocacy of my study.

I would like to thank MSc Tuan Le and Mr. Quoc Hung Vu, my closest friends, for their exertion to help me in the time I was in Korea.

Also, I would like to show my love for CIMEC laboratory and Sun - Moon - Love House, they are really my family, my moral support in Korea.

Last but not least there are various thanks to my father, my mother, my sisters, my brother and especially my wife and my children for their love, encouragement and sympathy for me not only in this thesis time but also in the whole of my life.

Thien Phuc Tran

Table of Contents

Acknowledgments	i
Table of Contents	iii
List of Figures	vi
List of Tables	ix
Abstract	x
Nomenclatures	xiii
1. Introduction	
1.1 Background and Motivation	1
1.2 Previous Research	3
1.3 Summary of Contributions and Outline of Thesis	7
2. System Modeling of the Mobile Manipulator	
2.1 Configuration of the Mobile Manipulator	12
2.1.1 The Requirement of the 3D Welding Task	12
2.1.2 Configuration of the Mobile Manipulator	13
2.2 Kinematic modeling of the Mobile Manipulator	15
2.2.1 The Associated Coordinate Frames	15
2.2.2 Kinematic Modeling of the Mobile Platform	17
2.2.3 Kinematic Modeling of the Manipulator	18
2.2.4 Kinematic Equation of the Welding Torch Tip	20
2.2.5 Tracking Errors	22
2.3 Dynamic modeling of the Mobile Manipulator	22
2.3.1 Dynamic Modeling of the Mobile Platform	25
2.3.2 Dynamic Modeling of the Manipulator	26

3. Hardware Design and Its Implementation of the Mobile Manipulator	
3.1 Tracking Errors Measurement	28
3.1.1 Measuring the Tracking Errors e_1 , e_3 and e_5	29
3.1.2 Measuring the Tracking Errors e_2 and e_4	31
3.2 Hardware of System and Its Implementation	33
3.2.1 Configuration of the Mobile Manipulator	33
3.2.2 Configuration of the Control System	34
4. Nonlinear Feedback Tracking Controller Design for Kinematic Model of the Mobile Manipulator	
4.1 Introduction	37
4.2 Kinematic Feedback Controller Design	38
4.3 Simulation and Experiment Results	42
4.4 Chapter Summary	50
5. Nonlinear Adaptive Tracking Controller Design for Kinematic Model of the Mobile Manipulator with the Unknown Parameter	
5.1 Introduction	51
5.2 Kinematic Adaptive Tracking Controller Design	52
5.3 Simulation and Experiment Results	57
5.4 Chapter Summary	65
6. Nonlinear Adaptive Tracking Controller Design of the Mobile Manipulator Based on Kinematics into Dynamics Approach	
6.1 Introduction	66
6.2 Adaptive Tracking Controller Design	67
6.3 Simulation and Experiment Results	73
6.4 Chapter Summary	82

7. Tracking Controller Design of the Mobile Manipulator Using Sliding Mode Technique	
7.1 Introduction	84
7.2 Tracking Controller Design Using Sliding Mode Technique	85
7.3 Simulation and Experiment Results	91
7.4 Chapter Summary	102
8. Conclusions	
8.1 Controllers in Comparison	104
8.2 Prospects of Topic and the Future Works	106
References	107
Publications and Conferences	117
Appendix	121

List of Figures

Figure 1.1	Multiple agents working in a coordinated environment	2
Figure 2.1	Geometric illustration for the requirement of a 3D welding task	13
Figure 2.2	Mobile manipulator configuration	13
Figure 2.3	Manipulator motion in welding process	14
Figure 2.4	Coordinate frames and state variables of the mobile manipulator	16
Figure 2.5	Kinematic relation of the mobile platform	17
Figure 2.6	Kinematic relation of the manipulator	19
Figure 2.7	Tracking errors description	21
Figure 3.1	CMU camera sensor	29
Figure 3.2	Error calculation diagram (for e_1 , e_3 and e_5)	30
Figure 3.3	Proximity sensor set	31
Figure 3.4	Error calculation diagram (for e_2 and e_4)	32
Figure 3.5	Configuration of the mobile manipulator	33
Figure 3.6	Configuration of the control system	34
Figure 3.7	Implementation of the control system	35
Figure 4.1	Block diagram of the kinematic feedback control system for mobile manipulator	41
Figure 4.2	Reference trajectory	42
Figure 4.3	Position tracking errors e_1 , e_2 and e_3	44
Figure 4.4	Orientation tracking errors e_4 and e_5	44
Figure 4.5	Angular velocity of the wheels	45
Figure 4.6	Angular velocity of the links	45
Figure 4.7	Reference trajectory and welding trajectory in the first	

	circular sector	46
Figure 4.8	Mobile manipulator in experiment	47
Figure 4.9	Tracking error e_1	47
Figure 4.10	Tracking error e_2	48
Figure 4.11	Tracking error e_3	48
Figure 4.12	Tracking error e_4	49
Figure 4.13	Tracking error e_5	49
Figure 5.1	Block diagram of the kinematic adaptive control system for mobile manipulator with unknown parameter	56
Figure 5.2	Tracking error e_1 , e_2 and e_3	58
Figure 5.3	Tracking error e_4 and e_5	59
Figure 5.4	Estimated value p_m	59
Figure 5.5	Angular velocity of the wheels	60
Figure 5.6	Angular velocity of the links	60
Figure 5.7	Welding trajectory and reference trajectory	61
Figure 5.8	Mobile manipulator in tracking experiment	61
Figure 5.9	Tracking error e_1	62
Figure 5.10	Tracking error e_2	63
Figure 5.11	Tracking error e_3	63
Figure 5.12	Tracking error e_4	64
Figure 5.13	Tracking error e_5	64
Figure 6.1	Block diagram of the second controller - feedback acceleration controller	71
Figure 6.2	Block diagram of the adaptive tracking control system for the mobile manipulator based on kinematics into dynamics approach	73
Figure 6.3	Tracking error e_1 , e_2 and e_3	76
Figure 6.4	Tracking error e_4 and e_5	76
Figure 6.5	Tracking error e_6 and e_7	77

Figure 6.6	Tracking error e_8 and e_9	77
Figure 6.7	Angular velocity of the wheels	78
Figure 6.8	Angular velocity of the links	78
Figure 6.9	Welding trajectory and reference trajectory	79
Figure 6.10	Mobile manipulator in tracking experiment	79
Figure 6.11	Tracking error e_1	80
Figure 6.12	Tracking error e_2	80
Figure 6.13	Tracking error e_3	81
Figure 6.14	Tracking error e_4	81
Figure 6.15	Tracking error e_5	82
Figure 7.1	Tracking error e_1 , e_2 and e_3	94
Figure 7.2	Tracking error e_4 and e_5	94
Figure 7.3	Sliding surface component S_1 without saturation function	95
Figure 7.4	Sliding surface component S_1 with saturation function	95
Figure 7.5	Sliding surface component S_2 without saturation function	96
Figure 7.6	Sliding surface component S_2 with saturation function	96
Figure 7.7	Sliding surface component S_3 without saturation function	97
Figure 7.8	Sliding surface component S_3 with saturation function	97
Figure 7.9	Sliding surface component S_4 without saturation function	98
Figure 7.10	Sliding surface component S_4 with saturation function	98
Figure 7.11	Reference trajectory and welding trajectory	99
Figure 7.12	Mobile manipulator in the tracking experiment	99
Figure 7.13	Tracking error e_1	100
Figure 7.14	Tracking error e_2	100
Figure 7.15	Tracking error e_3	101
Figure 7.16	Tracking error e_4	101
Figure 7.17	Tracking error e_5	102

List of Tables

Table 4.1	Numerical values of the system's parameters	43
Table 5.1	Numerical values of the system's parameters	57
Table 6.1	Numerical values of the system's parameters	73
Table 7.1	Numerical values of the system's parameters	92
Table 8.1	Controllers in comparison	104

Control of Mobile Manipulator for Tracking Smooth 3D Curved Welding Trajectory

Thien Phuc Tran

Department of Mechatronics Engineering, Graduate School

Pukyong National University

Abstract

The mobile manipulators are the hybrid generation of the mobile platform and the manipulator. The mobility of the mobile platform and the dexterity and agility of the manipulator are combined to form a mobile manipulation. Because of this inheritance, the mobile manipulator's work space is remarkably enlarged so many tasks that are impossible in the past, but now can be perfectly performed.

In this thesis, the goal is accomplishing a smooth 3D curved welding seam by the mobile manipulator. To fulfil this task, a mobile manipulator composed of a two-wheeled platform and a five-linked manipulator is used. For this purposed task, the welding torch tip should be controled to track the trajectory with a constant velocity and a correct gesture of the end effector, that is, keeping a constant inclined angle. To implement the purpose task, the robot is also composed of a camera sensor and a set of proximity sensors. In the experiment

steps of this study, the control system is designed by the integration of seven PIC18F452s including six for servo DC motor controllers and one for main controller. The communication between the main controller, as master, and three servo controllers, as slave, is performed via I2C communication.

Aiming to the tracking task, four controllers are proposed. They are listed as the following:

- *Nonlinear feedback tracking controller design* with the system's kinematic model. Herein, the uniform asymptotical stability of the system is guaranteed by Lyapunov - like analysis using Barbalat's lemma. The simultaneous convergence to zero of the tracking errors at the equilibrium point is also proved.
- *Nonlinear adaptive tracking controller design with unknown parameter* applied for kinematic model. The problem that the welding arc length can not be precisely measured in the welding process is solved by supplementing the unknown parameter concerned to the customary adaptive controller.
- *Nonlinear adaptive tracking controller design based on kinematic approach into dynamic approach*. In this controller, the system's dynamic characteristics are considered for enhancing the performance. By using the kinematic into dynamic approach, the sophisticated dynamic computations are replaced by the simple kinematic computations.
- *Tracking controller design using sliding mode technique*. The external disturbance problem is solved with this controller by using a robust control with sliding technique. Therein, a saturation function is also applied for eliminating the undesirable chattering phenomenon created by the imperfect control switching.

MatLab 7.0 and Simulink 6.0 software are used for evaluating the controllers in simulation step. The simulation results are shown to prove the validity of the controllers. The experiment step is also carefully performed and their results are presented for affirming the feasibility of applying the controller to the actual welding tasks.

This thesis has accomplished the following issues through the above implementation of developed control algorithms. Firstly, it makes an easier calculation with the assigning responsibilities for mobile platform and manipulator in the tracking task. Secondly, it makes a simpler modeling with using the unified model approach for design the united controller. Thirdly, it shows how to apply the adaptive control with unknown parameter to the welding mobile manipulator performing a 3D task. Fourthly, it applies the concept of the backstepping kinematics into dynamics to a welding mobile manipulator for simplifying the controller design. Fifthly, based on the robust sliding mode control technique, it solves the external disturbance problem for control a welding mobile manipulator.

All of them focus on the main goal of this research: performing a smooth 3D curved welding seam with a mobile manipulator.

Nomenclatures

Variables	Description	Units
$Oxyz$	world coordinate frame (pp. 15)	
$Cx_my_mz_m$	moving frame (pp. 15)	
q_m^C	joint angles of the manipulator in the moving frame (pp. 15)	
q_p^O	configuration of the platform in the world frame (pp. 16)	
q	configuration of the mobile manipulator (pp. 16)	
p_t^O	end effector position and orientation in the world frame (pp. 16)	
$C(x_C, y_C)$	the coordinate of the platform's center point (pp. 18)	
ϕ_C	heading angle of the platform (pp. 18)	[rad]
r	radius of the wheels (pp. 18)	[m]
b	distance from wheel to the symmetry axis (pp. 18)	[m]
v_{xy}	straight velocity of the platform in x-y plane (pp. 18)	[m/s]
ω_r	angular velocity of the right wheel (pp. 18)	[rpm]
ω_l	angular velocity of the left wheel (pp. 18)	[rpm]
ω_ϕ	angular velocity of the platform in x-y plane (pp. 18)	[rad/s]
r	radius of wheel (pp. 18)	[m]
θ_i	link variables ($i = 1-4$) (pp. 19)	[rad]
ω_i	angular velocity of the link ($i = 1-4$) (pp. 19)	[rad/s]
q_E	configuration of the torch tip (pp. 19)	
J	Jacobian matrix of the manipulator (pp. 19)	

l_i	length of the link ($i = 1-4$) (pp. 19)	[m]
ϕ_E	orientation angle of the end effector (pp. 20)	[rad]
ϕ_w	heading angle in the horizontal plane of the welding torch (pp. 20)	[rad]
p_m	projection of the manipulator on x-y plane (pp. 20)	[m]
ψ_w	vertical heading angle of the welding torch (pp. 22)	[rad]
ω_ψ	vertical angular velocity of the welding torch (pp. 22)	[rad/s]
e_i	tracking errors ($i = 1-5$) (pp. 22)	
$M(q)$	inertia matrix (pp. 23)	
$C(q, \dot{q})$	centripetal and Coriolis matrix (pp. 23)	
$F(q, \dot{q})$	friction and gravitational vector (pp. 23)	
$A(q)$	constraint matrix (pp. 23)	
λ	Lagrange multiplier (pp. 23)	
τ_d	disturbance torque vector (pp. 23)	[Nm]
$E(q)$	input transformation matrix (pp. 23)	
τ	input torque vector (pp. 23)	[Nm]
v_r	reference velocity of welding torch tip (pp. 39)	[m/s]
v_z	z component velocity of the welding torch tip (pp. 39)	[m/s]
V	Lyapunov function (pp. 39)	
k_i	weight factors of the controller (pp. 40)	
\hat{p}_m	estimated value of p_m (pp. 53)	[m]
\tilde{p}_m	estimated error of p_m (pp. 53)	[m]
v_c	velocity control input (pp. 67)	[m/s]
u	control law (pp. 67)	
m_c	mass of the platform's body (pp. 73)	[kg]

m_w	mass of the wheels (pp. 73)	[kg]
I_c	inertia moment of the platform's body (pp. 74)	[kgm ²]
I_w	inertia moment of the wheels (pp. 74)	[kgm ²]
m_i	mass of the links ($i = 1-4$) (pp. 74)	[kg]
I_i	inertia moment of the links ($i = 1-4$) (pp. 74)	[kgm ²]
S_i	sliding surface ($i = 1-4$) (pp. 86)	
Q_i	weight factors of the controller (pp. 87)	
P_i	weight factors of the controller (pp. 87)	
f_i	external disturbance (pp. 87)	[N]
Φ	boundary layer thickness (pp. 90)	

Subscripts

r	reference or desired value (pp. 22)
w	welding or actual value (pp. 22)
i	initial value (pp. 43)
n	new chosen value (pp. 70)

Prefix

Δ	error value (pp. 43)
----------	----------------------

Chapter 1

Introduction

1.1 Background and Motivation

There are various tasks in that the workers can be bored or harmed such as assembly, welding, rescue and mine clearing. In order to solve this problem, many kinds of automatic machine were invented. The workers have really evaded the heavy and dangerous works due to those machines. But day by day, the industry has progressed, the needs incessantly grow up and the higher level of automatic machine is necessary. With the background like that, the robot system is chosen as one of the solutions in this case. In fact, a great number of robots are furnished in numerous industrial fields such as ship building, automobile, electronic assembling, and pre-fabricated metal structure industries. Furthermore, they can be applied to the tasks exposed to the hazardous environments such as waste management and treatment, desolate exploration and even space operation. In order to extend the workspace, the fixed robots are replaced by the mobile robots. A lot of kinds of mobile robot such as mobile platform, biped robots, stewart platform, flying robot, and multi-leg robot are applied and a mobile manipulator is presumed to be a vintage mobile robot in industrial fields.

With a manipulator mounted on the mobile platform, the flexibility of a mobile manipulator is enhanced. Its workspace is enlarged so that many dexterous tasks can be performed by a mobile manipulator. Different from the others, mobile manipulator can be used in the 3D tasks hence human labor can be perfectly

replaced by this kind of robot.

The subject of this thesis is a mobile manipulator. It is made up of a five-linked manipulator mounted on a two-wheeled platform. Due to this configuration, a certain 3D task such as tracking the space welding trajectory can be fulfilled. Furthermore, with the mobile platform, the workspace of robot is enlarged many times and the result is that it can manufacture the big work pieces. For easy to image the ability of mobile manipulator, a conceptual example of the applications utilizing mobile manipulators is depicted in Fig. 1.1. In this figure, multiple mobile manipulators cooperatively perform material handling tasks.

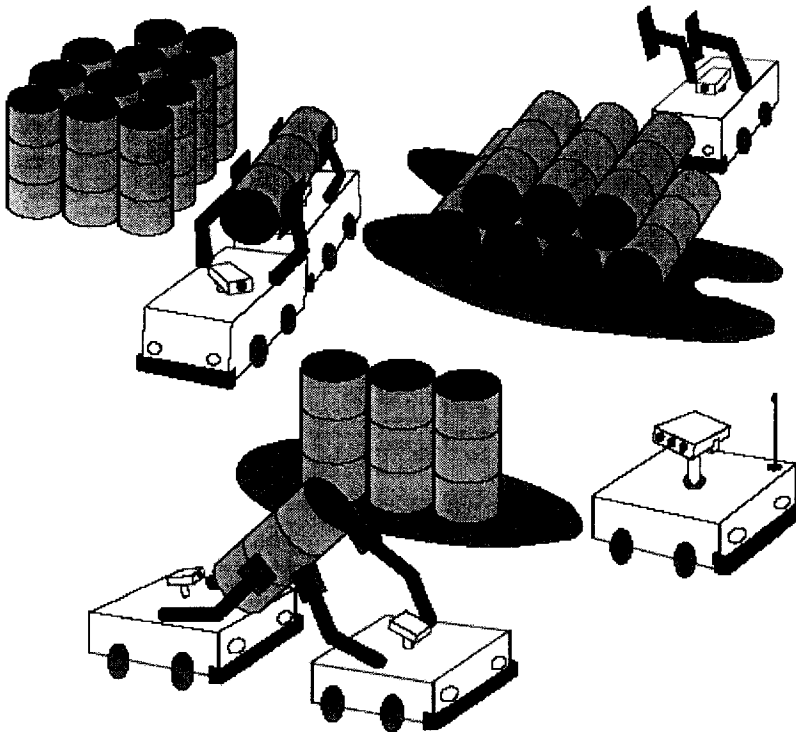


Fig. 1.1 Multiple agents working in a coordinated environment [16]

The object of this thesis is modeling, control, and tracking of the mobile

manipulator. The emphasis is placed on tracking the reference welding seam of welding torch tip clamped on the end effector. This tracking task is also guaranteed so that the velocity of welding torch tip is constant. Furthermore, the inclined angle between welding torch and the surface of welding seam is also set at a given value. All of them aim to obtain the satisfactory quality of the welding task.

In order to solve the above-mentioned tracking problem, the following issues will be addressed:

1. The hybrid constraint of mobile manipulator: non-holonomic constraint of wheeled mobile platform and holonomic constraint of manipulator.
2. The dynamic interaction between the mobile platform and manipulator.
3. The change of the parameters in the welding process such as the geometric dimension of the arc length of the welding torch.
4. The disturbance inputs on mobile manipulator.

1.2 Previous Research

Several different research domains are focused on in the research of the control of mobile manipulators. Because of consisting of mobile platform and manipulator, the researches of mobile platform and manipulator, separately, are based on as the background knowledge. Some of them have been extensively studied while others fairly new and relatively little research have been done. The main issues related to the topic of this thesis such as above-mentioned in the end of last subsection include several kinds of control technologies such as the kinematic and dynamic modeling of mobile platform, manipulator and mobile manipulator, the unified control and the decentralized control of mobile

manipulator, the tracking control of them, control of the system with unknown parameter, and control of the system with external disturbances. However, there is only a limited literature available on the issues of 3D trajectory tracking control for welding mobile manipulator although the advantage of a mobile manipulator over a conventional ground-fixed manipulator has been widely acknowledged.

Some previous significant researches classified according to its subjects, mobile platform, manipulator and mobile manipulator, are shown as the followings:

❖ *Motion control of the mobile platform*

There is a remarkable characteristic of the wheeled mobile robot systems: they must be affected by the non-holonomic constraints. The motion in the direction that is perpendicular with the symmetry of the mobile platform can not be performed by this system no matter what it is a two-wheeled platform, four-wheeled platform or four-wheeled platform with trailer. In this thesis, a two-wheeled platform is used, so it must be impacted by this constraint model.

Many researchers studied the wheeled mobile robot as a non-holonomic system. Bui et al ^{[14],[20],[21]} focused on a tracking controller design for a mobile platform with the tracking point outside of the mobile platform. They also mentioned about the adaptive control with unknown parameter and the solution for the external disturbance. Similarly, Dixon et al ^[19] developed an adaptive control method with unknown parameters in dynamic model for tracking and regulation a mobile robot. Jeon et al ^{[25],[34]}, Kam et al ^[29] concentrated on tracking control for a lattice type welding task. Xu et al ^[28] incorporated a biologically inspired shunting model into the conventional bang-bang

control for generating the real-time acceleration commands with the ability of producing the smooth, continuous velocities. Lefeber et al ^[31] developed an observer-based controller resulting in κ -exponential convergence of the tracking error of unicycle-type mobile platform. With the same objective, Chang et al ^[48] proposed an observer-based controller with an external disturbance attenuated to an arbitrarily pre-assigned level. Lee et al ^{[35],[39]}, Gusev et al ^[44] solved the tracking and regulation with saturation constraint by using the backstepping technique. A computed-torque controller with bounded external disturbance is discussed too. Fukao et al ^[38] used an adaptive backstepping approach for examining the kinematic model with unknown parameter. Relying on that, a torque adaptive controller is also proposed. Yang and Kim ^[40] focused on tracking problem with external disturbance and solving the problem by using sliding mode control. Fierro and Lewis ^[53] proposed an algorithm for easing the tracking problem of mobile platform from dynamics to kinematics. At last, a lot of researchers established the based knowledge for examining the kinematic and dynamic modeling of the mobile platform such as Sarkar et al ^[59], Deng et al ^[61], Burke et al ^[62], Yun et al ^[63], Khoukhi et al ^[66], Andrea-Novel et al ^[67] and Kanayama et al ^[70]

❖ *Motion control of the manipulator*

The control of manipulator is a fruitful area of research, development and manufacturing so it is specially concerned by a number of researchers. Zergeroglu et al ^[118] designed a model-based nonlinear controller for the tracking task of manipulator. Furthermore, the extra degrees of freedom of the redundant manipulator are used for

the sub-tasks. Tan and Xi ^[37] proposed a hybrid system approach combining the task level controller and the joint level controller for avoiding singularities. Tang and Guerrero ^[42] presented a robust decentralized control consisting of a linear state-feedback and a signal designed to compensate for the coupling among the joints, parameter uncertainty and bounded disturbances. Cheng et al ^[45] proposed the Singularity Isolation Plus Compact QP method for overcoming the singular configuration of a 6-DOF Puma manipulator by using the extra redundancy. Tarokh ^[47], Colbaugh et al ^[60] establish a decentralized controller for tracking task with torque disturbances. Especially, this design method did not require specific knowledge about the robot dynamics. Isobe et al ^[64] presented an approach for solving the inverse kinematics problem of manipulator. The problem of the singularity of the Jacobian and multiple solutions of the joint variables are also considered in this paper. Craig et al ^[75] focused on a computed-torque adaptive controller for tracking task with estimating parameters on-line such as payload, link mass and friction. Morgan and Ozguner ^[76] concentrated on the decentralized variable structure control algorithm with sliding mode.

❖ *Motion control of the mobile manipulator*

The control of mobile manipulator has been paid a special attention because of its dominant ability in applications. The researchers commonly discussed about tracking control, force control, unknown parameter and external disturbance.

Cheng and Tsai ^[22] developed the method for modeling and tracking control of two manipulator mounted on a mobile platform.

The proposed controller also fully compensates the coupled dynamics among the subsystems. Furuno et al ^[23] used a hierarchical gradient method with synthesizes the gradient function in a hierarchical manner based on the order of priority for trajectory planning problem. Bayle et al ^[24] proposed a generic approach to control a large class of mobile manipulators and the method to express the additional tasks corresponding to real experimental constraint. Tan and Xi ^[30] designed a task level action controller with combining the event-based planning and control method with the nonlinear feedback technique. Especially, the controller is based on the unified model approach but not the decentralized model approach. The controller also included the force control by using the extra degrees of freedom of the redundant manipulator. This objective is the same in Seraji ^{[52],[57]}. Yoo et al ^[33] solved the problem of path planning for combined motion of the mobile platform and manipulator with the concerning about manipulability measures. Dong et al ^[36], Yamamoto and Yun ^{[50],[54],[56]}, Hootsmans and Dubowsky ^{[65],[69]} discussed about tracking control problem with the consideration of interaction between the mobile platform and the manipulator. Khatib et al ^[49] proposed a decentralized control structure for cooperative tasks of multiple mobile manipulator systems. Liu and Lewis ^[71] also used a decentralized robust controller, but for overcoming the dynamic interaction of the mobile manipulator.

1.3 Summary of Contributions and Outline of Thesis

The followings are listed for showing the difference between this thesis and the previous researches:

- ❖ Assigning the responsibilities for mobile platform and manipulator in the tracking task so the calculation problem of system can be eased.
- ❖ Using the unified model approach for design the united controller so its configuration is simpler.
- ❖ Applying the adaptive control with unknown parameter to the welding mobile manipulator performing a 3D task.
- ❖ Using the concept of the backstepping kinematics into dynamics to simplify the controller design of a welding mobile manipulator.
- ❖ Applying the sliding mode control for solving the external disturbance problem for control a welding mobile manipulator.

This thesis consists of eight chapters. The content and summary of contribution in each chapter is summarized as follows:

Chapter 1 : The background of the issue is provided so the necessary of this research is set up. Some previous researches about the same field are summarized for showing the context of the problem and the trend of the other nearby problems. The summary of the contributions of this thesis as well as the outline of thesis content are also shown in this chapter.

Chapter 2 : The modeling of system is presented in this chapter. Both kinematic model and dynamic model are considered. Similarly, the system is investigated in the aspects of mobile platform, manipulator and mobile manipulator. The kinematic and dynamic relationships between the input components, the actuators, and the

output component, the end effector are mainly stated in this chapter. All relationships are expressed based on the physics analyses kinematics and dynamics of mechanical system. In here, the fundamental knowledge is provided as a mathematic tool for examining the problem in later chapters.

Chapter 3 : The chapter is divided to two parts, one for error measurement and one for describing the hardware implementation. The first part of chapter is reserved for showing how to get the error from the feedback signals of the sensors. These calculations are derived from the geometric relationships between the sensors mounted on mobile manipulator and the desired welding trajectory. A set of camera sensor (Logitech cam) and a set of two proximities are used for receiving the difference between welding torch tip and desired trajectory. In the second part, the structure of electronic hardware is obviously portrayed. The method for controlling the actuators and communicating the feedback sensors is also completely presented. It can be used for deeply understanding the experiments in the later chapters.

Chapter 4 : Based on the kinematic model of manipulator described in chapter 2, a feedback control is proposed. The errors vector is established from desired data and feedback signal of sensor for calculating the velocity commands to actuators. The Lyapunov approach is used for stabilizing the system in tracking task. A nonlinear feedback controller is proposed in here, and the simulation is preformed for proving the validity of the algorithm. The experiments are also carried out for showing the feasibility of using kinematic model

control for the mobile manipulator in a certain 3D task.

Chapter 5 In practice, the distance from torch tip to the desired point on the welding trajectory can be varied because the arc length of the torch is influenced by many other parameters such as the current intensity of the supplied power, and the geometric quality of the welding surface. The calculations based on the kinematic model of system are influenced by this variation. For overcoming this problem, an adaptive law with unknown parameter is applied to the mobile manipulator control. The unknown parameter is predicted and an update rule is proposed for increasing the flexibility of the mobile manipulator in the welding process. Some simulations and experiments are also fulfilled for affirming the correctness of the proposed algorithm.

Chapter 6 : In the motion, the mobile manipulator is still affected by many kinds of force such as inertia, centripetal, gravity and coriolis forces. All of them are taken into consideration in this chapter. For easing the control task, a combined kinematic/dynamic control law is developed using backstepping and asymptotic stability is guaranteed by Lyapunov theory. A feedback velocity control inputs are designed for making the position errors asymptotically stable. Another feedback velocity following control law is also designed such that the velocities of the mobile manipulator converge asymptotically to the given velocity inputs. For calculating the required torques for the actual mobile manipulator, a conventional computed-torque controller is used. As well as the previous chapter, the simulations and the experiments are carefully carried out for

reinforcing the proposed algorithm.

Chapter 7 : The external disturbances are considered in this chapter. In order to increase the ability of mobile manipulator for suffering the disturbances and to increase the accuracy of the mobile manipulator, a controller using the sliding mode control method is applied. A novel sliding mode control law is proposed for asymptotically stabilizing the mobile manipulator to the desired welding trajectory. It is shown that the proposed scheme is robust to the bounded external disturbances. Like the previous chapter, a conventional computed-torque controller is used for calculating the required torques for the actual mobile manipulator. The chattering phenomenon is also mentioned and a saturation function is proposed for overcoming this phenomenon. The simulation and experiment results are used for demonstrating the effectiveness of accurate tracking capability and the robust performance of the proposed algorithm.

Chapter 8 : This chapter is reserved for comparing the controllers that are proposed in the previous chapters. The contributions of thesis are also summarized concretely. Herein, the prospect of thesis and some future works are enumerated.

Chapter 2

System Modeling of the Mobile Manipulator

Two objectives are aimed in this chapter, that is, firstly, an appropriate configuration of mobile manipulator is chosen for performing the 3D welding task. The following modelings will be eased so much with this logical choice. Secondly, the mathematical model of mobile manipulator is establishing for designing the controller in the later chapters.

2.1 Configuration of the Mobile Manipulator

2.1.1 The Requirement of the 3D Welding Task

A smooth 3D curved welding seam is described in a vertical curved surface. For guaranteeing the quality of the welding seam, the following has to be obtained by the mobile manipulator in the welding process. The orientation of the welding torch should lie in the normal plane of the welding trajectory at the welding point. It should be also inclined with 45 degrees with respect to the intersectional line between the normal plane and the welding trajectory surface at welding point. In the next subsection, the configuration of the mobile manipulator and the assignment for the mobile platform and manipulator will be supposed for strictly satisfying this requirement. The requirement is clearly illustrated in Fig. 2.1.

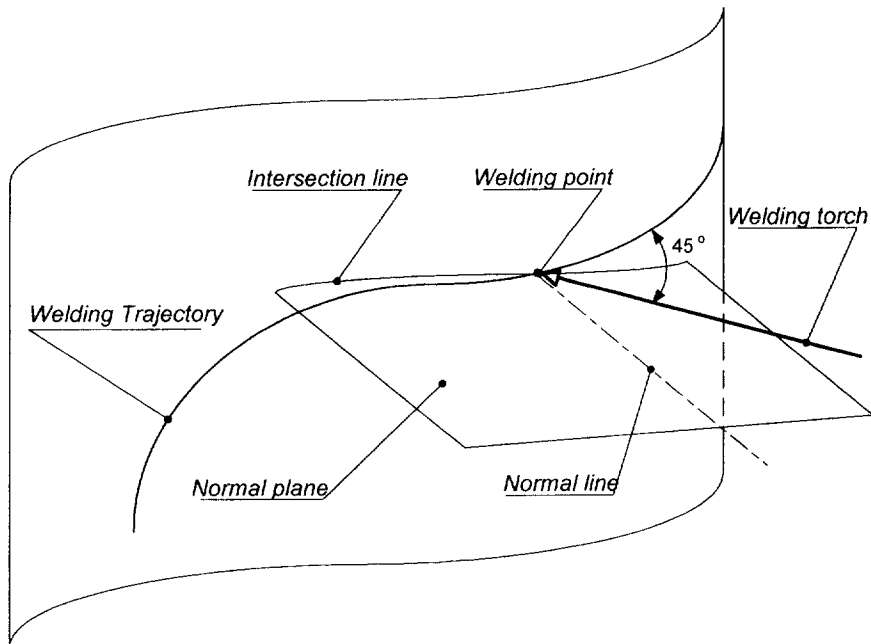


Fig. 2.1 Geometric illustration for the requirement of 3D welding task

2.1.2 Configuration of the Mobile Manipulator

- 1- Camera sensor
- 2- Welding torch
- 3- Link 2
- 4- Link 1
- 5- Link 0
- 6- Mobile Platform
- 7, 8, 9, 10- Revolute joint
- 11- Link 3+4

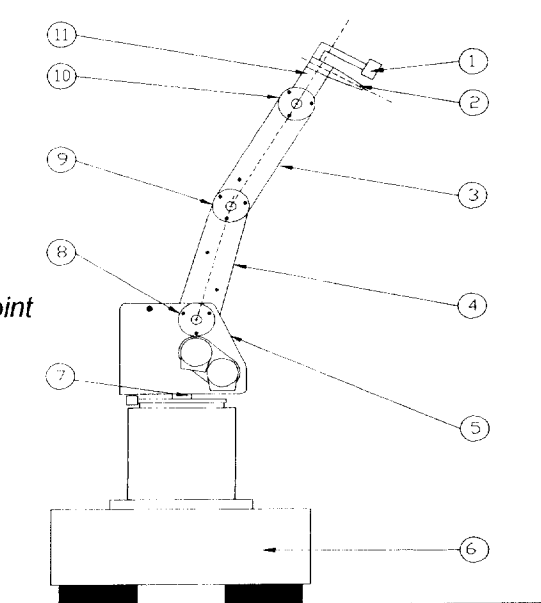


Fig. 2.2 Mobile manipulator configuration

A two wheeled mobile platform is used as a component of the mobile manipulator. The wheels of the mobile platform are independently driven by separate motors. A caster is also furnished for supporting the body of mobile platform. The position for setting up the manipulator is chosen at the middle of the common center line of two wheels.

A five degrees of freedom manipulator is mounted on the mobile platform of the mobile manipulator. The rotational motion of first link of manipulator (link 0) is not used in the welding process, but only for choosing what side of the mobile platform is the active side before the welding process.

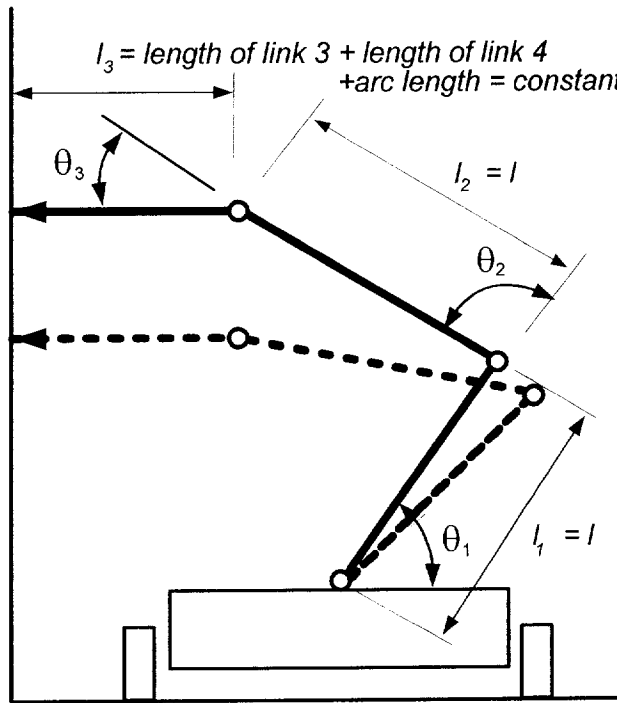


Fig. 2.3 Manipulator motion in welding process

According to the requirement mentioned in the last subsection (2.1.1), in the configuration of the manipulator, the torch orientation is fixed on the tilt of 45 degrees with respect to the link direction of the fourth link. Thereto, the link

direction of the fourth link always is kept in the perpendicular direction of the welding trajectory surface at the welding point, that is to say, parallel with the ground (see in the Fig. 2.3 for more detail). With the above condition, the torch orientation always lies in the normal plane of the welding trajectory at the welding point, and is inclined with 45 degrees with respect to the tangent line of the welding trajectory at the welding point. At last, the appropriate gesture of the torch at the certain welding point will be assured by the corresponding rotation of the last link.

In order to perform the welding task, the separate assignments for the mobile platform and the manipulator are made as the following: the duty of tracking the vertical curved surface in which the welding trajectory lies on is carried out by the mobile platform, and the duty of reaching to the altitude of the welding point is executed by the manipulator.

2.2 Kinematic Modeling of the Mobile Manipulator

3.1.1 The Associated Coordinate Frames

Two coordinate frames are set up for investigating the system model (see Fig. 2.4 for more detail). Together with both of coordinate frame, for easy reference, all the definitions of the state variables for mobile manipulator, mobile platform and the manipulator are listed as the following:

- $Oxyz$: world coordinate frame, it is also the inertia coordinate frame.
- $Cx_my_mz_m$: moving frame, it is the frame attached on the mobile manipulator.
- $q_m^C = \{\theta_1, \theta_2, \theta_3, \theta_4\}^T$: joint angles of the manipulator in the moving

frame.

- $q_p^O = \{x_c, y_c, \phi\}^T$: configuration of the platform in the world frame.

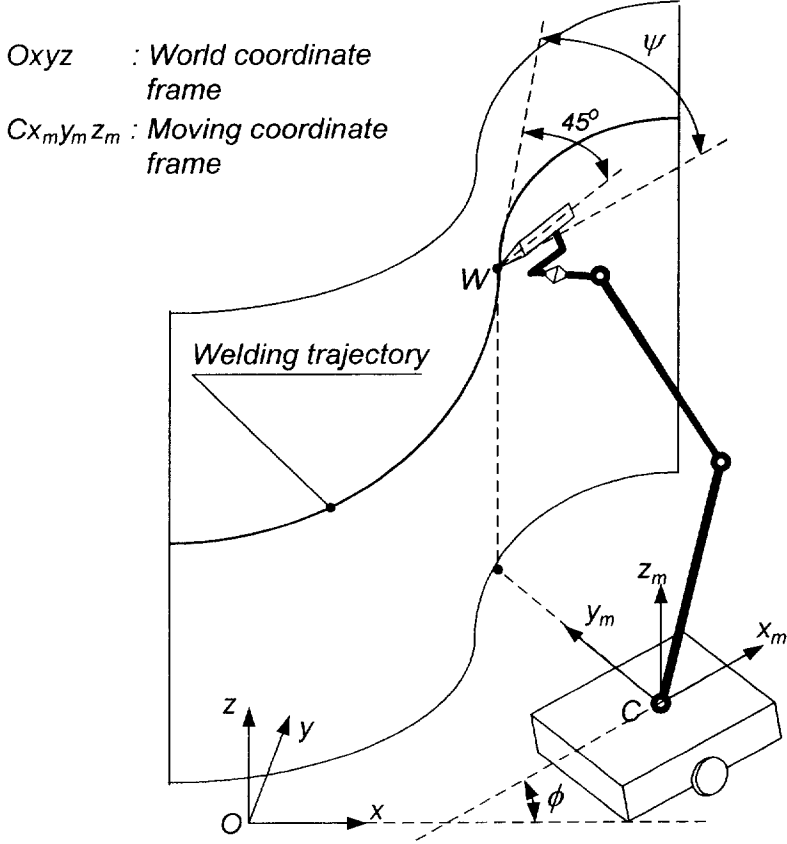


Fig. 2.4 Coordinate frames and state variables of the mobile manipulator

- $q = \{x_c, y_c, \phi, \theta_1, \theta_2, \theta_3, \theta_4\}^T$: configuration of the mobile manipulator.
- $p_i^O = \{x_w, y_w, z_w, \phi, \psi, \theta\}^T$: end effector position and orientation in the world frame.

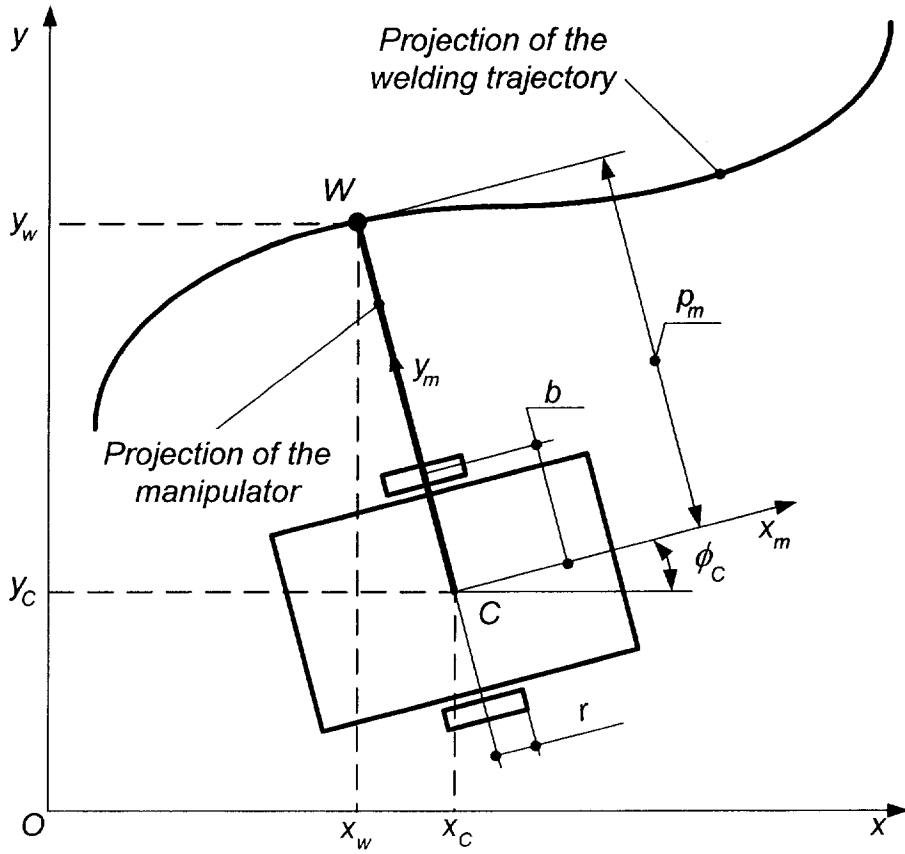


Fig. 2.5 Kinematic relation of the mobile platform (bird's-eye-view)

3.1.2 Kinematic Modeling of the Mobile Platform

The kinematic equation of the platform can be described as the following:

$$\begin{bmatrix} \dot{x}_C \\ \dot{y}_C \\ \dot{\phi}_C \\ \dot{\theta}_r \\ \dot{\theta}_l \end{bmatrix} = \begin{bmatrix} \cos \phi_C & 0 \\ \sin \phi_C & 0 \\ 0 & 1 \\ 1/r & b/r \\ 1/r & -b/r \end{bmatrix} \begin{bmatrix} v_{xy} \\ \omega_\phi \end{bmatrix} \quad (2.1)$$

where $q_p = [x_C \ y_C \ \phi_C \ \theta_r \ \theta_l]^T$ is the generalized coordinate of the mobile platform, see in Fig. 2.5 for more detail, $C(x_C, y_C)$ is the coordinate of the platform's center point, ϕ_C is the heading angle of the platform, $\dot{\theta}_r, \dot{\theta}_l$ are the angular velocities of the right and left wheels of the mobile platform, r, b are radius of the wheel and the distance from wheel to the symmetry axis, respectively, v_{xy} and ω_ϕ are the straight and angular velocity of the mobile platform in x-y plane, respectively and are supposed be bounded values.

It is assumed that the wheels of the mobile platform do not slip. So, the velocity of C must be kept in the direction of the symmetry axis of the mobile platform and its wheels must purely roll. The constraints are expressed as follows:

$$A(q_p)\dot{q}_p = 0 \quad (2.2)$$

or for this case:
$$\begin{bmatrix} -\sin\phi_C & \cos\phi_C & 0 & 0 & 0 \\ \cos\phi_C & \sin\phi_C & b & -r & 0 \\ \cos\phi_C & \sin\phi_C & -b & 0 & -r \end{bmatrix} \begin{bmatrix} \dot{x}_C \\ \dot{y}_C \\ \dot{\phi}_C \\ \dot{\theta}_r \\ \dot{\theta}_l \end{bmatrix} = 0 \quad (2.3)$$

3.1.3 Kinematic Modeling of the Manipulator

In practice, the manipulator is considered as a planar mechanism with three links as shown in Fig. 2.3. Furthermore, in welding process, to retain the appropriate direction of the torch with respect to the welding trajectory, the last link is always fixed in the horizontal direction. The constraint can be expressed as the following:

$$\begin{cases} \theta_1 + \theta_2 + \theta_3 = \pi \\ \omega_1 + \omega_2 + \omega_3 = 0 \end{cases} \quad (2.4)$$

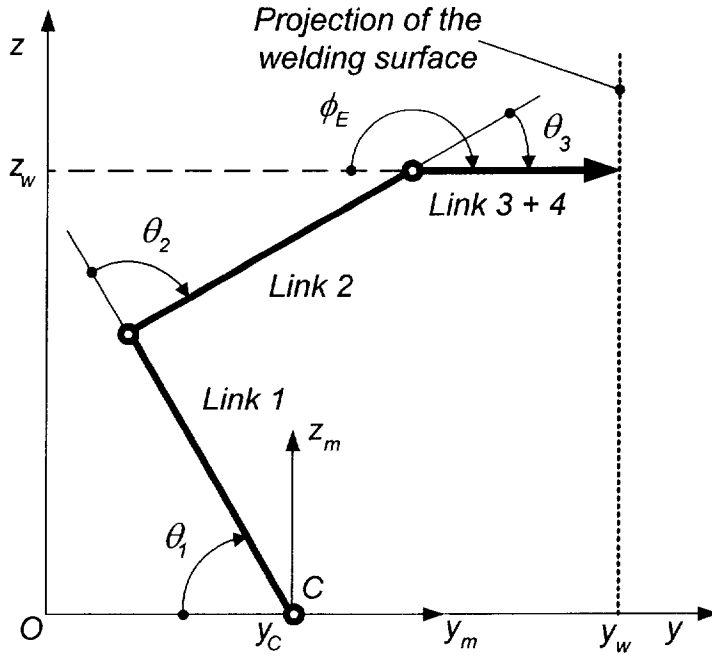


Fig. 2.6 Kinematic relation of the manipulator

where θ_i and ω_i are the link variables and the angular velocities of the i^{th} link of the manipulator.

The kinematic equation of the manipulator can be described as the following:

$$\dot{q}_E = J(q_m)\dot{q}_m \quad (2.5)$$

where q_E is the configuration of the torch tip, J is the Jacobian matrix of the manipulator, q_m is the link variable of the manipulator.

In case of the planar three-link manipulator, (2.5) can be re-expressed as:

$$\begin{bmatrix} \dot{x}_E \\ \dot{z}_E \\ \dot{\phi}_E \end{bmatrix} = \begin{bmatrix} J_{11} & J_{12} & J_{13} \\ J_{21} & J_{22} & J_{23} \\ J_{31} & J_{32} & J_{33} \end{bmatrix} \begin{bmatrix} \dot{\theta}_1 \\ \dot{\theta}_2 \\ \dot{\theta}_3 \end{bmatrix} \quad (2.6)$$

where l_i is the length of i^{th} link, and $S_{ij} = \sin(\theta_i + \theta_j)$, $C_{ij} = \cos(\theta_i + \theta_j)$,
 $J_{11} = l_2 S_3 + l_1 S_{23}$, $J_{12} = l_2 S_3$, $J_{13} = 0$, $J_{21} = l_3 + l_2 C_1 + l_1 C_{23}$, $J_{22} = l_3 + l_2 C_3$,
 $J_{23} = l_3$, $J_{31} = J_{32} = J_{33} = 1$, ϕ_E is the orientation angle of the end effector.

The inverse kinematic equation is defined as:

$$\begin{bmatrix} \omega_1 \\ \omega_2 \\ \omega_3 \end{bmatrix} = \begin{bmatrix} \dot{\theta}_1 \\ \dot{\theta}_2 \\ \dot{\theta}_3 \end{bmatrix} = \begin{bmatrix} J_{11}^{-1} & J_{12}^{-1} & J_{13}^{-1} \\ J_{21}^{-1} & J_{22}^{-1} & J_{23}^{-1} \\ J_{31}^{-1} & J_{32}^{-1} & J_{33}^{-1} \end{bmatrix} \begin{bmatrix} \dot{y}_E \\ \dot{z}_E \\ \dot{\phi}_E \end{bmatrix} \quad (2.7)$$

where $J_{11}^{-1} = l_2 C_3$, $J_{12}^{-1} = -l_2 S_3 - l_1 S_{23}$, $J_{13}^{-1} = l_2 l_3 S_3$, $J_{21}^{-1} = -l_2 C_3 - l_1 C_{23}$,
 $J_{22}^{-1} = l_2 S_3 + l_1 S_{23}$, $J_{23}^{-1} = -l_2 l_3 S_3 - l_1 l_3 S_{23}$, $J_{31}^{-1} = l_1 C_{23}$, $J_{32}^{-1} = -l_1 S_{23}$,
 $J_{33}^{-1} = l_1 l_3 S_{23} + l_1 l_3 S_2$.

3.1.4 Kinematic Equation of the Welding Torch Tip

The relationship between the welding point W and the center of the mobile platform C can be expressed as the following:

$$\begin{bmatrix} x_w \\ y_w \\ z_w \\ \phi_w \end{bmatrix} = \begin{bmatrix} x_C - p_m \sin \phi_C \\ y_C + p_m \cos \phi_C \\ z_C + l_1 \sin \theta_1 + l_2 \sin(\theta_1 + \theta_2) \\ \phi_C \end{bmatrix} \quad (2.8)$$

where p_m is the distance from the projection of the manipulator torch tip on the x-y plane to the center C of platform, ϕ_w is the heading angle in the horizontal plane of the welding torch and ϕ_C is the heading angle of the mobile platform.

Combining the derivative of (2.8) and the angular velocity of the torch yields the kinematic equation for the welding torch tip as follows:

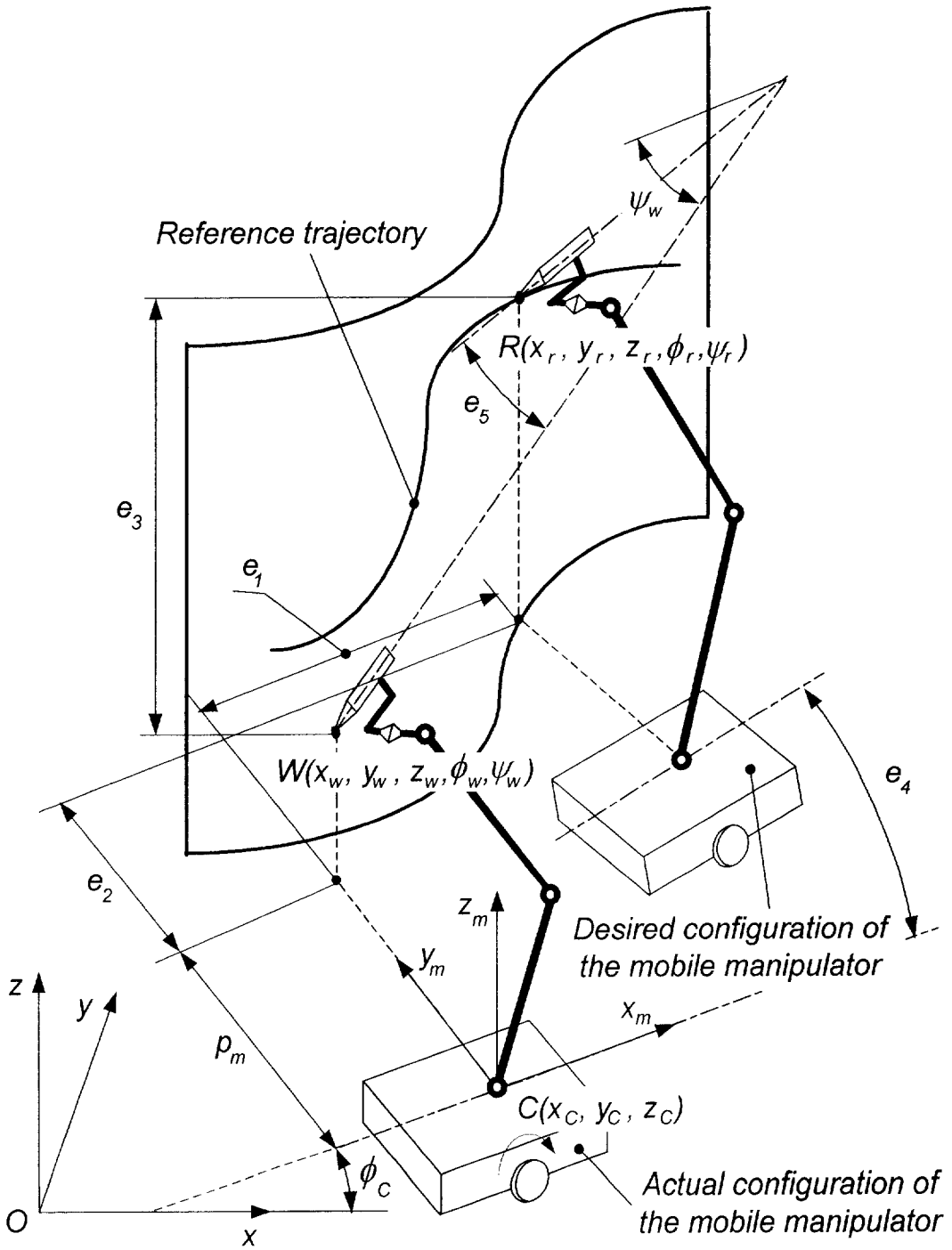


Fig. 2.7 Tracking errors description

$$\begin{bmatrix} \dot{x}_w \\ \dot{y}_w \\ \dot{z}_w \\ \dot{\phi}_w \\ \dot{\psi}_w \end{bmatrix} = \begin{bmatrix} \cos\phi_C - p_m \cos\phi_C & 0 & 0 & 0 \\ \sin\phi_C - p_m \sin\phi_C & 0 & 0 & 0 \\ 0 & 0 & l_1 \cos\theta_1 + l_2 \cos(\theta_1 + \theta_2) & 0 \\ 0 & 1 & 0 & 0 \\ 0 & 0 & 0 & 1 \end{bmatrix} \begin{bmatrix} v_{xy} \\ \omega_\phi \\ \omega_l \\ \omega_2 \\ \omega_\psi \end{bmatrix} \quad (2.9)$$

where ψ_w and ω_ψ are the heading angle and the angular velocity of the welding torch in vertical plane, respectively. It is assumed that ω_ψ is bounded.

3.1.5 Tracking errors

Vector $[e_1 \ e_2 \ e_3 \ e_4 \ e_5]^T$ is denoted as the vector of the tracking error that is the difference between the welding point W and the reference point R (see Fig. 2.7 for more detail). This vector is expressed as:

$$\begin{bmatrix} e_1 \\ e_2 \\ e_3 \\ e_4 \\ e_5 \end{bmatrix} = \begin{bmatrix} \cos\phi_w & \sin\phi_w & 0 & 0 & 0 \\ -\sin\phi_w & \cos\phi_w & 0 & 0 & 0 \\ 0 & 0 & 1 & 0 & 0 \\ 0 & 0 & 0 & 1 & 0 \\ 0 & 0 & 0 & 0 & 1 \end{bmatrix} \begin{bmatrix} x_r - x_w \\ y_r - y_w \\ z_r - z_w \\ \phi_r - \phi_w \\ \psi_r - \psi_w \end{bmatrix} \quad (2.10)$$

where the subscript r and w imply reference and welding (or desired and actual), respectively.

2.3 Dynamic Modeling of the Mobile Manipulator

The dynamic equation and the constraint equation of the mobile manipulator using the Lagrangian approach can be described as the following (Lewis et al ^[8], Lin and Goldenberg ^[27]):

$$M(q)\ddot{q} + C(q, \dot{q})\dot{q} + F(q, \dot{q}) + A^T(q)\lambda + \tau_d = E(q)\tau \quad (2.11)$$

$$A(q)\dot{q} = 0 \quad (2.12)$$

where $q \in \mathbb{R}^p$ is p generalized coordinates, $M(q) \in \mathbb{R}^{p \times p}$ is the symmetric and positive definite inertia matrix, $C(q, \dot{q}) \in \mathbb{R}^{p \times p}$ is the centripetal and Coriolis matrix, $F(q, \dot{q}) \in \mathbb{R}^p$ is the friction and gravitational vector, $A(q) \in \mathbb{R}^{r \times p}$ is the constraint matrix, $\lambda \in \mathbb{R}^r$ is the Lagrange multiplier, $\tau_d \in \mathbb{R}^p$ is the disturbance vector, $E(q) \in \mathbb{R}^{p \times (p-r)}$ is the input transformation matrix, $\tau \in \mathbb{R}^{p-r}$ is the torque input vector, and r is the number of the kinematic constraints.

In (2.11), the following properties are established (Lewis et al ^[8], Lin and Goldenberg ^[27])

Property 1: The inertia matrix and generalized coordinate are bounded.

$$\begin{aligned} M_{\min} I_p &\leq M(q) \leq M_{\max} I_p \\ C(q, \dot{q}) &\leq C_b(q) \|\dot{q}\| \end{aligned} \quad (2.13)$$

where M_{\min}, M_{\max} are the positive scalar constants depending on the mass properties and the constraint matrix, I_p is the identity matrix, and $C_b(q)$ is the positive function of q . This mobile manipulator is a revolute joint robot, so this term is a finite constant (Lewis et al ^[8], Lin and Goldenberg ^[27]).

Property 2: The skew symmetric property.

$$\begin{aligned} \dot{M} - 2C &= -(\dot{M} - 2C)^T \\ \dot{M} &= C + C^T \end{aligned} \quad (2.14)$$

The generalized coordinate vector can be expressed as $q = (q_v^T, q_r^T)^T$, where $q_v \in \mathbb{R}^m$ describes the generalized coordinates in (2.11), and $q_r \in \mathbb{R}^n$ is the free

generalized coordinates. With $p = m + n$ and $A_v(q_v) \subset \mathbb{R}^{r \times m}$, eq. (2.12) can be re-expressed as the following:

$$A_v(q_v)\dot{q}_v = 0 \quad (2.15)$$

This mobile manipulator is fully actuated, and the equation (2.11) is rewritten in another form as the following:

$$\begin{aligned} \begin{pmatrix} M_{11} & M_{12} \\ M_{21} & M_{22} \end{pmatrix} \begin{pmatrix} \ddot{q}_v \\ \ddot{q}_r \end{pmatrix} + \begin{pmatrix} C_{11} & C_{12} \\ C_{21} & C_{22} \end{pmatrix} \begin{pmatrix} \dot{q}_v \\ \dot{q}_r \end{pmatrix} + \begin{pmatrix} F_1 \\ F_2 \end{pmatrix} \\ + \begin{pmatrix} A_v^T(q_v)\lambda \\ 0 \end{pmatrix} + \begin{pmatrix} \tau_{d1} \\ \tau_{d2} \end{pmatrix} = \begin{pmatrix} E_v \tau_v \\ \tau_r \end{pmatrix} \end{aligned} \quad (2.16)$$

where $\tau_v \subset \mathbb{R}^{m-r}$ is the actuated torque vector of the constrained coordinates, $E_v \subset \mathbb{R}^{m \times (m-r)}$ is the input transformation matrix, $\tau_r \subset \mathbb{R}^n$ is the actuated torque vector of the free coordinates, and $\tau_{d1} \subset \mathbb{R}^m, \tau_{d2} \subset \mathbb{R}^n$ are the disturbance torques.

There exists a full rank and bounded matrix $S_v(q_v) \subset \mathbb{R}^{m \times (m-r)}$ formed by $(m-r)$ columns that span the null space of $A_v(q_v)$ defined in (2.15) as the following:

$$S_v^T(q_v)A_v^T(q_v) = 0 \quad (2.17)$$

There exists an auxiliary vector $v(t) \subset \mathbb{R}^{m-r}$ so that for all t

$$\dot{q}_v = S(q_v)v(t) \quad (2.18)$$

and its derivative form is

$$\ddot{q}_v = S(q_v)\dot{v} + \dot{S}(q_v)v \quad (2.19)$$

Property 3:

$$\begin{aligned}\dot{M}_{11} - 2C_{11} &= -(\dot{M}_{11} - 2C_{11})^T \\ \dot{M}_{22} - 2C_{22} &= -(\dot{M}_{22} - 2C_{22})^T\end{aligned}\tag{2.20}$$

Property 4:

$$\begin{aligned}\dot{M}_{21} &= C_{21} + C_{12}^T \\ \dot{M}_{12} &= M_{21}^T\end{aligned}\tag{2.21}$$

Property 5:

$$\begin{aligned}\|S^T M_{11} S\| &\leq \overline{M_{11b}} \\ \|M_{12}\| &\leq M_{12b} \\ \|M_{21}\| &\leq M_{21b} \\ \|M_{22}\| &\leq M_{22b}\end{aligned}\tag{2.22}$$

where $\overline{M_{11b}}, M_{12b}, M_{21b}, M_{22b}$ are the positive constants.

Property 6:

$$\begin{aligned}\|S^T C_{11} S\| &\leq \overline{C_{11b}} \|\dot{q}\| \\ \|C_{12}\| &\leq C_{12b} \|\dot{q}\| \\ \|C_{21}\| &\leq C_{21b} \|\dot{q}\| \\ \|C_{22}\| &\leq C_{22b} \|\dot{q}\|\end{aligned}\tag{2.23}$$

where $\overline{C_{11b}}, C_{12b}, C_{21b}, C_{22b}$ are the positive constants.

2.3.1 Dynamic Modeling of the Mobile Platform

From (2.15) and (2.16), the mobile platform's dynamics can be expressed as:

$$M_{11}\ddot{q}_v + M_{12}\ddot{q}_r + C_{11}\dot{q}_v + C_{12}\dot{q}_r + F_l + A_v^T \lambda + \tau_{dl} = E_v \tau_v \quad (2.24)$$

$$A_v(q_v)\dot{q}_v = 0.$$

Substituting (2.18), (2.19) into (2.24) obtains

$$S^T M_{11} S \ddot{v} + S^T M_{11} \dot{S} \dot{v} + S^T M_{12} \ddot{q}_r + S^T C_{11} S \dot{v} + S^T C_{12} \dot{q}_r + S^T F_l + S^T \tau_{dl} = S^T E_v \tau_v \quad (2.25)$$

Equation (2.25) can be re-written as:

$$\overline{M_{11}} \ddot{v} + \overline{C_{11}} \dot{v} + \overline{\tau_{dl}} = \tau_v \quad (2.26)$$

where $\overline{C_{11}} = S^T C_{11} S + S^T M_{11} \dot{S}$, $\overline{\tau_{dl}} = S^T (M_{12} \ddot{q}_r + C_{12} \dot{q}_r + F_l + \tau_{dl})$,
 $\overline{M_{11}} = S^T M_{11} S$, $S^T E_v = I$.

Property 7:

$$\dot{\overline{M_{11}}} - 2\overline{C_{11}} = -(\dot{\overline{M_{11}}} - 2C_{11})^T \quad (2.27)$$

Herein, it is assumed that the disturbance on the platform, the friction and the gravity of the platform are bounded.

2.3.2 Dynamic Modeling of the Manipulator

From (2.16), the dynamics for the manipulator can be expressed as:

$$M_{21}\ddot{q}_v + M_{22}\ddot{q}_r + C_{21}\dot{q}_v + C_{22}\dot{q}_r + F_2 + \tau_{d2} = \tau_r \quad (2.28)$$

Equation (2.28) can be re-written as:

$$\overline{M_{22}}\ddot{q}_r + \overline{C_{22}}\dot{q}_r + \overline{\tau_{d2}} = \tau_r \quad (2.29)$$

where $\overline{M_{22}} = M_{22}$, $\overline{C_{22}} = C_{22}$, $\overline{\tau_{d2}} = M_{21}\ddot{q}_v + C_{21}\dot{q}_v + F_2 + \tau_{d2}$.

As is mentioned in the last sub-section, it is assumed that the disturbance on the manipulator, the friction and the gravity on the manipulator are bounded. In summary, the dynamic model of the mobile manipulator can be described by the (2.18), (2.26) and (2.29).

Chapter 3

Hardware Design and Implementation of the Mobile Manipulator

How to measure the tracking errors and how to build the hardware of the mobile manipulator are the subjects that will be clarified in this chapter. The control system exerted on the mobile manipulator is the feedback control with the sensors. The feedback signal from the sensors plays a very important role in the control scheme, so they should be carefully and accurately measured. The configuration of the mobile manipulator is chosen based on the analysis of the task of the mobile manipulator. Relied on that configuration, the hardware of the control system is adequately built.

3.1 Tracking Errors Measurement

As mentioned in the last chapter, the tracking errors of the system are the difference between the welding point and the reference point, and they are defined as the following (see Fig. 2.7 for more detail):

- ❖ The error along the x_m axis of the moving frame $Cx_my_mz_m$ is denoted by e_1 .
- ❖ The error along the y_m axis of the moving frame $Cx_my_mz_m$ is denoted by e_2 .
- ❖ The error along the z_m axis of the moving frame $Cx_my_mz_m$ is denoted by e_3 .

- ❖ The error of the heading angle of the mobile platform in the plane Cx_my_m is denoted by e_4 .
- ❖ The error of the heading angle of the welding torch in the plane that is parallel with the plane Cx_mz_m is denoted by e_5 .

For detecting these errors, a camera and a set of proximity mounted on the end effector are used. Both of them are the non-contact sensors so the random errors that are produced by the rough surface of welding trajectory can be avoided. The errors e_1 , e_3 and e_5 are measured by the camera sensor and the errors e_2 and e_4 are measured by the proximity sensor set.

3.1.1 Measuring the Tracking Errors e_1 , e_3 and e_5

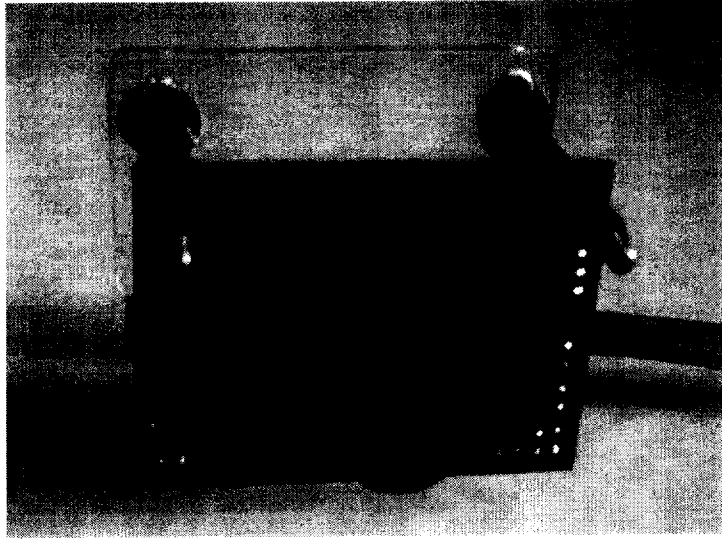


Fig. 3.1 CMU camera sensor

The CMU camera sensor is shown in Fig. 3.1 and the diagram for measuring the errors is shown in Fig. 3.2. The tracking error components e_1 , e_3 and e_5 are calculated by using the difference between the center of view window C_0 and the center of detected object C_d . A camera sensor is mounted on the third link (eye-in-

hand) so that its coordinate frame $Ex_e y_e z_e$ is always parallel with the moving coordinate frame $Cx_m y_m z_m$ and the center of the view window of the camera coincides with the welding torch tip of the mobile manipulator. The outputs of this professional camera are the coordinates of the boundary box of detected object ($F_1(x_{F_1}, y_{F_1})$, $F_2(x_{F_2}, y_{F_2})$) and the coordinates of the estimated center of detected object $C_c(x_c, y_c)$.

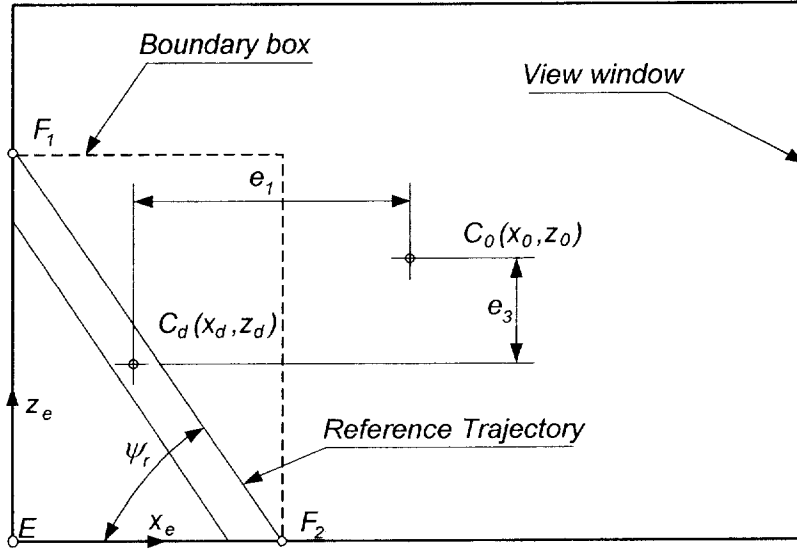


Fig. 3.2 Error calculation diagram (for e_1 , e_3 and e_5)

From Fig. 3.2, the errors e_1 , e_3 and e_5 can be expressed as following:

$$\begin{aligned} e_1 &= x_c - x_0 \\ e_3 &= y_c - y_0 \\ e_5 &= \psi_r - \psi_w = \text{atan}\left(\frac{y_{F_1} - y_{F_2}}{x_{F_1} - x_{F_2}}\right) - \psi_w \end{aligned} \quad (3.1)$$

where ψ_r and ψ_w are desired and actual heading angle of the welding torch at the welding point.

The value ψ_w is measured by a rotational potentiometer attached on the third link. This potentiometer was pre-calibrated so that the difference from the horizon to the center line of the torch, that is, the angle ψ_w is shown by its output.

Herein, as for the error e_5 , there are various cases of what sides that the detected object is intersected with the view window. According to a certain case, the error value e_5 has a little bit of difference with respect to the value in (3.2), but it is trivial enough to omit. So (3.2) can be used for calculating the errors with proper precise results at anywhere.

3.1.2 Measuring the Tracking Errors e_2 and e_4

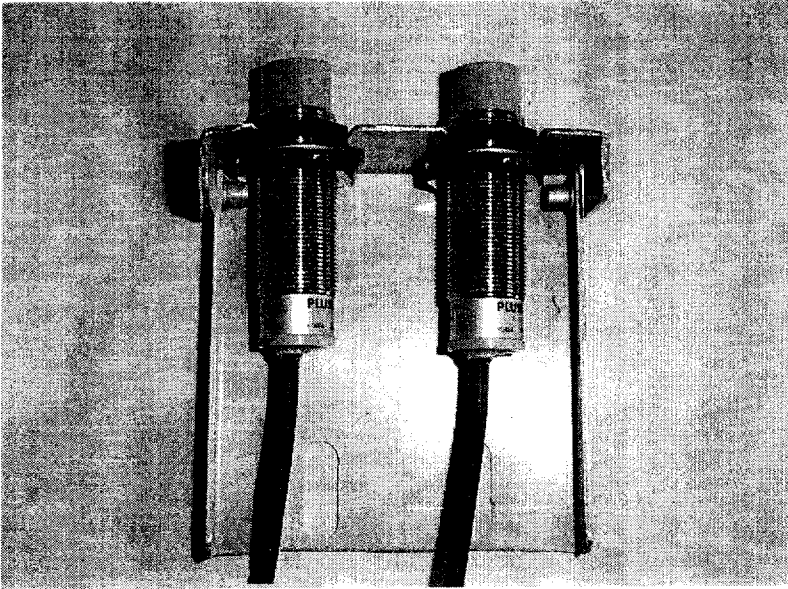


Fig. 3.3 Proximity sensor set

In order to measure the tracking error components e_2 and e_4 , one sensor set is applied as shown in Fig. 3.3. In Fig. 3.4, the sensor set that is also mounted on the third link is composed of two proximities so that they are put on the line parallel with motion direction of the mobile platform.

distance between the proximities l_p so it can be ignored without any remarkable influencing the accuracy of the welding seam.

3.2 Hardware of the System and Its Implementation

3.2.1 Configuration of the Mobile Manipulator

As mentioned in the previous chapter, the driving system of the mobile manipulator is composed of six DC motors with proper gearboxes. Some timing driving-belts are used because of the structural conditions and the load lessening, especial in the manipulator. A caster wheel is also equipped for mobile platform to support its body. Both camera sensor and proximity set are installed on the end of third link, above the welding torch. The configuration of the mobile manipulator is shown in Fig. 3.5.

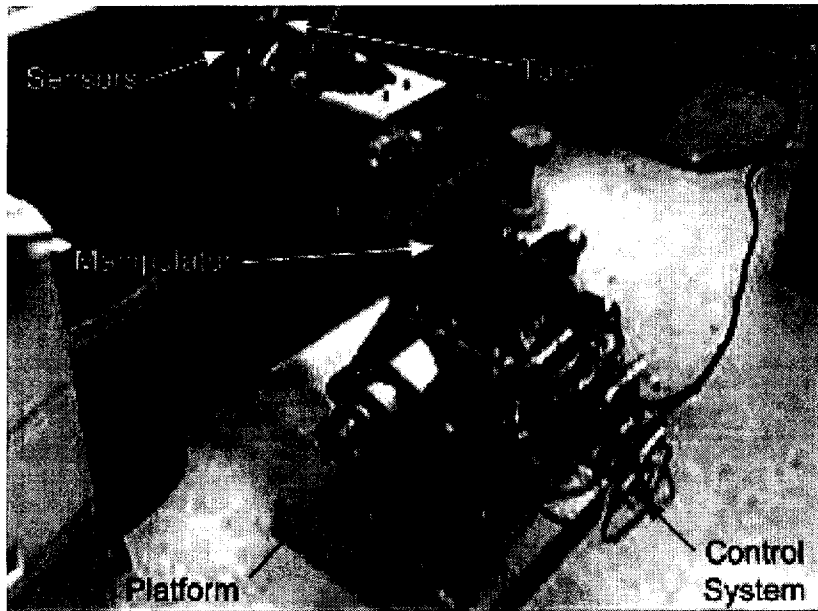


Fig. 3.5 Configuration of the mobile manipulator

3.2.2 Configuration of the Control System

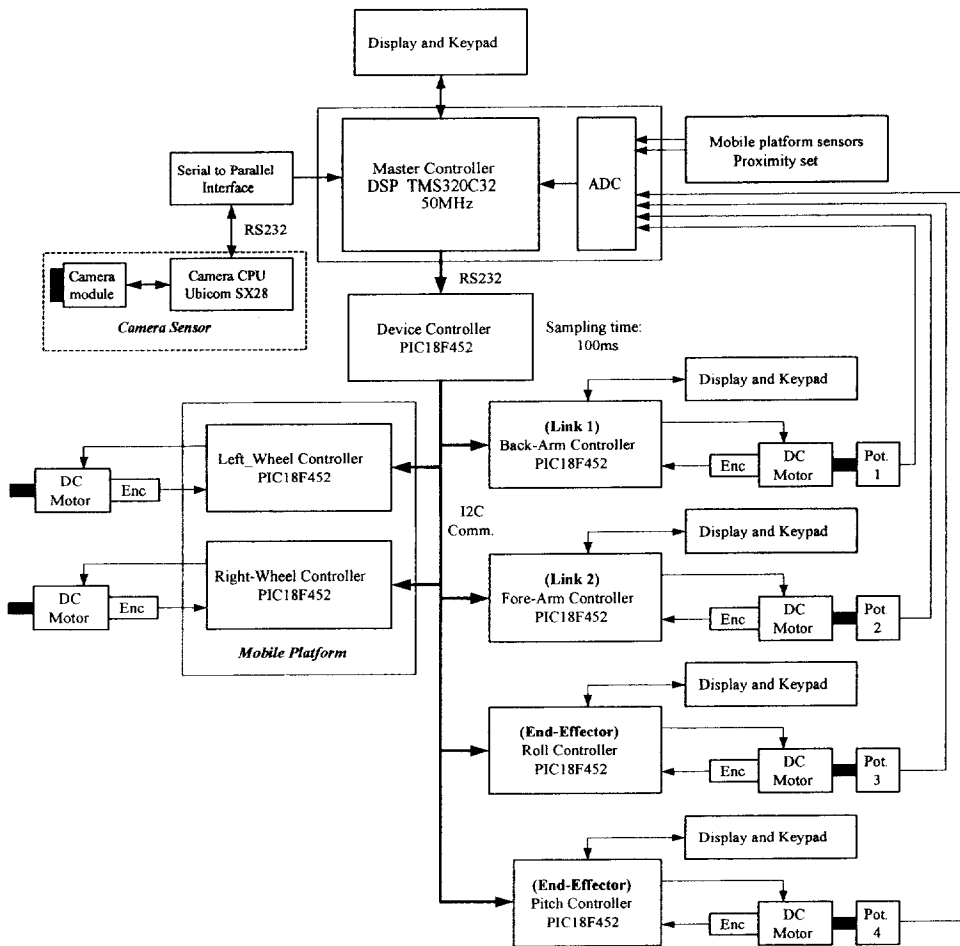


Fig. 3.6 Configuration of the control system

A DSP-PIC based control system was developed for the mobile manipulator because a certain complicated control law can be managed by such a system. The hardware of the control system was modularized in terms of the function of the components of the system. It is based on the integration of two levels of controllers: device controller and master controller.

The former is constructed by seven PIC18F452 microprocessors. Therein, one PIC18F452 is used for playing the role of an interface between the two levels. The

others are the left-wheel controller and the right-wheel controller for the mobile platform, the back-arm controller and the fore-arm controller for the two links, the roll motion controller and the pitch motion controller for the end-effector. The latter is based on TMS320C32 DSP processor which renders the control law and sends command to the device controller.



Fig. 3.7 Implementation of the control system

The device controllers are DC motor drivers that perform the indirect servo control using one encoder. There are six A/D ports used on the master controller: two A/D ports are connected to the two proximities for sensing the errors e_2 and e_4 of the mobile platform, as mentioned in sub-section 3.1.2, and the four others are used to measure the rotational angles of the links and the end-effector. The

interface controller links to the servo controllers via I2C communication and links to the master controller via RS232 communication.

Additionally, the master controller receives signal from camera sensor for detecting the errors between the welding torch and the reference trajectory. The whole configuration of the control system is shown in Fig. 3.6.

For operation, the master controller receives the signals from the sensors to calculate the errors as mentioned in sub-section 3.1.1 and 3.1.2, the controller manages based on these errors with the sampling time of 100ms, and the command signals are sent to the six servo controllers, respectively. The implementation of the control system is given in Fig. 3.7.

Chapter 4

Nonlinear Feedback Tracking Controller Design for Kinematic Model of the Mobile Manipulator

4.1 Introduction

In this chapter, a tracking controller for the mobile manipulator is discussed. Therein, the controlled variables - position and orientation of the end effector - are measured by the sensors, and the measured information is fed back to the controller to adjust the controlled variables. The mathematical model that is used in the controller design is the kinematic model. Based on this kinematic model and applying the Lyapunov method, the control inputs - command velocities for the motors driving the wheels of mobile platform and the links of manipulator - are computed to satisfy the stability of the system.

The simulations are performed with Matlab 7.0 and Simulink 6.0. In this step, the weight factor is correspondingly chosen with the initial value of the configuration of mobile manipulator. The graphs showing the relationship between the input and the output signals are carefully analyzed for proving the validity of the algorithm in theoretic aspect.

Various experiments are earnestly exerted for investigating the performance of the mobile manipulator in practical welding process. This experiment results are also used to adjust the weight factors of controller for obtaining the faster

converging and the more stable system. The practical feasibility of this controller design is clearly shown by this step.

4.2 Kinematic Feedback Controller Design

As mentioned the sub-section 2.2.5, the tracking errors of the system are assumed to be bounded and they can be expressed as the following (see Fig. 2.7 for more detail):

$$\begin{bmatrix} e_1 \\ e_2 \\ e_3 \\ e_4 \\ e_5 \end{bmatrix} = \begin{bmatrix} \cos \phi_w & \sin \phi_w & 0 & 0 & 0 \\ -\sin \phi_w & \cos \phi_w & 0 & 0 & 0 \\ 0 & 0 & 1 & 0 & 0 \\ 0 & 0 & 0 & 1 & 0 \\ 0 & 0 & 0 & 0 & 1 \end{bmatrix} \begin{bmatrix} x_r - x_w \\ y_r - y_w \\ z_r - z_w \\ \phi_r - \phi_w \\ \psi_r - \psi_w \end{bmatrix} \quad (4.1)$$

Herein, tracking is concerned as the objective so a controller should be found out so that it can make the mobile manipulator obtaining $e_i \rightarrow 0$ with respect to $t \rightarrow \infty$. In the other word, the welding point W becomes to coincide with its reference point R , or the actual configuration concurs with the desired configuration of the end effector.

Easily, the derivative form of the errors in Eq. (4.1) can be established as the following:

$$\begin{bmatrix} \dot{e}_1 \\ \dot{e}_2 \\ \dot{e}_3 \\ \dot{e}_4 \\ \dot{e}_5 \end{bmatrix} = \begin{bmatrix} v_r \cos \psi_r \cos e_4 \\ v_r \cos \psi_r \sin e_4 \\ v_r \sin \psi_r \\ \omega_{\phi r} \\ \omega_{\psi r} \end{bmatrix} + \begin{bmatrix} -1 & e_2 + p_m & 0 & 0 \\ 0 & -e_1 & 0 & 0 \\ 0 & 0 & -1 & 0 \\ 0 & -1 & 0 & 0 \\ 0 & 0 & 0 & -1 \end{bmatrix} \begin{bmatrix} v_{xy} \\ \omega_{\phi} \\ v_z \\ \omega_{\psi} \end{bmatrix} \quad (4.2)$$

where, v_r is the reference velocity in the welding trajectory, it is assumed as a bounded and constant value; v_{xy} is the x-y component velocity of the mobile platform; v_z is the z component velocity of the end effector of the manipulator; ω_ϕ and ω_ψ are the derivative form of the heading angle ϕ and ψ , respectively; and p_m is the projection of the manipulator on x-y plane.

A candidate Lyapunov function is proposed as the following: (it is also chosen so that to be positive definite function)

$$V = \frac{1}{2}e_1^2 + \frac{1}{2}e_2^2 + \frac{1}{2}e_3^2 + \frac{1 - \cos e_4}{k_2} + \frac{1}{2}e_5^2 \quad (4.3)$$

The derivative form of (4.3) can be expressed as:

$$\begin{aligned} \dot{V} &= e_1 \dot{e}_1 + e_2 \dot{e}_2 + e_3 \dot{e}_3 + \frac{\sin e_4}{k_2} \dot{e}_4 + e_5 \dot{e}_5 \\ &= e_1 (v_r \cos \psi_r \cos e_4 - v_{xy} + e_2 \omega_\phi + p_m \omega_\phi) + \\ &\quad e_2 (v_r \cos \psi_r \sin e_4 - e_1 \omega_\phi) + e_3 (v_r \sin \psi_r - v_z) + \\ &\quad \frac{\sin e_4}{k_2} (\omega_{\phi r} - \omega_\phi) + e_5 (\omega_{\psi r} - \omega_\psi) \\ &= e_1 (v_r \cos \psi_r \cos e_4 - v_{xy} + p_m \omega_\phi) + e_2 v_r \cos \psi_r \sin e_4 + \\ &\quad e_3 (v_r \sin \psi_r - v_z) + \frac{\sin e_4}{k_2} (\omega_{\phi r} - \omega_\phi) + e_5 (\omega_{\psi r} - \omega_\psi) \end{aligned} \quad (4.4)$$

The control variables are chosen as the following:

$$\begin{cases} v_{xy} = p_m (\omega_{\phi r} + k_2 e_2 v_r \cos \psi_r + k_4 \sin e_4) + v_r \cos \psi_r \cos e_4 + k_1 e_1 \\ v_z = v_r \sin \psi_r + k_3 e_3 \\ \omega_\phi = \omega_{\phi r} + k_2 e_2 v_r \cos \psi_r + k_4 \sin e_4 \\ \omega_\psi = \omega_{\psi r} + k_5 e_5 \end{cases} \quad (4.5)$$

where k_1, k_2, k_3, k_4, k_5 are positive values.

Substituting Eq. (4.5) into Eq.(4.4), eliminating the similar terms for simplifying, the brief form of \dot{V} can be expressed as the following:

$$\dot{V} = -k_1 e_1^2 - k_3 e_3^2 - \frac{k_4}{k_2} \sin^2 e_4 - k_5 e_5^2 \leq 0 \quad (4.6)$$

For proving $e_i \rightarrow 0$ as $t \rightarrow \infty$, the Barbalat's lemma is used in the following procedure. As for first condition of the lemma, because $\dot{V} \leq 0$, so error vector e is bounded. Furthermore, referring Eq. (4.3), when e is bounded, V has a finite limit as $t \rightarrow \infty$. As for second condition of the lemma, the value of the derivative of \dot{V} is calculated as below:

$$\frac{d\dot{V}}{dt} = -2k_1 e_1 \dot{e}_1 - 2k_3 e_3 \dot{e}_3 - \frac{2k_4}{k_2} \dot{e}_4 \sin e_4 \cos e_4 - 2k_5 e_5 \dot{e}_5 \quad (4.7)$$

Obviously, because e_i and \dot{e}_i are bounded, the derivative of \dot{V} is bounded too. (The bounded-ness of \dot{e}_i is resulted by the smoothness of welding trajectory and the constant velocity of welding torque tip throughout the welding process). Therefore \dot{V} satisfies the sufficient condition of a uniformly continuous function. According to two above-mentioned conditions, by Barbalat's lemma, the result is obtained as $\lim_{t \rightarrow \infty} \dot{V} = 0$.

Now, Eq. (4.6) can be re-written as follows:

$$0 = -k_1 e_1^2 - k_3 e_3^2 - \frac{k_4}{k_2} \sin^2 e_4 - k_5 e_5^2 \quad (4.8)$$

Eq. (4.8) implies that $\lim_{t \rightarrow \infty} [e_1 \quad e_3 \quad e_4 \quad e_5]^T = 0$. As a result of $e_4 = 0$, the welding heading angle and reference heading angle of mobile platform coincide,

that is to say, $\omega_\phi = \omega_\phi$. Referring Eq. (4.5), in the third row, when two previous conditions occur, the result is $\lim_{t \rightarrow \infty} e_2 = 0$.

After everything mentioned above, a conclusion can be inferred: the equilibrium point $e_i = 0$ is uniformly asymptotically stable.

Based on the kinematic relationships in section 2.2, the control input of system can be expressed as the following:

$$\begin{bmatrix} \omega_r \\ \omega_l \\ \omega_1 \\ \omega_2 \\ \omega_4 \end{bmatrix} = \begin{bmatrix} \frac{1}{r} & 0 & \frac{b}{r} & 0 \\ \frac{1}{r} & 0 & -\frac{b}{r} & 0 \\ 0 & \frac{\sin \theta_{12}}{l \sin \theta_2} & 0 & 0 \\ 0 & \frac{-\sin \theta_1 - \sin \theta_{12}}{l \sin \theta_2} & 0 & 0 \\ 0 & 0 & 0 & 1 \end{bmatrix} \begin{bmatrix} v_{xy} \\ v_z \\ \omega_\phi \\ \omega_\psi \end{bmatrix} \text{ and } \omega_3 = -\omega_1 - \omega_2 \quad (4.9)$$

The development of the control system can be illustrated by the following block diagram:

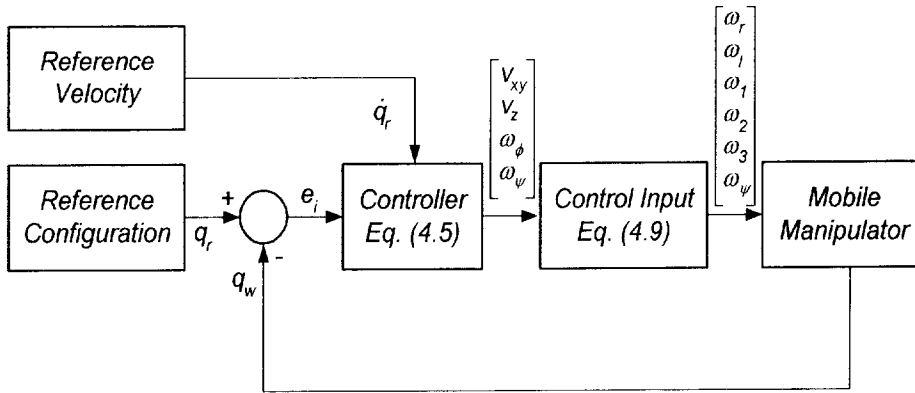


Fig. 4.1 Block diagram of the kinematic feedback control system for mobile manipulator

4.3 Simulation and Experiment Results

The reference trajectory used in simulation is made on the vertical curved surface. This smooth curve is constituted by three one-fourth circular sectors 200mm in diameter. The contact points of the circular sectors are chosen so that the reference trajectory can be a smooth curve. The circular sectors are successively put in the y-z plane, x-y plane, and x-z plane. The reference trajectory is shown in the Fig. 4.2.

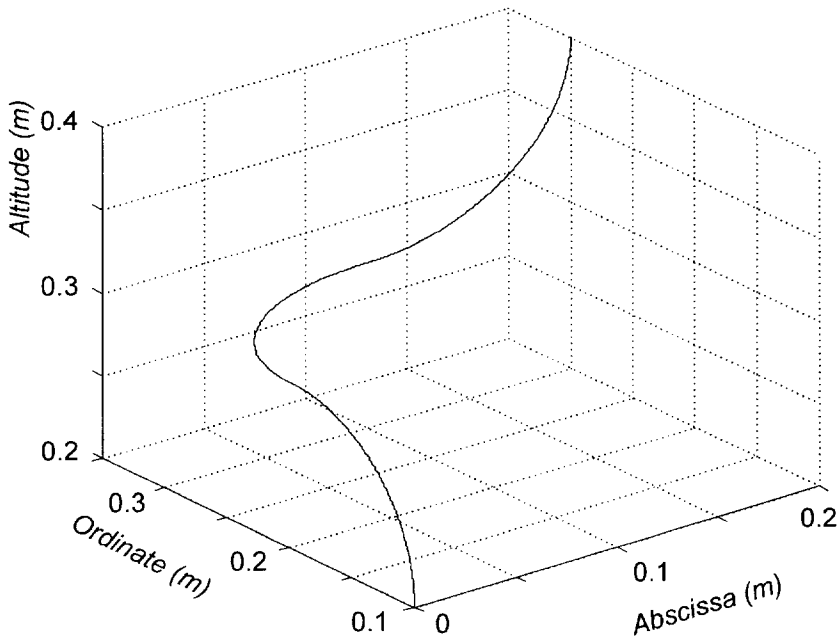


Fig. 4.2 Reference trajectory

During the welding process, for obtaining the best quality of the welding seam, the velocity of the desired point in welding trajectory is remained in constant of 7.5mm/s. The initial configuration of the mobile robot is set at the values so that the errors are at usual rate of the welding process.

The values of the mobile manipulator's parameters used in the simulation are given in Table 4.1 as shown below:

Table 4.1 Numerical values of the system's parameters

Parameters	Description	Values	Units
r	Radius of the wheels	0.03	m
b	Half of the wheel-to-wheel distance	0.15	m
$l_1 = l_2 = l$	Length of the first and second link	0.222	m
$l_3 + l_4$	Length of the third + fourth link	0.172	m
p_m	Projection of the manipulator on Oxy	0.38	m
Δx_i	Initial position error in x direction	0.01	m
Δy_i	Initial position error in y direction	0	m
Δz_i	Initial position error in z direction	0.01	m
$\Delta \phi_i$	Initial orientation error in horizontal	$\pi/22$	rad
$\Delta \psi_i$	Initial orientation error in vertical	$\pi/22$	rad
k_1	Weight factor of the controller	1.5	
k_2	Weight factor of the controller	100	
k_3	Weight factor of the controller	1	
k_4	Weight factor of the controller	10	
k_5	Weight factor of the controller	5	

The tracking errors of the mobile manipulator in the welding process are shown in the first two Figs. 4.3 and 4.4. Therein, the position tracking errors converge to zero after about five seconds. More quickly, it takes only about one second, the orientation tracking errors converge to zero. This good performance of the system is obtained due to the reasonable choice of the weight factor of controller. According to the results of various simulations, an interesting result

can be inferred, that is, each weight factor set only makes the good performance on the corresponding range of the initial errors.

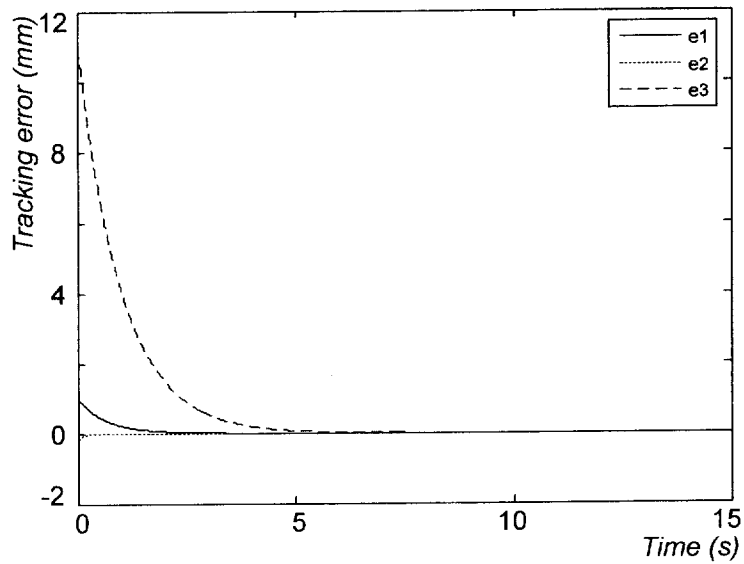


Fig. 4.3 Position tracking errors e_1 , e_2 and e_3

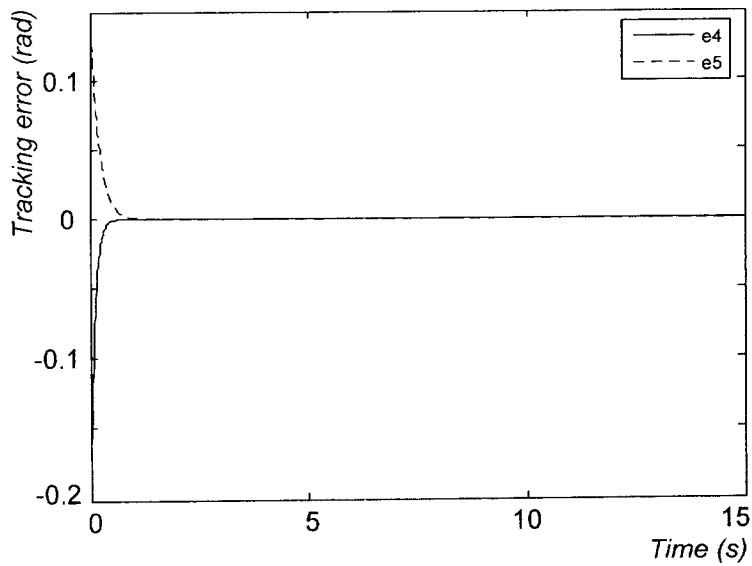


Fig. 4.4 Orientation tracking errors e_4 and e_5

The control input parameters - velocities of the wheels and links - are shown in Figs. 4.5 and 4.6. In Fig. 4.7, the performance of the system in the first circular sector is displayed with the reference trajectory for easy to compare.

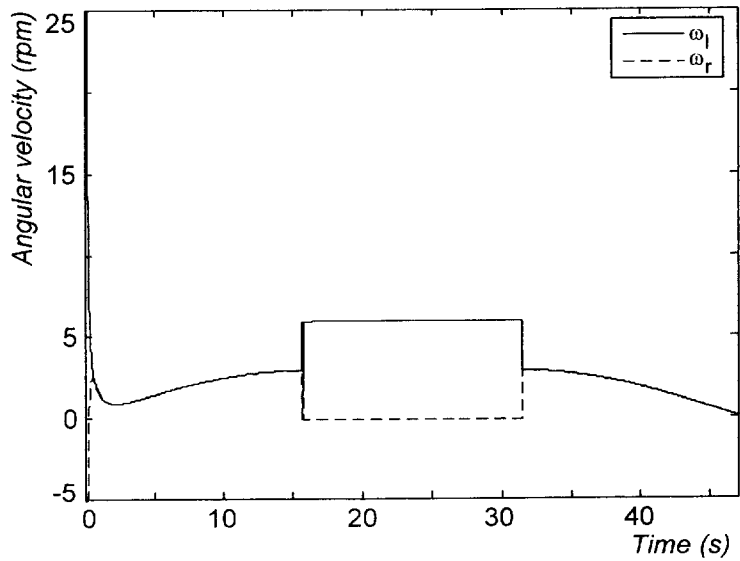


Fig. 4.5 Angular velocity of the wheels

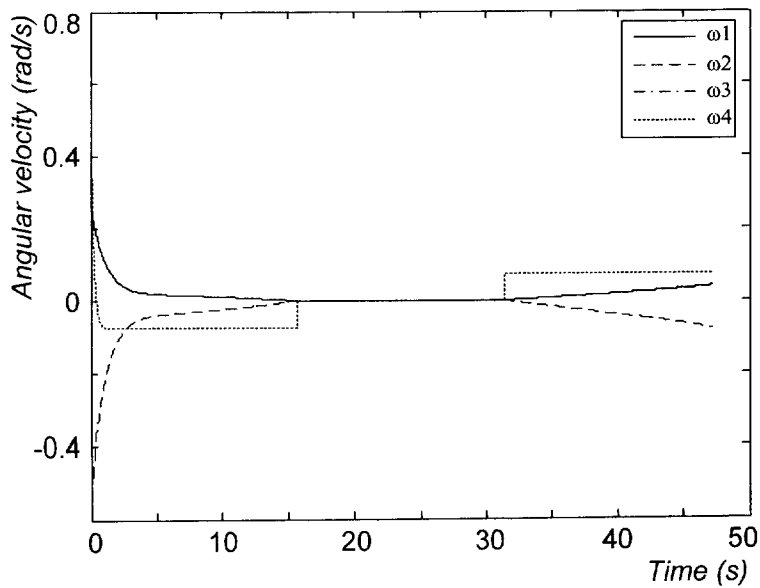


Fig. 4.6 Angular velocity of the links

The actual trajectory, in Fig. 4.7, quickly coincides with the desired trajectory, only after a very short distance from the initial position, even if the initial errors are remarkable. It can be implied that the proposed algorithm satisfied the "simulation test" so it is ready for experimental examining.

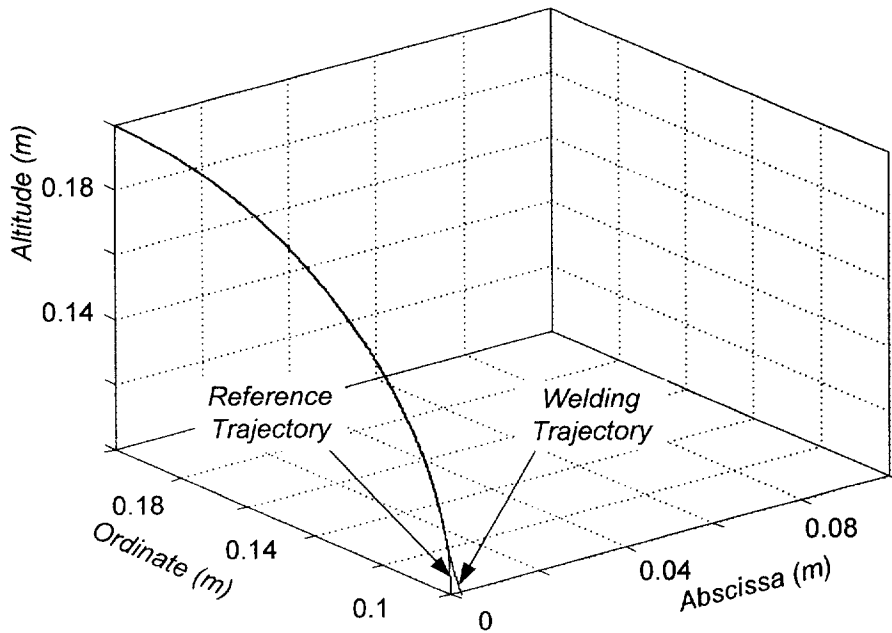


Fig. 4.7 Reference trajectory and welding trajectory in the first circular sector

The mobile manipulator and its experimental environment are shown in Fig. 4.8. It shows the experiment about verifying the tracking ability of the controller. The experiment results of the system's performance are consecutively shown in Figs. 4.9-13. In those Figs., the simulation results are also depicted for a convenient comparison. The measured values of the position error are even very small deviations, not exceed 1 mm. Similarly, the orientation errors do not also surpass 0.01 radian (about a half of one degree). It can be accepted those values in the welding process.

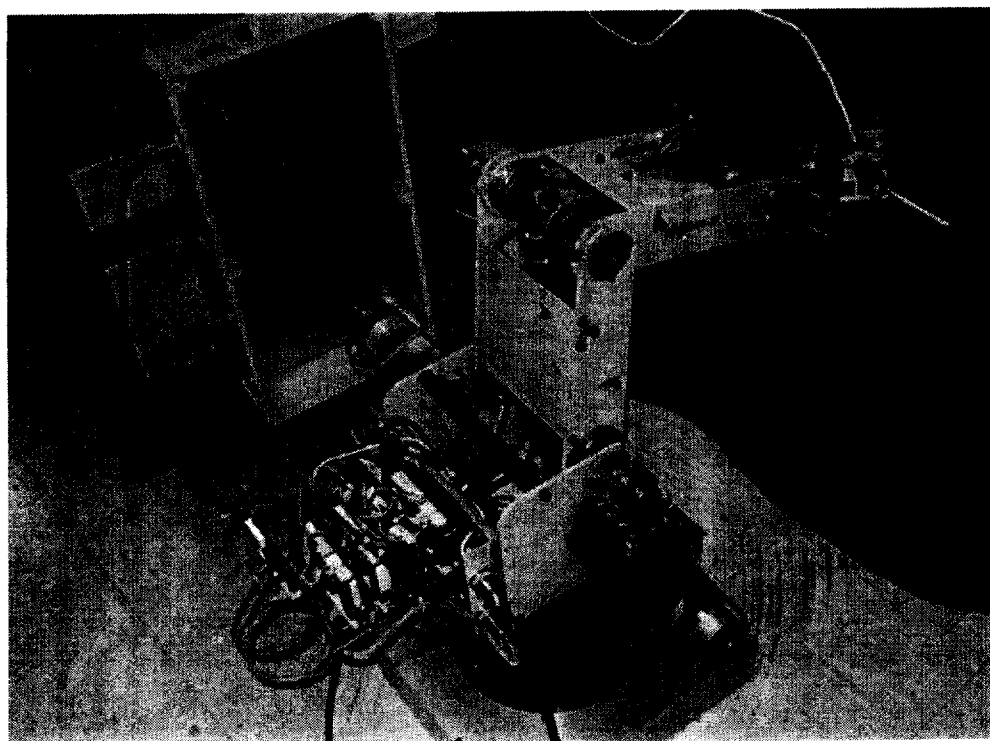


Fig. 4.8 Mobile manipulator in experiment

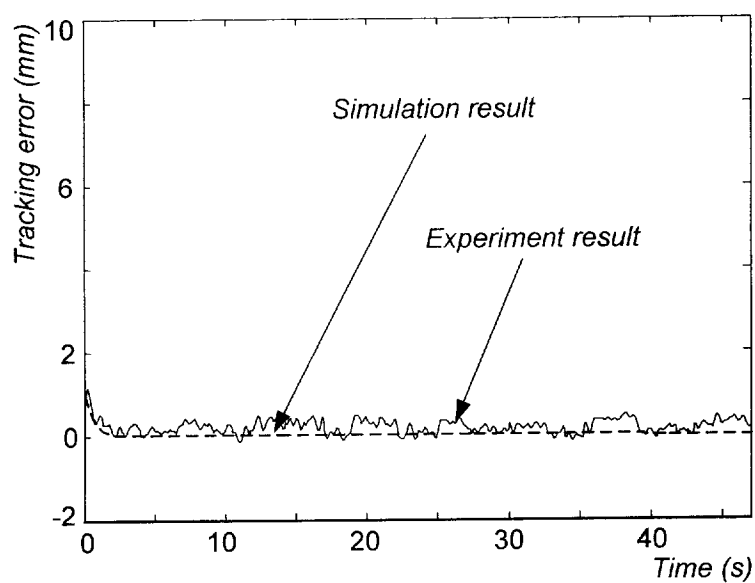


Fig. 4.9 Tracking error e_l

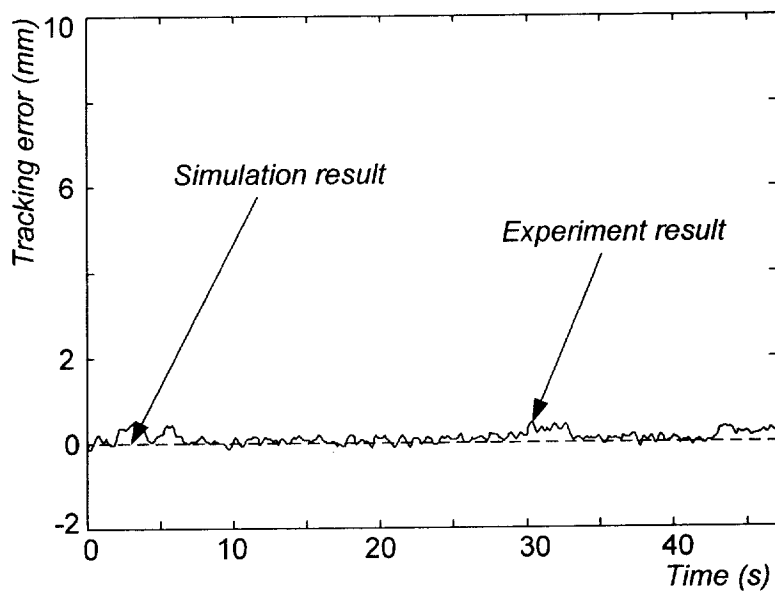


Fig. 4.10 Tracking error e_2

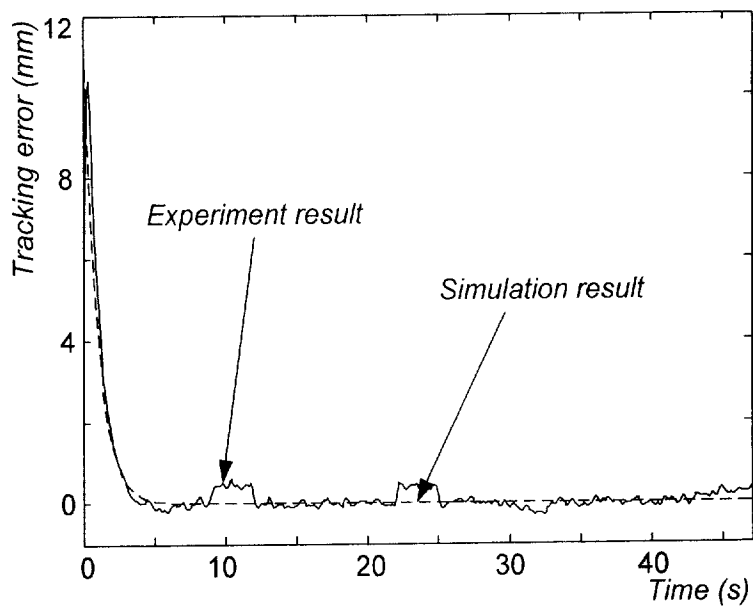


Fig. 4.11 Tracking error e_3

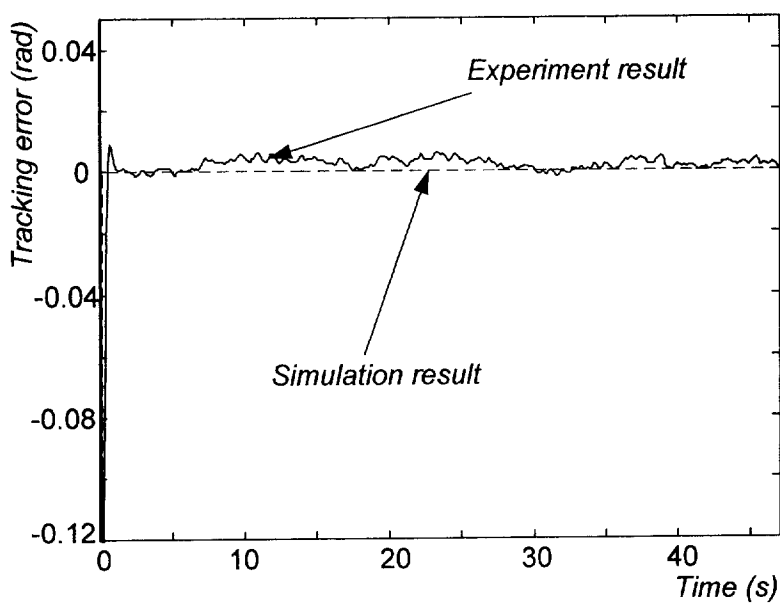


Fig. 4.12 Tracking error e_4

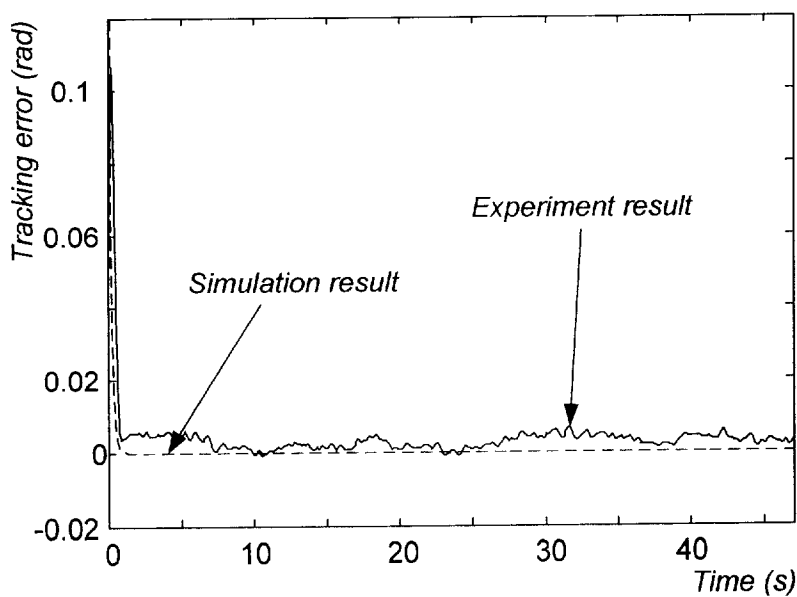


Fig. 4.13 Tracking error e_5

4.4 Chapter Summary

A simple nonlinear feedback control algorithm based on the kinematic model of a mobile manipulator is proposed in this chapter. Even if the controller is very simple and easy for applying, it also shows the ability to make a good performance for the mobile manipulator in 3D tracking duty. The uniform asymptotical stability of the system is guaranteed by Lyapunov - like analysis using Barbalat's lemma. It also proves that at the equilibrium point, the tracking errors simultaneously equal to zero. The affirmation in terms of the theory is made out by the simulation step and the experiment step is performed for confirming the feasibility of algorithm in actual welding process.

The contribution in this chapter:

- ❖ Establishing a nonlinear feedback controller based on the kinematic model for a mobile manipulator performing the smooth 3D curved welding trajectory.
- ❖ Specifying a set of weight factors used in this mobile manipulator's controller for satisfying the rate of initial deviation: 0-20mm with position error and 0-0.3rad with orientation error.

Chapter 5

Nonlinear Adaptive Tracking Controller Design for Kinematic Model of the Mobile Manipulator with Unknown Parameter

5.1 Introduction

In the practice, not every parameters of the mobile manipulator are exactly known. For example, the diameters of the wheels of the mobile platform are worn day by day, the lengths of the links are unknown because of the manufactured or the assembled errors, and the physical quantity values of the system such as the inertia moments are not exactly measured because of the sophisticated form of the robot components. The accuracy of the kinematic computation will be intensively influenced by those unknown parameters. A mobile manipulator is even suffered a tough unknown parameter, it is the length of welding arc. In practice, the length of welding arc is varied upon various other parameters such as the current intensity of power supplied, and the geometric quality of the welding surface. Furthermore, the welding arc length variation is uninterrupted and very hard to be predicted. In this chapter, an adaptive tracking controller based on the kinematic model is proposed for solving the unknown parameter problem. Like the previous chapter, the stability of the system is once more proved by using the Lyapunov technique. The simulations are performed for showing the good performance of the system in

the suffering with the unknown parameter problem. The experiments are carried out for affirming the flexibility and adaptation of the mobile manipulator in the welding process with unknown kinematic parameter.

5.2 Kinematic Adaptive Tracking Controller Design

According to the sub-section 2.2.5, the tracking errors of the system can be expressed as the following:

$$\begin{bmatrix} e_1 \\ e_2 \\ e_3 \\ e_4 \\ e_5 \end{bmatrix} = \begin{bmatrix} \cos \phi_w & \sin \phi_w & 0 & 0 & 0 \\ -\sin \phi_w & \cos \phi_w & 0 & 0 & 0 \\ 0 & 0 & 1 & 0 & 0 \\ 0 & 0 & 0 & 1 & 0 \\ 0 & 0 & 0 & 0 & 1 \end{bmatrix} \begin{bmatrix} x_r - x_w \\ y_r - y_w \\ z_r - z_w \\ \phi_r - \phi_w \\ \psi_r - \psi_w \end{bmatrix} \quad (5.1)$$

The main objective of this chapter is still tracking control so that a controller for the mobile manipulator should be found out to obtain $e_i \rightarrow 0$ as $t \rightarrow \infty$, that is, for making the welding point W to become to coincide with its reference point R . Based on the kinematic relationship shown in section 2.2, the impact of the unknown parameters should be illustrated. In the other word, they should be represented in the control law for investigating their influence on the performance of the system.

Easily, the derivative form of the tracking errors is established as follows

$$\begin{bmatrix} \dot{e}_1 \\ \dot{e}_2 \\ \dot{e}_3 \\ \dot{e}_4 \\ \dot{e}_5 \end{bmatrix} = \begin{bmatrix} v_r \cos \psi_r \cos e_4 \\ v_r \cos \psi_r \sin e_4 \\ v_r \sin \psi_r \\ \omega_{\phi r} \\ \omega_{\psi r} \end{bmatrix} + \begin{bmatrix} -1 & e_2 + p_m & 0 & 0 \\ 0 & -e_1 & 0 & 0 \\ 0 & 0 & -1 & 0 \\ 0 & -1 & 0 & 0 \\ 0 & 0 & 0 & -1 \end{bmatrix} \begin{bmatrix} v_{xy} \\ \omega_{\phi} \\ v_z \\ \omega_{\psi} \end{bmatrix} \quad (5.2)$$

where v_r is the reference velocity in the welding trajectory, and is bounded and large than zero; v_{xy} is the x-y component velocity of v_r ; v_z is the z component velocity of v_r ; $\omega_{\phi r}$ and $\omega_{\psi r}$ are reference rotational velocity of the welding torch in horizontal plane and vertical plane, respectively.

The projection of manipulator in x-y plane is denoted by p_m . In practice, the value of parameter p_m is always varied because the arc length of the torch depends on many other parameters such as the current intensity of the power supplied, and the geometric quality of the welding surface. Thus, an adaptive controller is designed to obtain the control objective by using the estimates of the parameter p_m . Also, the estimated value and the estimated error of p_m are denoted by \hat{p}_m and \tilde{p}_m , respectively. Their relationship is described in the following equation:

$$\hat{p}_m = p_m + \tilde{p}_m, \quad (5.3)$$

$$\dot{\hat{p}}_m = \dot{\tilde{p}}_m, \quad (5.4)$$

Using the above definition, Eq. (5.2) can be re-expressed as follows:

$$\begin{bmatrix} \dot{e}_1 \\ \dot{e}_2 \\ \dot{e}_3 \\ \dot{e}_4 \\ \dot{e}_5 \end{bmatrix} = \begin{bmatrix} v_r \cos \psi_r \cos e_4 \\ v_r \cos \psi_r \sin e_4 \\ v_r \sin \psi_r \\ \omega_{\phi r} \\ \omega_{\psi r} \end{bmatrix} + \begin{bmatrix} -1 & e_2 + \hat{p}_m & 0 & 0 \\ 0 & -e_1 & 0 & 0 \\ 0 & 0 & -1 & 0 \\ 0 & -1 & 0 & 0 \\ 0 & 0 & 0 & -1 \end{bmatrix} \begin{bmatrix} v_{xy} \\ \omega_{\phi} \\ v_z \\ \omega_{\psi} \end{bmatrix} \quad (5.5)$$

A positive definite function is chosen as the candidate Lyapunov function and is expressed as the following:

$$V = \frac{1}{2}e_1^2 + \frac{1}{2}e_2^2 + \frac{1}{2}e_3^2 + \frac{1 - \cos e_4}{k_2} + \frac{1}{2}e_5^2 + \frac{1}{2k_6}\hat{p}_m^2 \quad (5.6)$$

The derivative form of (4.6) is expressed as the following:

$$\begin{aligned}
\dot{V} &= e_1 \dot{e}_1 + e_2 \dot{e}_2 + e_3 \dot{e}_3 + \frac{\sin e_4}{k_2} \dot{e}_4 + e_5 \dot{e}_5 + \frac{\hat{p}_m}{k_6} \dot{\hat{p}}_m \\
&= e_1 (v_r \cos \psi_r \cos e_4 - v_{xy} + e_2 \omega_\phi + \hat{p}_m \omega_\phi) + \\
&\quad e_2 (v_r \cos \psi_r \sin e_4 - e_1 \omega_\phi) + e_3 (v_r \sin \psi_r - v_z) + \\
&\quad \frac{\sin e_4}{k_2} (\omega_{\phi r} - \omega_\phi) + e_5 (\omega_{\psi r} - \omega_\psi) + \frac{\hat{p}_m}{k_6} \dot{\hat{p}}_m \\
&= e_1 (v_r \cos \psi_r \cos e_4 - v_{xy}) + e_3 (v_r \sin \psi_r - v_z) + \\
&\quad \frac{\sin e_4}{k_2} (k_2 e_2 v_r \cos \psi_r + \omega_{\phi r} - \omega_\phi) + e_5 (\omega_{\psi r} - \omega_\psi) \\
&\quad + \hat{p}_m (\omega_\phi e_1 + \frac{\dot{\hat{p}}_m}{k_6})
\end{aligned} \tag{5.7}$$

An adaptive control law with the unknown parameter p_m is chosen as the following:

$$\begin{cases}
v_{xy} = v_r \cos \psi_r \cos e_4 + k_1 e_1 \\
v_z = v_r \sin \psi_r + k_3 e_3 \\
\omega_\phi = \omega_{\phi r} + k_2 e_2 v_r \cos \psi_r + k_4 \sin e_4 \\
\omega_\psi = \omega_{\psi r} + k_5 e_5 \\
\dot{\hat{p}}_m = -k_6 \omega_\phi e_1
\end{cases} \tag{5.8}$$

where $k_1, k_2, k_3, k_4, k_5, k_6$ are positive values.

Substituting Eq. (5.8) into Eq. (5.7), \dot{V} can be re-expressed as the following:

$$\dot{V} = -k_1 e_1^2 - k_3 e_3^2 - \frac{k_4}{k_2} \sin^2 e_4 - k_5 e_5^2 \leq 0 \tag{5.9}$$

It is the same of previous chapter, for proving $\lim_{t \rightarrow \infty} e_i = 0$ and the estimated value \hat{p}_m converges to a certain value, the Barbalat's lemma is used once more for \dot{V} . In examining the function \dot{V} for the first condition of the lemma, because $\dot{V} \leq 0$, so error vector e is bounded. Furthermore, referring Eq. (5.6), when e is bounded, V has a finite limit as $t \rightarrow \infty$. In investigating the function \dot{V} for the second condition of the lemma, the value of the derivative of \dot{V} is computed as the following:

$$\frac{d\dot{V}}{dt} = -2k_1 e_1 \dot{e}_1 - 2k_3 e_3 \dot{e}_3 - \frac{2k_4}{k_2} \dot{e}_4 \sin e_4 \cos e_4 - 2k_5 e_5 \dot{e}_5 \quad (5.10)$$

Obviously, because \dot{e}_i are bounded, the derivative of \dot{V} is bounded too. Therefore \dot{V} satisfies the sufficient condition of a uniformly continuous function. According to two above-mentioned conditions, by Barbalat's lemma, the result is obtained as $\dot{V} \rightarrow 0$ as $t \rightarrow \infty$.

Now, Eq. (5.9) can be re-written as follows:

$$0 = -k_1 e_1^2 - k_3 e_3^2 - \frac{k_4}{k_2} \sin^2 e_4 - k_5 e_5^2 \quad (5.11)$$

Eq. (5.11) implies that $\lim_{t \rightarrow \infty} [e_1 \ e_3 \ e_4 \ e_5]^T = 0$. As a result of $e_4 = 0$, the welding heading angle and reference heading angle of mobile platform coincide, that is to say, $\omega_\phi = \omega_{\phi^r}$. Referring Eq. (5.8), in the third row, when the previous conditions occur, the result is $\lim_{t \rightarrow \infty} e_2 = 0$. After everything mentioned above, a conclusion can be inferred: the equilibrium point $e_i = 0$ is uniformly asymptotically stable.

From the last row of Eq. 5.8, when $e_l = 0$, $\dot{\hat{p}}_m = 0$, that is to say, the velocity of the variation of \hat{p}_m equals to 0, in the other word, the estimated value of p_m will converge to a certain value.

Based on the kinematic relationships in section 2.2, the control input of system can be expressed as the following:

$$\begin{bmatrix} \omega_r \\ \omega_l \\ \omega_1 \\ \omega_2 \\ \omega_\psi \\ \dot{\hat{p}}_m \end{bmatrix} = \begin{bmatrix} 1/r & 0 & b/r & 0 \\ 1/r & 0 & -b/r & 0 \\ 0 & \frac{\sin \theta_{12}}{l \sin \theta_2} & 0 & 0 \\ 0 & \frac{-\sin \theta_1 - \sin \theta_{12}}{l \sin \theta_2} & 0 & 0 \\ 0 & 0 & 0 & 1 \\ 0 & 0 & -k_6 e_1 & 0 \end{bmatrix} \begin{bmatrix} v_{xy} \\ v_z \\ \omega_\phi \\ \omega_\psi \end{bmatrix} \quad (5.12)$$

and $\omega_3 = -(\omega_1 + \omega_2)$

The block diagram of algorithm is shown as follows.

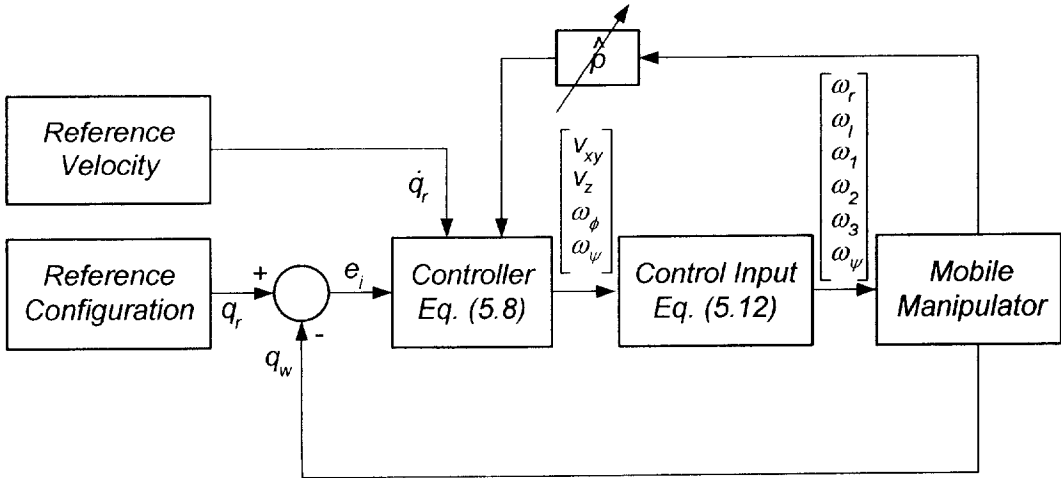


Fig. 5.1 Block diagram of the kinematic adaptive control system for mobile manipulator with unknown parameter

5.3 Simulation and Experiment Results

In this chapter, the simulations are performed with using the same reference trajectory as the last chapter. It is depicted in Fig. 4.2. Matlab 7.0 and Simulink 6.0 are also invoked to perform the simulations. The initial position and oriental errors of the mobile manipulator's end effector are set up with average rate like in the last chapter's simulation. Some parameter values of the system used in the simulation are given in Table 5.1.

Table 5.1 Numerical values of the system's parameters

Parameters	Description	Values	Units
r	Radius of the wheels	0.03	m
b	Half of the wheel-to-wheel distance	0.15	m
$l_1 = l_2 = l$	Length of the first and second link	0.222	m
$l_3 + l_4$	Length of the third + fourth link	0.172	m
p_m	Projection of the manipulator on Oxy	0.38	m
\hat{p}_m	Estimated initial value of p_m	0.386	m
Δx_i	Initial position error in x direction	0.01	m
Δy_i	Initial position error in y direction	0	m
Δz_i	Initial position error in z direction	0.01	m
$\Delta \phi_i$	Initial orientation error in horizontal	$\pi/22$	rad
$\Delta \psi_i$	Initial orientation error in vertical	$\pi/22$	rad
k_1	Weight factor of the controller	1.8	
k_2	Weight factor of the controller	2.5	
k_3	Weight factor of the controller	2	

k_4	Weight factor of the controller	1	
k_5	Weight factor of the controller	1.5	
k_6	Weight factor of the controller	57	

In Figs. 5.2 and 5.3, the position tracking errors and orientation tracking errors converge to zero after about 4 seconds. It can be inferred that the proposed algorithm can make the good performance for the system in simulation step. Fig. 5.4 shows the variation of the estimation value \hat{p}_m respect to time. Therein, the estimated value quickly converges after only about 1 sec. It demonstrates the flexibility of the system for suffering the unknown parameter problem. The angular velocities of wheels and links are shown in Figs. 5.5 and 5.6. One can compare the performance of the system with the desired trajectory by paying attention to Fig. 5.7.

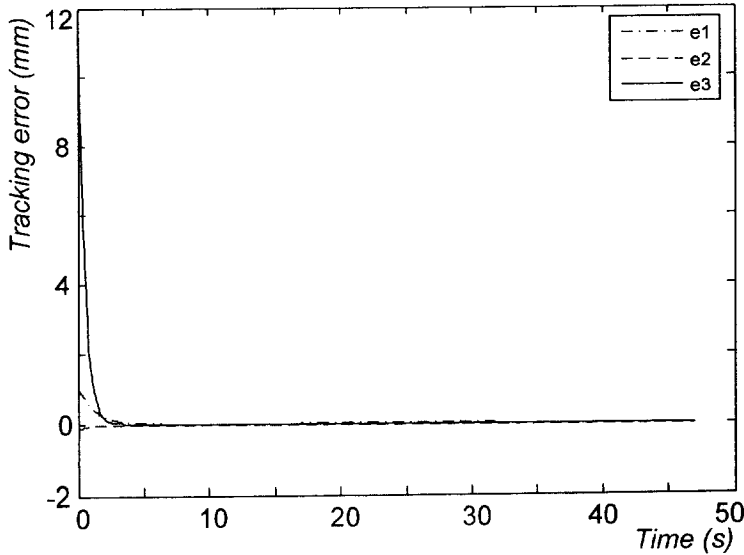


Fig. 5.2 Tracking errors e_1 , e_2 , and e_3

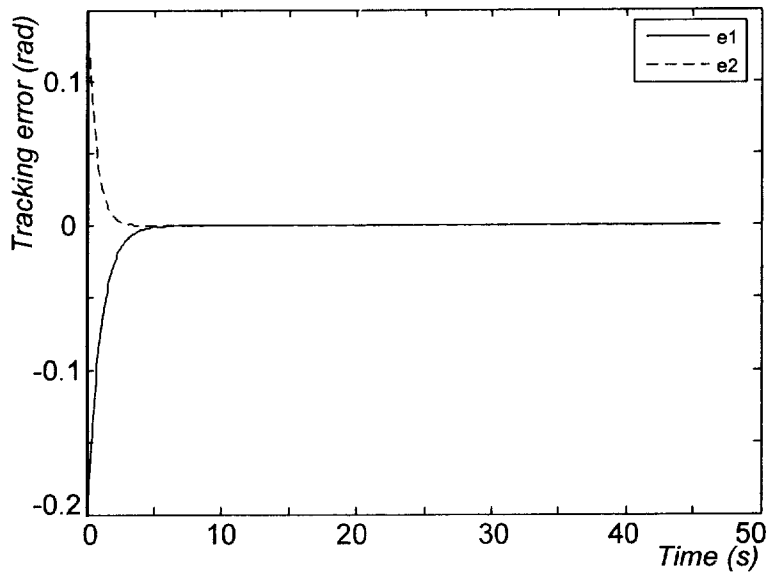


Fig. 5.3 Tracking errors e_4 , and e_5

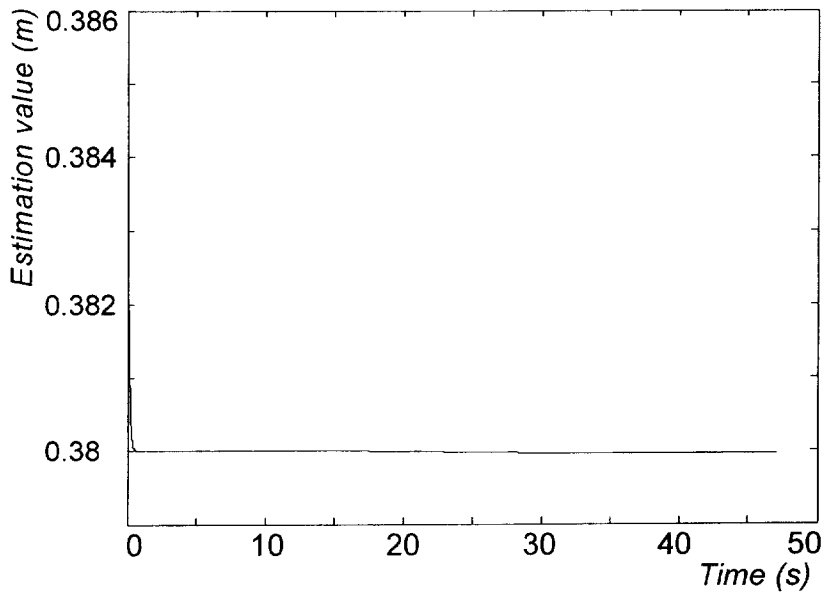


Fig. 5.4 Estimated value p_m

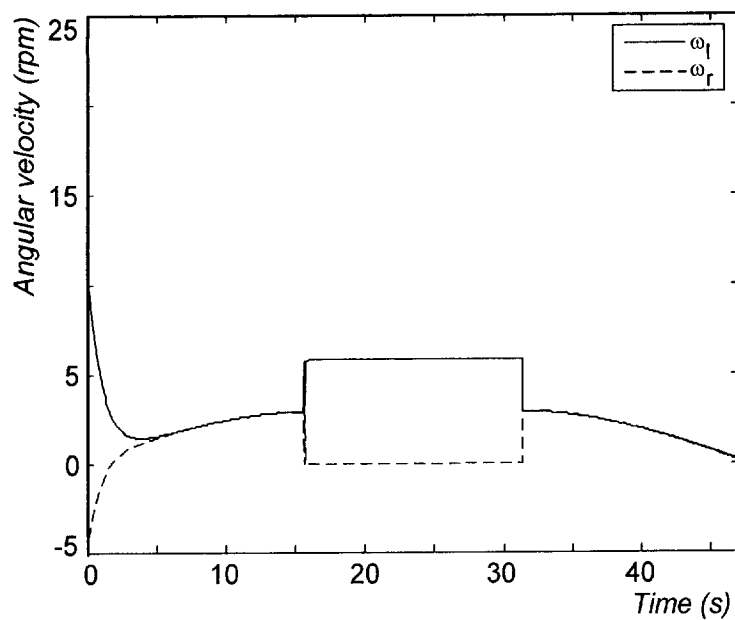


Fig. 5.5 Velocity of the wheels

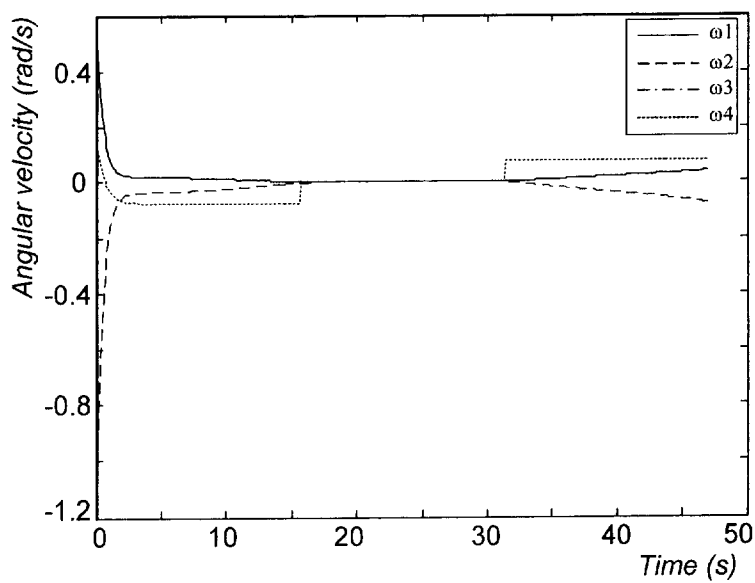


Fig. 5.6 Velocity of the links

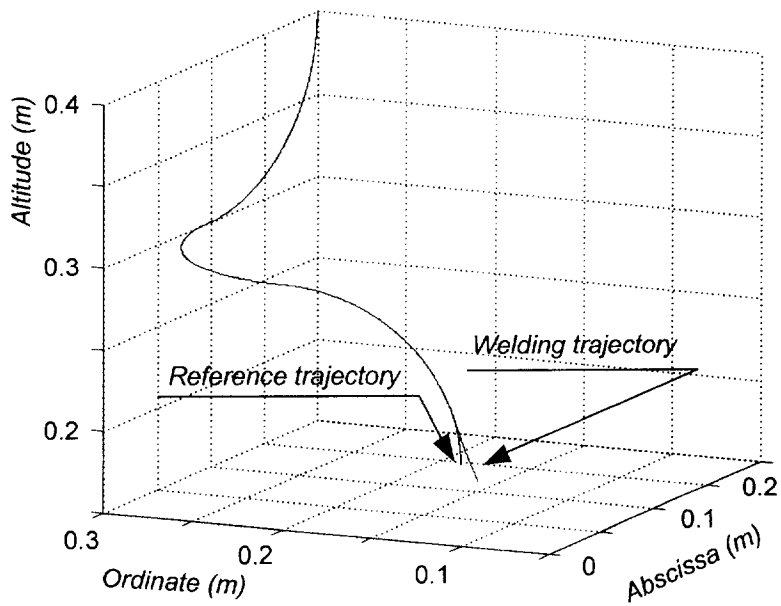


Fig. 5.7 Welding trajectory and reference trajectory

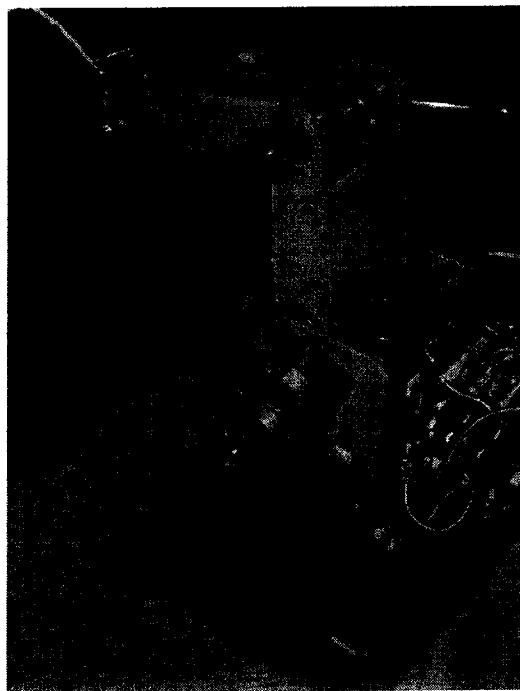


Fig. 5.8 Mobile manipulator in tracking experiment

The mobile manipulator in the tracking experiment is shown in Fig. 5.8. The experiment results are depicted in Figs. 5.9-13. In those Figs., the simulation results are also correspondingly re-supported so it is easy investigating the accuracy of the performance of the system.

The error values in experiment step do not exceed 1mm in position deviation and 1.5 degrees in orientation deviation from the simulation values even if the initial errors are set up at the remarkable values. The experiments also show the validity of the adaptive control law for estimating an unknown parameter, that is to say, the system performance is acceptable even if the controller based on the kinematic model and the parameter uninterruptedly varied throughout the welding process. Form those results, it can be implied about the feasibility of proposed algorithm for applied on a certain 3D welding process with the estimated parameters.

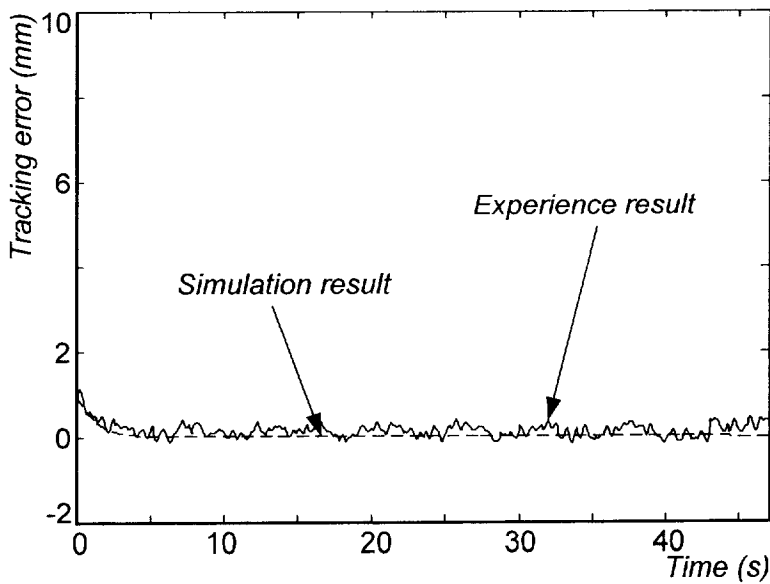


Fig. 5.9 Tracking error e_l

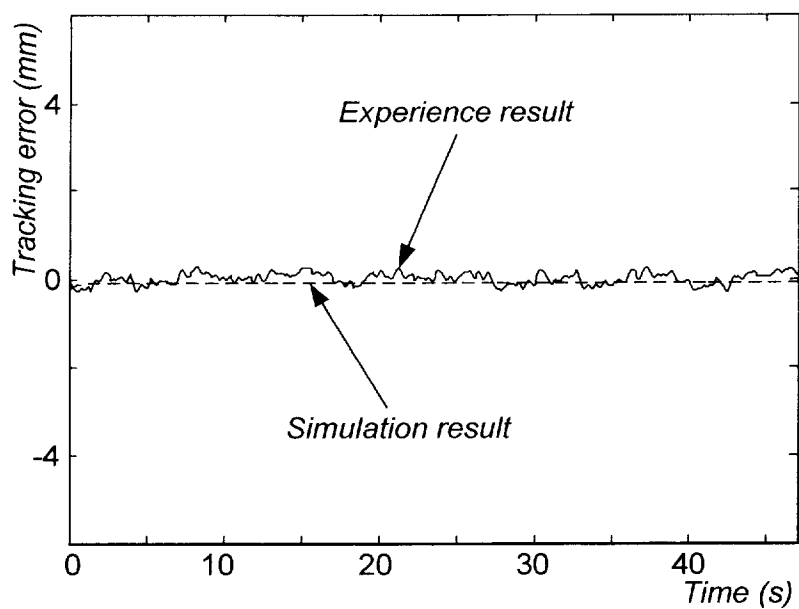


Fig. 5.10 Tracking error e_2

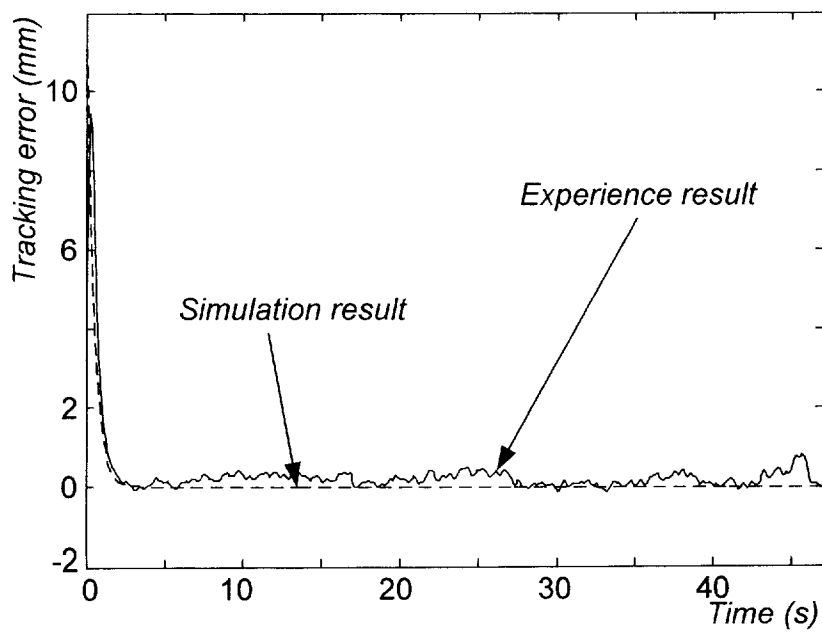


Fig. 5.11 Tracking error e_3

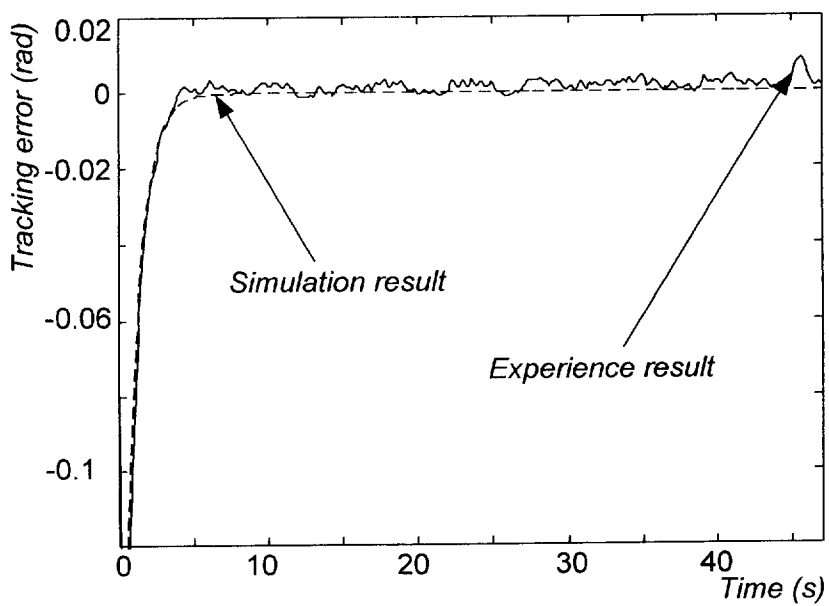


Fig. 5.12 Tracking error e_4

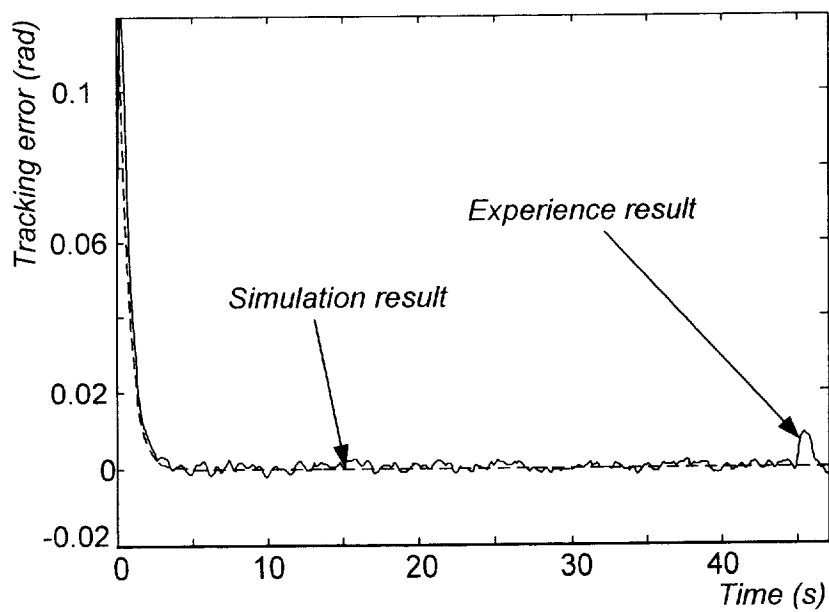


Fig. 5.13 Tracking error e_5

5.4 Chapter Summary

This controller is the update version of the controller in chapter 4. Although the last chapter's controller owned the good ability to be applied to a certain 3D welding process, it also required the perfect knowledge of kinematic characteristics of the mobile manipulator. Overcoming this serious weak point, with the compensating of an unknown parameter adaptive control law, this controller shows its flexibility in operation. Concretely, a common problem occurring in a customary welding process - the welding arc length can not be precisely measured - is solved by the new controller. The simulations and experiments are also performed for verifying the validity of the controller and their results with the acceptable performance of system in the operation prove the feasibility of controller in applying to a mobile manipulator exerting a 3D welding task.

The contribution in this chapter:

- ❖ Demonstrating how to design a nonlinear adaptive controller with concerning the unknown parameter of the system for the mobile manipulator.

Chapter 6

Nonlinear Adaptive Tracking Controller Design of the Mobile Manipulator Based on Kinematics into Dynamics Approach

6.1 Introduction

In this chapter, the dynamic model of the system is investigated. For the easy calculations, a tracking controller design based on a hybrid kinematic/dynamic concept is developed. A rigorous dynamic extension method is proposed for taking into account the specific dynamics of the system to convert a steering system command into control inputs of the actual mobile manipulator. Based on selecting a velocity control for steering system as shown in chapter 4, a controller is designed for converting such a velocity control into a torque control for the actual mobile manipulator, that is to say, converting the kinematic into dynamic concept. Therefore, the dynamic characters of the system such as the mass and inertia moment can be taken into account in this controller. The controller is established in according to the following order:

- First, a kinematic feedback controller is designed for steering system to make the position error asymptotically stable.
- Second, a second step controller is contributed to the system: the feedback velocity following controller. It is designed to make the actual velocity of the

mobile manipulator converge asymptotically to the given velocity inputs.

- Third, the signals of the second controller are used by a computed-torque feedback controller to compute the required torques for the actuators of the actual mobile manipulator.

6.2 Adaptive Tracking Controller Design Based on Kinematics into Dynamics Approach

As aforementioned, this controller design is developed for converting the dynamic control problem into the kinematic control problem. This method is aimed for the purpose to make easy the complication of a control algorithm using the dynamic model and in addition the dynamic characters of the system are still involved. The controller is constructed by three steps: first, finding a velocity control input $\mathbf{v}_c = f_c(e, \mathbf{v}_r, k, t)$ so that $\lim_{t \rightarrow \infty} (q_r - q) = 0$, second, establishing an auxiliary feedback control law $\mathbf{u} = \dot{\mathbf{v}}_c + \mathbf{K}(\mathbf{v}_c - \mathbf{v})$ so that $\mathbf{v} \rightarrow \mathbf{v}_c$ as $t \rightarrow \infty$, and third, computing the applied torques using the dynamic modeling as shown in section 2.3.

Vector $[e_1 \ e_2 \ e_3 \ e_4 \ e_5]^T$ is denoted as the vector of the tracking error that is the difference between the welding position $W(x_w, y_w, z_w, \phi_w, \psi_w)$ and the reference position $R(x_r, y_r, z_r, \phi_r, \psi_r)$ (see sub-section 2.2.5 for more detail). This vector is expressed as:

$$\begin{bmatrix} e_1 \\ e_2 \\ e_3 \\ e_4 \\ e_5 \end{bmatrix} = \begin{bmatrix} \cos \phi_w & \sin \phi_w & 0 & 0 & 0 \\ -\sin \phi_w & \cos \phi_w & 0 & 0 & 0 \\ 0 & 0 & 1 & 0 & 0 \\ 0 & 0 & 0 & 1 & 0 \\ 0 & 0 & 0 & 0 & 1 \end{bmatrix} \begin{bmatrix} x_r - x_w \\ y_r - y_w \\ z_r - z_w \\ \phi_r - \phi_w \\ \psi_r - \psi_w \end{bmatrix} \quad (6.1)$$

where ϕ_r is the reference heading angle of the platform; ϕ_w is the welding heading angle of the platform; ψ_r is the reference heading angle of the torch; and ψ_w is the welding heading angle of the torch. The subscript r and w imply reference and welding, respectively.

Tracking control is concerned as the objective of this design. Thereby, a control rule should be found out so that $\lim_{t \rightarrow \infty} e_i = 0$, that is to say, the actual point W and desired point R coincide.

The derivative of the tracking errors is expressed as:

$$\begin{bmatrix} \dot{e}_1 \\ \dot{e}_2 \\ \dot{e}_3 \\ \dot{e}_4 \\ \dot{e}_5 \end{bmatrix} = \begin{bmatrix} v_r \cos \psi_r \cos e_4 \\ v_r \cos \psi_r \sin e_4 \\ v_r \sin \psi_r \\ \omega_{\phi r} \\ \omega_{\psi r} \end{bmatrix} + \begin{bmatrix} -I & e_2 + p_m & 0 & 0 \\ 0 & -e_1 & 0 & 0 \\ 0 & 0 & -I & 0 \\ 0 & -I & 0 & 0 \\ 0 & 0 & 0 & -I \end{bmatrix} \begin{bmatrix} v_{xy} \\ \omega_{\phi} \\ v_z \\ \omega_{\psi} \end{bmatrix} \quad (6.2)$$

where v_r is the reference velocity in the welding trajectory, it is bounded and large than zero; v_{xy} is the x-y component velocity of v_r ; v_z is the z component velocity of v_r ; $\omega_{\phi r}$ and $\omega_{\psi r}$ are reference angular velocity in horizontal plane and vertical, respectively; and p_m is the projection of the manipulator on x-y plane.

The candidate Lyapunov function is chosen as follows, with the note: it should be a positive definite function:

$$V = \frac{1}{2} e_1^2 + \frac{1}{2} e_2^2 + \frac{1}{2} e_3^2 + \frac{1 - \cos e_4}{k_2} + \frac{1}{2} e_5^2 \quad (6.3)$$

Easily, the derivative form of the chosen Lyapunov function can be established as the following:

$$\begin{aligned}
\dot{V} &= e_1 \dot{e}_1 + e_2 \dot{e}_2 + e_3 \dot{e}_3 + \frac{\sin e_4}{k_2} \dot{e}_4 + e_5 \dot{e}_5 \\
&= e_1 (v_r \cos \psi_r \cos e_4 - v_{xy} + e_2 \omega_\phi + p_m \omega_\phi) + \\
&\quad e_2 (v_r \cos \psi_r \sin e_4 - e_1 \omega_\phi) + e_3 (v_r \sin \psi_r - v_z) + \\
&\quad \frac{\sin e_4}{k_2} (\omega_{\phi r} - \omega_\phi) + e_5 (\omega_{\psi r} - \omega_\psi) \\
&= e_1 (v_r \cos \psi_r \cos e_4 - v_{xy} + p_m \omega_\phi) + e_2 v_r \cos \psi_r \sin e_4 + \\
&\quad e_3 (v_r \sin \psi_r - v_z) + \frac{\sin e_4}{k_2} (\omega_{\phi r} - \omega_\phi) + e_5 (\omega_{\psi r} - \omega_\psi)
\end{aligned} \tag{6.4}$$

The velocity control input (or auxiliary velocity) for steering system to perform the tracking problem is chosen as the following:

$$\mathbf{v}_c = \begin{bmatrix} v_{xy} \\ v_z \\ \omega_\phi \\ \omega_\psi \end{bmatrix} = \begin{bmatrix} p_m \omega_\phi + v_r \cos \psi_r \cos e_4 + k_1 e_1 \\ v_r \sin \psi_r + k_3 e_3 \\ \omega_{\phi r} + k_2 e_2 v_r \cos \psi_r + k_4 \sin e_4 \\ \omega_{\psi r} + k_5 e_5 \end{bmatrix} \tag{6.5}$$

where k_1, k_2, k_3, k_4, k_5 are the positive values.

Using above velocity control input, Eq. (6.4) can be re-written as:

$$\dot{V} = -k_1 e_1^2 - k_3 e_3^2 - \frac{k_4}{k_2} \sin^2 e_4 - k_5 e_5^2 \leq 0 \tag{6.6}$$

The derivative form of \mathbf{v}_c is written as below:

$$\dot{\mathbf{v}}_c = \begin{bmatrix} \dot{p}_m \omega_\phi + p_m \dot{\omega}_\phi + \cos \psi_r (\dot{v}_r \cos e_4 - v_r \dot{e}_4 \sin e_4) + k_1 \dot{e}_1 \\ \dot{v}_r \sin \psi_r + k_3 \dot{e}_3 \\ \dot{\omega}_{\phi r} + k_2 \cos \psi_r (\dot{e}_2 v_r + e_2 \dot{v}_r) + k_4 \dot{e}_4 \cos e_4 \\ \dot{\omega}_{\psi r} + k_5 \dot{e}_5 \end{bmatrix} \tag{6.7}$$

The auxiliary velocity errors $\mathbf{e}_c = [e_6 \quad e_7 \quad e_8 \quad e_9]^T$ are expressed as below:

$$\mathbf{e}_c = \mathbf{v} - \mathbf{v}_c = \begin{bmatrix} v_1 - v_{xy} \\ v_2 - v_z \\ v_3 - \omega_\phi \\ v_4 - \omega_\psi \end{bmatrix} \quad (6.8)$$

The objective of second controller is to find out an adaptive control rule to obtain $\mathbf{e}_c \rightarrow 0$ as $t \rightarrow \infty$, so that the auxiliary velocity become coincide with designed velocity. Easily, the derivative form of this error is obtained as following:

$$\dot{\mathbf{e}}_c = \dot{\mathbf{v}} - \dot{\mathbf{v}}_c = \mathbf{u} - \dot{\mathbf{v}}_c \quad (6.9)$$

The following new candidate Lyapunov function is chosen (it is also a positive definite function):

$$V_n = \frac{1}{2}e_1^2 + \frac{1}{2}e_2^2 + \frac{1}{2}e_3^2 + \frac{1 - \cos e_4}{k_2} + \frac{1}{2}e_5^2 + \frac{1}{2}e_6^2 + \frac{1}{2}e_7^2 + \frac{1}{2}e_8^2 + \frac{1}{2}e_9^2 \quad (6.10)$$

$$\begin{aligned} \dot{V}_n &= e_1\dot{e}_1 + e_2\dot{e}_2 + e_3\dot{e}_3 + \frac{\sin e_4}{k_2}\dot{e}_4 + e_5\dot{e}_5 + e_6\dot{e}_6 + e_7\dot{e}_7 + e_8\dot{e}_8 + e_9\dot{e}_9 \\ &= \dot{V} + e_6\dot{e}_6 + e_7\dot{e}_7 + e_8\dot{e}_8 + e_9\dot{e}_9 \end{aligned} \quad (6.11)$$

In order that the system gets stable, \dot{V}_n should satisfy negative value, in other words, the condition for the stability of system can be expressed as

$$\mathbf{e}_c^T \dot{\mathbf{e}}_c \leq 0 \quad (6.12)$$

From Eq. (6.9), one can write

$$\mathbf{e}_c^T \dot{\mathbf{e}}_c = \mathbf{e}_c^T (\mathbf{u} - \dot{\mathbf{v}}_c) \quad (6.13)$$

Herein, a nonlinear feedback acceleration control input (second controller) is chosen as the following:

$$\mathbf{u} = \dot{\mathbf{v}}_c - \mathbf{K} \mathbf{e}_c \quad (6.14)$$

where $\mathbf{K} = \begin{bmatrix} k_6 & 0 & 0 & 0 \\ 0 & k_7 & 0 & 0 \\ 0 & 0 & k_8 & 0 \\ 0 & 0 & 0 & k_9 \end{bmatrix}$ is a positive definite matrix.

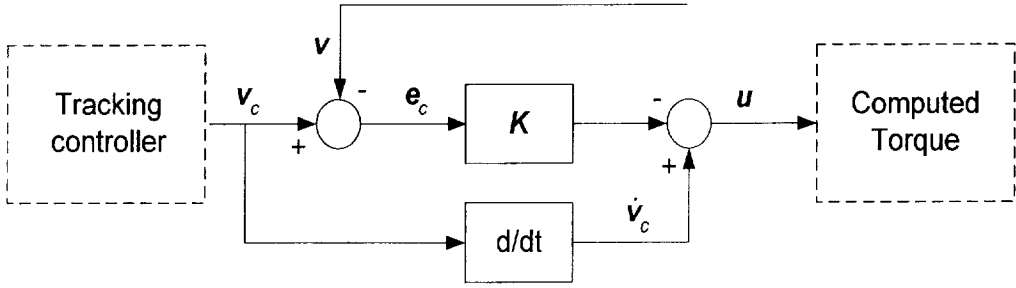


Fig. 6.1 Block diagram of the second controller - feedback acceleration controller

For proving that $\lim_{t \rightarrow \infty} [e_1 \ e_2 \ e_3 \ e_4 \ e_5]^T = 0$, herein the Barbalat's lemma is used as following. As for first condition of the lemma, because $\dot{V}_n \leq 0$, so error vector \mathbf{e} is bounded. Furthermore, referring Eq. (6.10), when \mathbf{e} is bounded, V_n has a finite limit as $t \rightarrow \infty$. As for second condition of the lemma, the value of the derivative of \dot{V}_n is calculated as below:

$$\begin{aligned} \frac{d\dot{V}_n}{dt} = & -2k_1 e_1 \dot{e}_1 - 2k_3 e_3 \dot{e}_3 - \frac{2k_4}{k_2} \dot{e}_4 \sin e_4 \cos e_4 - 2k_5 e_5 \dot{e}_5 - 2k_6 e_6 \dot{e}_6 - \\ & 2k_7 e_7 \dot{e}_7 - 2k_8 e_8 \dot{e}_8 - 2k_9 e_9 \dot{e}_9 \end{aligned} \quad (6.15)$$

Obviously, because \dot{e}_i are bounded, the derivative of \dot{V}_n is bounded too. Therefore \dot{V}_n satisfies the sufficient condition of a uniformly continuous function. According to two above-mentioned conditions, by Barbalat's lemma, the result is obtained as $\lim_{t \rightarrow \infty} \dot{V}_n = 0$.

Now, Eq. (6.11) can be re-written as follows:

$$0 = -k_1 e_1^2 - k_3 e_3^2 - \frac{k_4}{k_2} \sin^2 e_4 - k_5 e_5^2 - k_6 e_6^2 - k_7 e_7^2 - k_8 e_8^2 - k_9 e_9^2 \quad (6.16)$$

Eq. (6.16) implies that $\lim_{t \rightarrow 0} [e_1 \ e_3 \ e_4 \ e_5]^T = 0$. As a result of $e_4 = 0$, the welding heading angle and reference heading angle of mobile platform coincide, that is to say, $\omega_\phi = \omega_{\phi_r}$. Referring Eq. (6.5), in the third row, when two previous conditions occur, the result is $\lim_{t \rightarrow \infty} e_2 = 0$.

After everything mentioned above, a conclusion can be inferred: the equilibrium point $e_i = 0$ is uniformly asymptotically stable.

Base on the dynamic relationship in sections 2.3.1 and 2.3.2, the control input of the system can be calculated by the following equations:

$$\boldsymbol{\tau} = \overline{\mathbf{M}}\dot{\mathbf{v}} + \overline{\mathbf{C}}\mathbf{v} + \overline{\boldsymbol{\tau}}_d \quad (6.17)$$

where $\boldsymbol{\tau} = [\boldsymbol{\tau}_v \ \boldsymbol{\tau}_r]^T$ is the vector of applied torques on mobile platform's and manipulator's actuators, $\overline{\mathbf{M}} = \begin{bmatrix} \overline{\mathbf{M}}_{11} & 0 \\ 0 & \overline{\mathbf{M}}_{22} \end{bmatrix}$, $\dot{\mathbf{v}} = \mathbf{u}$ - the control law of the second controller, $\overline{\mathbf{C}} = \begin{bmatrix} \overline{\mathbf{C}}_{11} & 0 \\ 0 & \overline{\mathbf{C}}_{22} \end{bmatrix}$, $\mathbf{v} = [\mathbf{v}_v \ \mathbf{v}_r]^T$ is the actual velocity vector fed back from the plant of system, $\overline{\boldsymbol{\tau}}_d = [\overline{\boldsymbol{\tau}}_{d1} \ \overline{\boldsymbol{\tau}}_{d2}]^T$.

The block diagram of algorithm is shown as the following

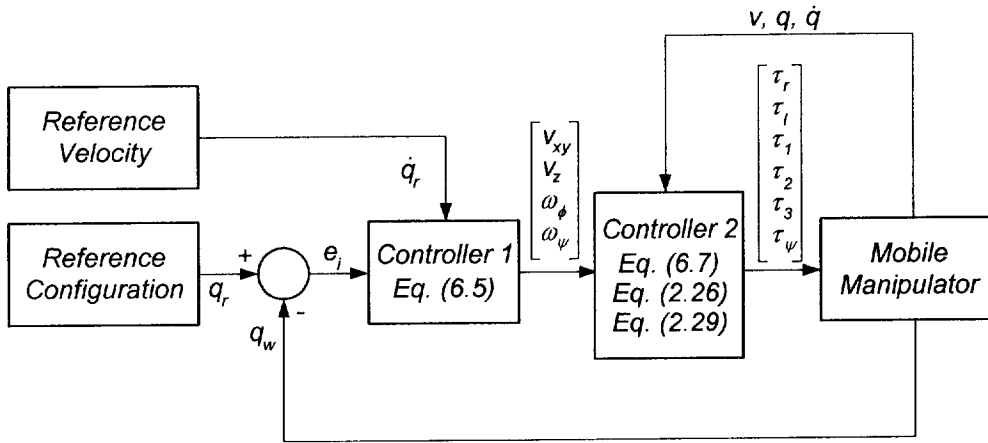


Fig. 6.2 Block diagram of the adaptive tracking control system for mobile manipulator based on kinematics into dynamics approach

6.3 Simulation and Experiment Results

Like the previous chapters, the reference trajectory as shown in Fig. 4.2 is chosen for simulation step. The initial errors for the end effector of the mobile manipulator are in the same case. Four more weight factors are supplemented for the second controller, they were chosen for the best convergence of the velocity tracking errors. The values of the system's characteristic parameter used in the simulation are given in Table 6.1.

Table 6.1 Numerical values of the system's parameters

Parameters	Description	Values	Units
r	Radius of the wheels	0.03	m
b	Half of the wheel-to-wheel distance	0.15	m
$l_1 = l_2 = l$	Length of the first and second link	0.222	m
$l_3 + l_4$	Length of the third + fourth link	0.172	m

Table 6.1 Numerical values of the system's parameters

Parameters	Description	Values	Units
r	Radius of the wheels	0.03	m
b	Half of the wheel-to-wheel distance	0.15	m
$l_1 = l_2 = l$	Length of the first and second link	0.222	m
$l_3 + l_4$	Length of the third + fourth link	0.172	m
p_m	Projection of the manipulator on Oxy	0.38	m
Δx_i	Initial position error in x direction	0.01	m
Δy_i	Initial position error in y direction	0	m
Δz_i	Initial position error in z direction	0.01	m
$\Delta \phi_i$	Initial orientation error in horizontal	$\pi/22$	rad
$\Delta \psi_i$	Initial orientation error in vertical	$\pi/22$	rad
k_1	Weight factor of the controller	1.3	
k_2	Weight factor of the controller	1.4	
k_3	Weight factor of the controller	1	
k_4	Weight factor of the controller	1.2	
k_5	Weight factor of the controller	2.5	
k_6	Weight factor of the controller	1.5	
k_7	Weight factor of the controller	1.2	
k_8	Weight factor of the controller	2.5	
k_9	Weight factor of the controller	1.5	
m_c	Mass of the platform's body	4	Kg
m_w	Mass of the wheels	0.5	Kg

I_c	Inertia moment of the platform's body	0.31	Kgm ²
I_w	Inertia moment of the wheels	4.5×10^{-4}	Kgm ²
m_1	Mass of the first link	2	Kg
m_2	Mass of the second link	1.5	Kg
$m_{(3+4)}$	Mass of the set (third + fourth links)	0.8	Kg
I_1	Inertia moment of the first link	0.31	Kgm ²
I_2	Inertia moment of the second link	0.27	Kgm ²
I_{3+4}	Inertia moment of the set (3+4)	0.22	Kgm ²
$I_{4+torch}$	Inertia moment of fourth link + torch	0.013	Kgm ²

In Fig. 6.3, all position tracking errors converge to zero after about seven seconds. The orientation tracking errors more quickly converge to zero in nearly four seconds (Fig. 6.4). Especially, in the case of the error e_5 , it even takes only about two seconds for e_5 goes to zero. In Figs. 6.5 and 6.6, the velocity tracking errors are in the same case: less than three seconds, they converge to zero. However, the angular velocity tracking errors show a little sudden unstable in very short time at the junction points between two adjacent circular sectors. At those places, the angular velocities of the orientation motion change their state: from still to motion or vice versa. But in general, the stability of the system is still guaranteed by the controllers. Figs 6.7 and 6.8 show the output angular velocities of the mobile platform's wheels and the manipulator's links, respectively. In the last Fig. of the simulation step, Fig. 6.9, the orbit of welding torch tip is depicted with the desired orbit. They reveal the ability of this algorithm in making the good performance to the system. The simulation results prove the validity of the

proposed algorithm. The mobile manipulator and the experimental environment are shown in Fig. 6.10.

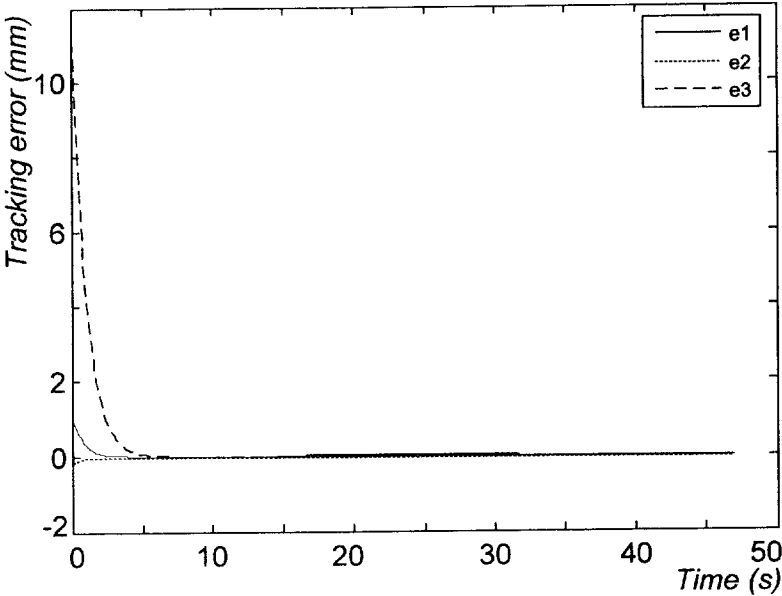


Fig. 6.3 Tracking errors e_1 , e_2 and e_3

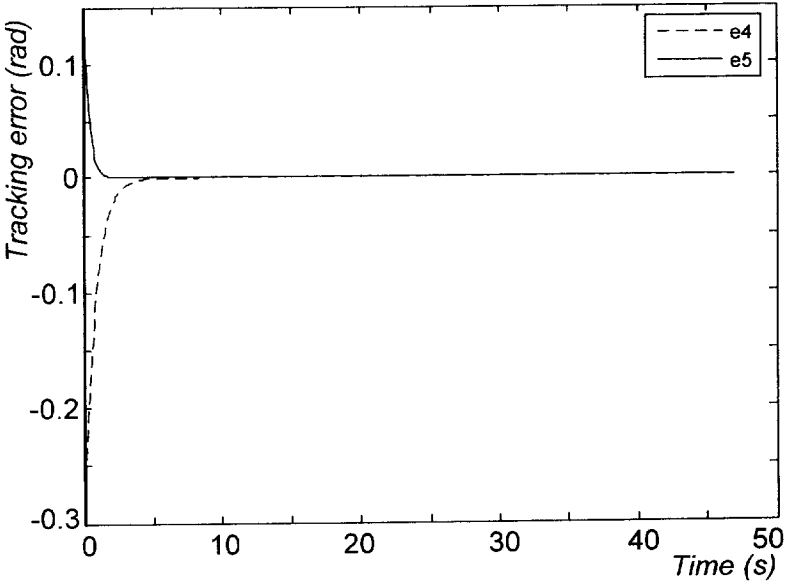


Fig. 6.4 Tracking errors e_4 and e_5

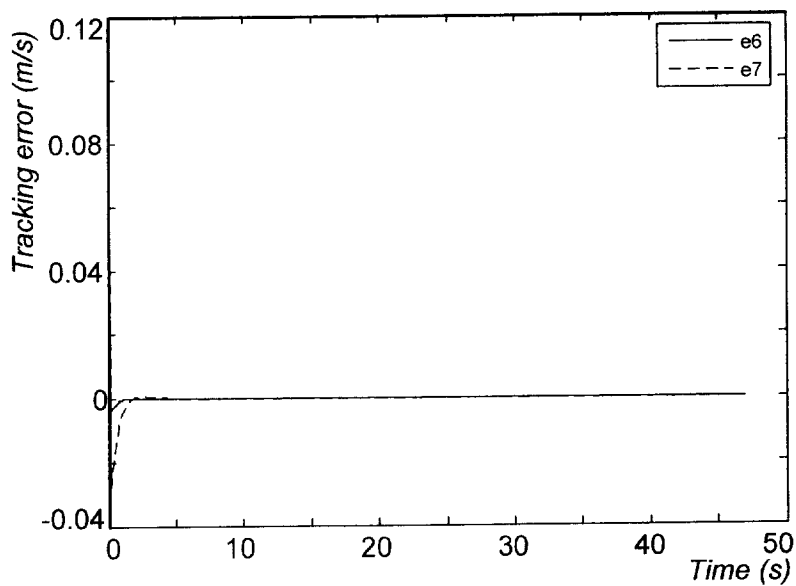


Fig. 6.5 Tracking errors e_6 and e_7

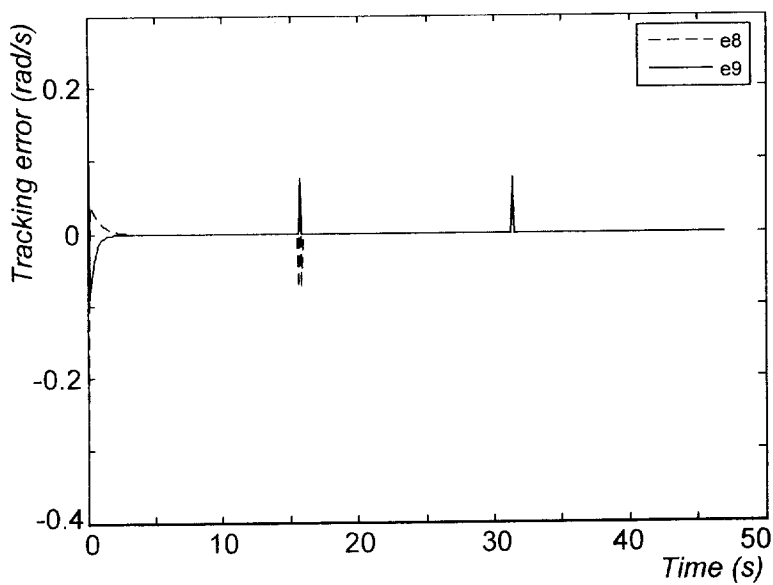


Fig. 6.6 Tracking errors e_8 and e_9

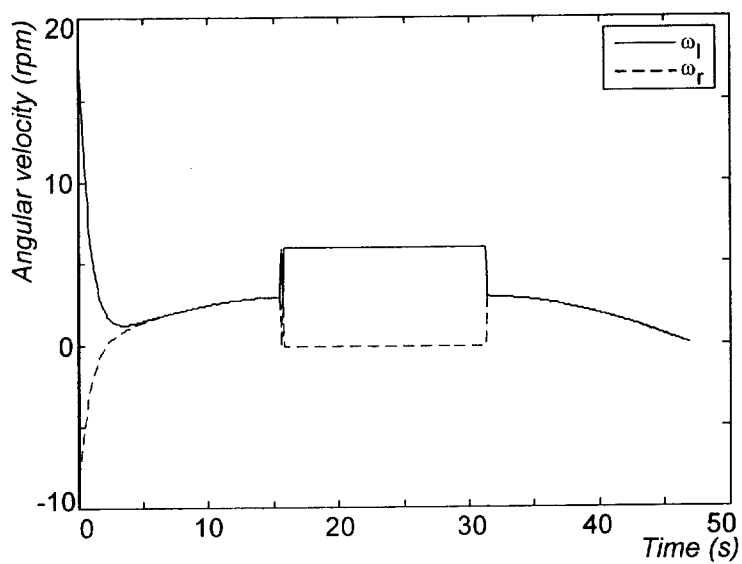


Fig. 6.7 Angular velocity of the wheels

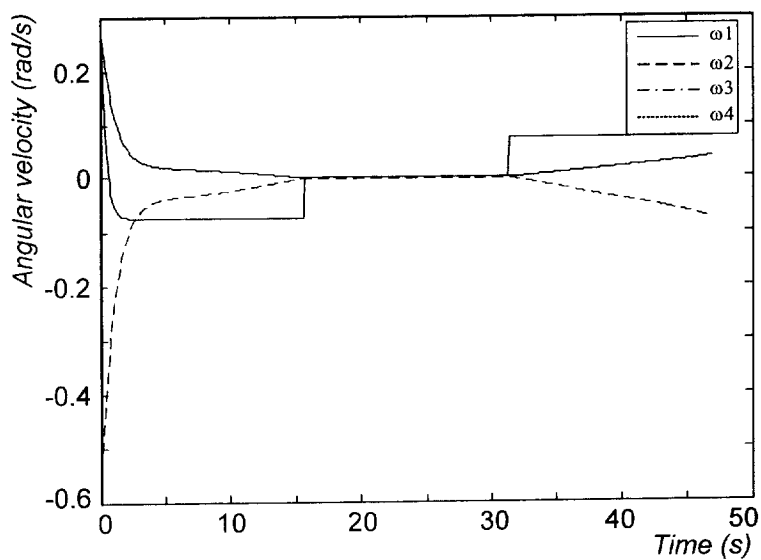


Fig. 6.8 Angular velocity of the links

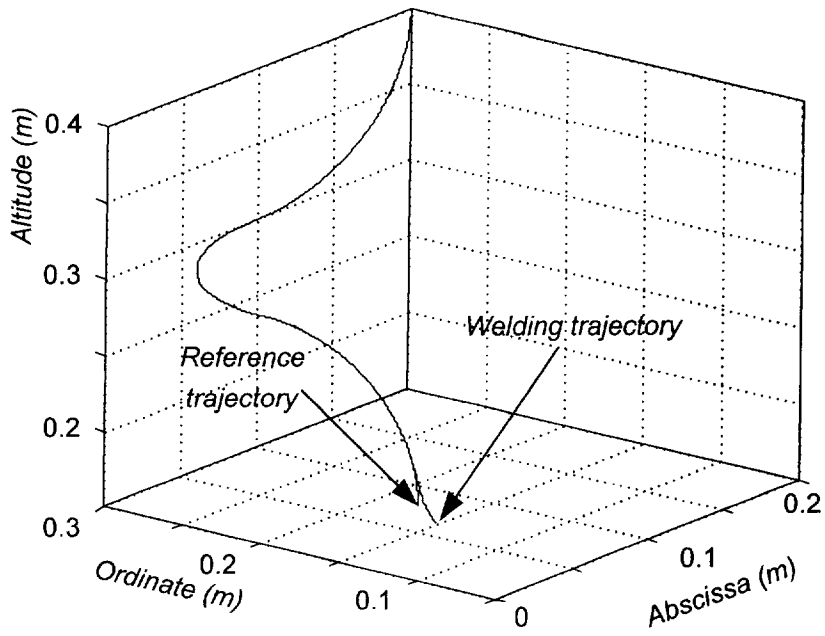


Fig. 6.9 The reference trajectory and the welding trajectory

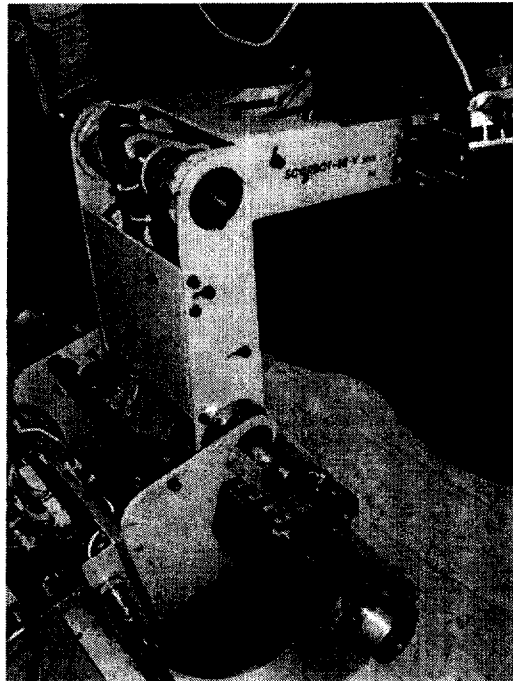


Fig. 6.10 Mobile manipulator in tracking experiment

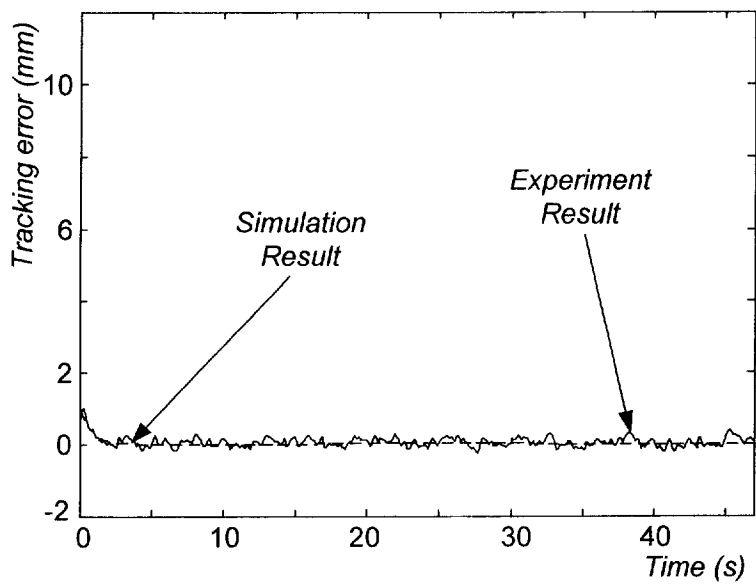


Fig. 6.11 Tracking errors e_1

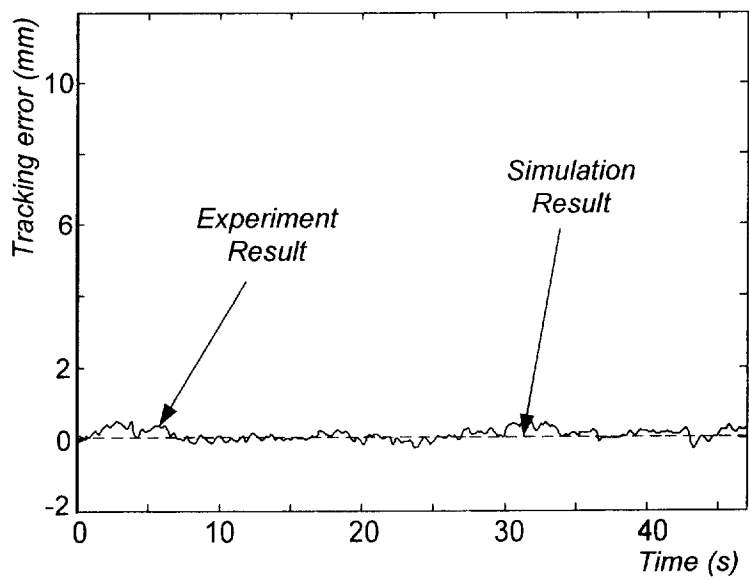


Fig. 6.12 Tracking errors e_2

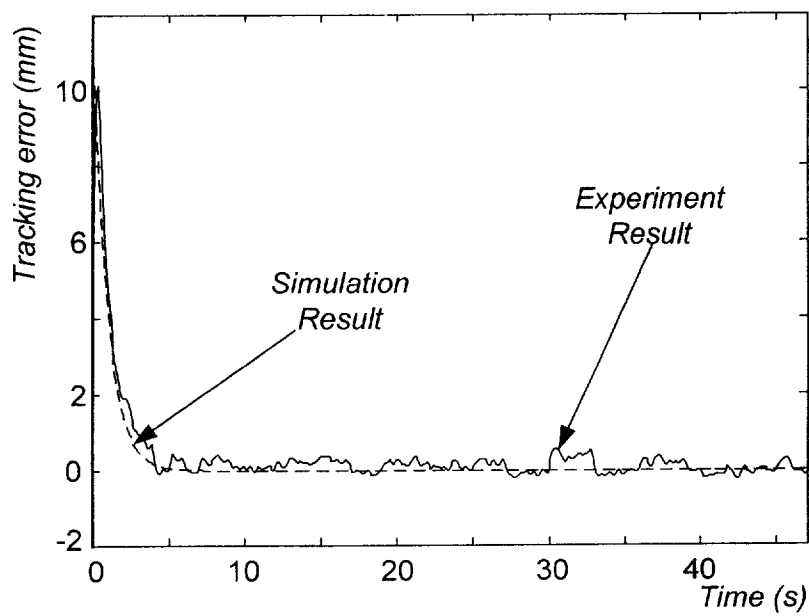


Fig. 6.13 Tracking errors e_3

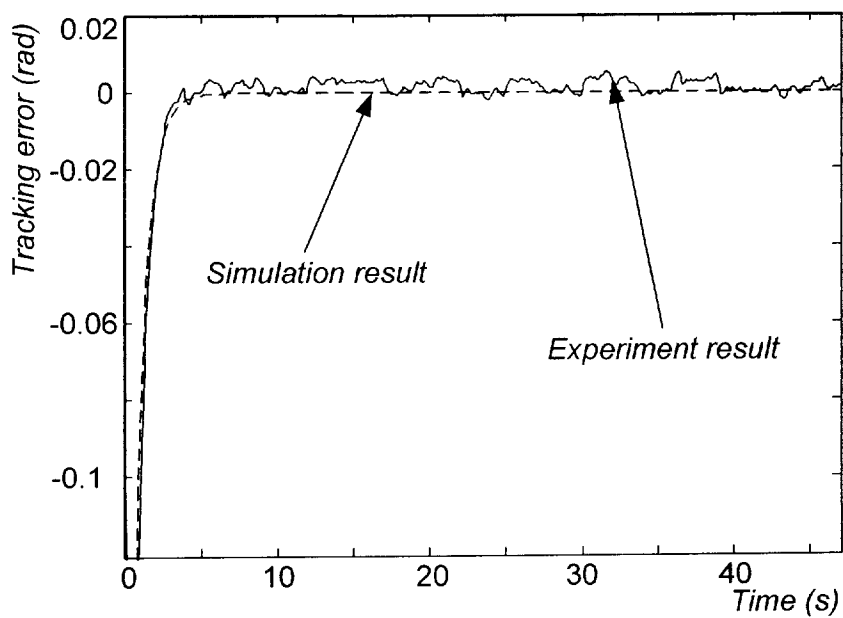


Fig. 6.14 Tracking errors e_4

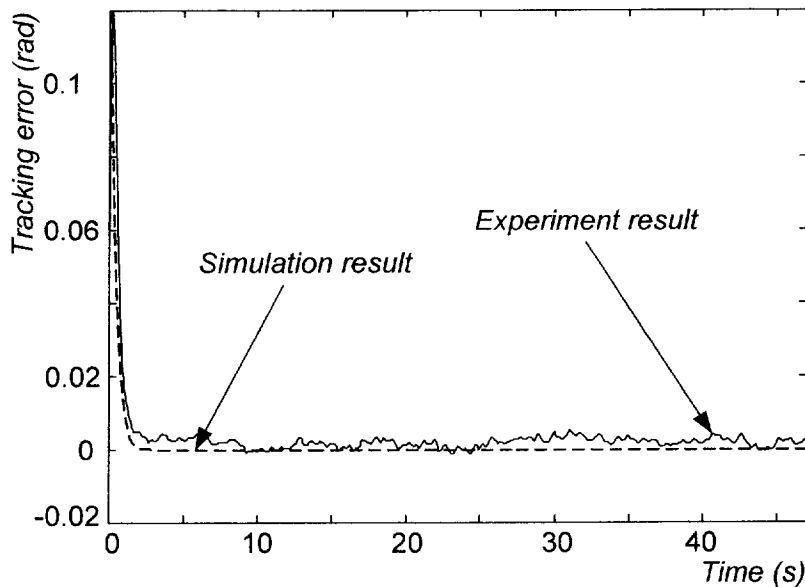


Fig. 6.15 Tracking errors e_5

The experiment results - the tracking errors - are developed in Figs. 6.11-15. In those Figs., the performance of the system also achieves a high accuracy. The tracking errors are even about 1mm in position deviation and 0.01rad in orientation deviation. These values can be perfectly accepted in an actual welding process.

6.4 Chapter Summary

This control algorithm is based on the concept of kinematic into dynamic method so it makes easy the computation in applying. In this chapter, the controller design is contributed by two steps, first, to making the control law to choose the velocity control for the steering system, and second, to construct another controller for computing the applied torques. Because the first step controller is the same controller that is used in chapter four so the whole controller of this chapter can be counted as an enhanced version of the chapter four's

controller. The dynamic characteristics of the system are concerned by the supplemented controller - the second step controller. Thus, this controller really gets the dynamic behavior for the mobile manipulator. By means of referring to the simulation and experiment results, one can realize that the controller can be exerted to a 3D welding task.

The contribution in this chapter:

- ❖ Introducing the dynamic behavior to the system.
- ❖ Easing the sophisticated dynamic calculations by the simple kinematic calculations.

Chapter 7

Tracking Controller Design of the Mobile Manipulator Using Sliding Mode Technique

7.1 Introduction

In chapter 6, the computed-torque control is used to calculate the input torques for the actuators. Therein, all system parameters are assumed to be the known parameters. In practice, not every parameters of the system model can be exactly defined. Therefore, a nonlinear system as the mobile manipulator will be suffering the strong effects by the modeling inaccuracies. Furthermore, the system is also impacted by the external disturbances. For overcoming these problems, a simple approach to robust control, so-called sliding mode control technique, with the bound estimation is exerted in this chapter. By using sliding mode robust control, the high order of the mobile manipulator can be reduced to a first order system. The problem of maintaining stability and consistent performance in the face of modeling imprecision is solved by this technique. However, due to the imperfections in the practice switching of control law, the performance of the system is deteriorated by a phenomenon so-called the chattering. In this chapter, for eliminating this phenomenon, a saturation function is also applied. The simulations of proposed controller are performed for assuring the validity of this algorithm. The elimination of chattering phenomenon in the sliding surfaces is

also illustrated by the figures. The experiments are also carefully performed to affirm the feasibility of this method for the mobile manipulator in a 3D welding process.

7.2 Tracking Controller Design Using Sliding Mode Technique

As mentioned the sub-section 2.2.5, the tracking errors of the system can be expressed as the following:

$$\begin{bmatrix} e_1 \\ e_2 \\ e_3 \\ e_4 \\ e_5 \end{bmatrix} = \begin{bmatrix} \cos \phi_w & \sin \phi_w & 0 & 0 & 0 \\ -\sin \phi_w & \cos \phi_w & 0 & 0 & 0 \\ 0 & 0 & 1 & 0 & 0 \\ 0 & 0 & 0 & 1 & 0 \\ 0 & 0 & 0 & 0 & 1 \end{bmatrix} \begin{bmatrix} x_r - x_w \\ y_r - y_w \\ z_r - z_w \\ \phi_r - \phi_w \\ \psi_r - \psi_w \end{bmatrix} \quad (7.1)$$

The control objective is to find out a robust control law for the mobile manipulator to track a 3D reference trajectory with considering the external bounded disturbances, in other words, obtain $e_i \rightarrow 0$ as $t \rightarrow \infty$ for the welding point W to become to coincide with its reference point R in the case of the occurring of the disturbance on the system.

The derivative form of Eq. (7.1) is expressed as:

$$\begin{bmatrix} \dot{e}_1 \\ \dot{e}_2 \\ \dot{e}_3 \\ \dot{e}_4 \\ \dot{e}_5 \end{bmatrix} = \begin{bmatrix} v_r \cos \psi_r \cos e_4 \\ v_r \cos \psi_r \sin e_4 \\ v_r \sin \psi_r \\ \omega_{\phi r} \\ \omega_{\psi r} \end{bmatrix} + \begin{bmatrix} -1 & e_2 + p_m & 0 & 0 \\ 0 & -e_1 & 0 & 0 \\ 0 & 0 & -1 & 0 \\ 0 & -1 & 0 & 0 \\ 0 & 0 & 0 & -1 \end{bmatrix} \begin{bmatrix} v_{xy} \\ \omega_{\phi} \\ v_z \\ \omega_{\psi} \end{bmatrix} \quad (7.2)$$

where v_r is the reference velocity in the welding trajectory, it is assumed to be bounded; v_{xy} is the x-y component velocity of v ; v_z is the z component velocity of v ; ω_ϕ, ω_ψ are the derivative form of the angle ϕ, ψ that are the heading angle of the mobile platform and the welding torch, respectively, they are assumed the bounded values; and p_m is the distance between the projection of the manipulator on x-y plane and the center of the mobile platform.

Continuously, the second derivative of the error vector (7.1) is calculated as the following:

$$\begin{bmatrix} \ddot{e}_1 \\ \ddot{e}_2 \\ \ddot{e}_3 \\ \ddot{e}_4 \\ \ddot{e}_5 \end{bmatrix} = \begin{bmatrix} -\dot{e}_4 v_r \cos \psi_r \sin e_4 + \dot{e}_2 \omega_\phi - \dot{v}_{xy} + (e_2 + p_m) \dot{\omega}_\phi \\ \dot{e}_4 v_r \cos \psi_r \cos e_4 - \dot{e}_1 \omega_\phi - e_1 \dot{\omega}_\phi \\ -\dot{v}_z \\ \dot{\omega}_{\phi r} - \dot{\omega}_\phi \\ \dot{\omega}_{\psi r} - \dot{\omega}_\psi \end{bmatrix} \quad (7.3)$$

Herein, for guaranteeing the stability of the system, a vector of the time varying sliding surface is defined as the following:

$$\mathbf{S} = \begin{bmatrix} S_1 \\ S_2 \\ S_3 \\ S_4 \end{bmatrix} = \begin{bmatrix} \dot{e}_1 + k_1 e_1 + |e_2| \text{sgn}(e_1) \\ \dot{e}_4 + k_4 e_4 \\ \dot{e}_3 + k_3 e_3 \\ \dot{e}_5 + k_5 e_5 \end{bmatrix} \quad (7.4)$$

where k_1, k_3, k_4, k_5 are the positive values.

From (2.26) and (2.29), it is assumed that the disturbance vectors can be expressed as the multipliers of the matrices \overline{M}_{11} and \overline{M}_{22} , respectively (it satisfies the uncertainty matching condition with a known boundary).

$$\begin{aligned}\overline{\tau_{d1}} &= \overline{\mathbf{M}_{11}} \mathbf{f}_v, \mathbf{f}_v = \begin{bmatrix} f_{v1} & f_{v2} \end{bmatrix}^T \\ \overline{\tau_{d2}} &= \overline{\mathbf{M}_{22}} \mathbf{f}_r, \mathbf{f}_r = \begin{bmatrix} f_{r1} & f_{r2} \end{bmatrix}^T\end{aligned}\quad (7.5)$$

where $f_{v1}, f_{v2}, f_{r1}, f_{r2}$ are bounded.

The control input is defined by the computed-torque method as the following (Lewis et al [8])

$$\overline{\mathbf{M}}(q)\dot{h}_r + \overline{\mathbf{C}}(q, \dot{q})h + \overline{\mathbf{M}}(q)u = \tau \quad (7.6)$$

where $\mathbf{u} = [u_1 \ u_2 \ u_3 \ u_4]^T$ is the control law which determines the error dynamics. Substituting the above proposed control law into the dynamic equations of system (2.26) and (2.29) yields

$$\dot{h} + f = \dot{h}_r + u \Rightarrow \dot{h} - \dot{h}_r = u - f$$

$$\text{or in this case } \begin{bmatrix} \dot{v}_{xy} - \dot{v}_{xyr} \\ \dot{\omega}_{\phi} - \dot{\omega}_{\phi r} \\ \dot{v}_z - \dot{v}_{zr} \\ \dot{\omega}_{\psi} - \dot{\omega}_{\psi r} \end{bmatrix} = \begin{bmatrix} u_1 \\ u_2 \\ u_3 \\ u_4 \end{bmatrix} - \begin{bmatrix} f_{v1} \\ f_{v2} \\ f_{r1} \\ f_{r2} \end{bmatrix} \quad (7.7)$$

Referring Eq. (7.4), the derivative form of the vector sliding surface S is expressed as the following:

$$\dot{S} = \begin{bmatrix} \ddot{e}_1 \\ \ddot{e}_4 \\ \ddot{e}_3 \\ \ddot{e}_5 \end{bmatrix} + \begin{bmatrix} k_1 \dot{e}_1 + |\dot{e}_2| \text{sgn}(e_1) \\ k_4 \dot{e}_4 \\ k_3 \dot{e}_3 \\ k_5 \dot{e}_5 \end{bmatrix}$$

$$\begin{aligned}
&= - \begin{bmatrix} \dot{v}_{xy} - \dot{v}_{xyr} \\ \dot{\omega}_{\phi} - \dot{\omega}_{\phi r} \\ \dot{v}_z - \dot{v}_{zr} \\ \dot{\omega}_{\psi} - \dot{\omega}_{\psi r} \end{bmatrix} + \begin{bmatrix} (e_2 + p_m)\dot{\omega}_{\phi} + \dot{e}_2\omega_{\phi} \\ -\dot{e}_4v_r \cos\psi_r \sin e_4 \\ 0 \\ 0 \end{bmatrix} + \begin{bmatrix} k_1\dot{e}_1 + |\dot{e}_2|\text{sgn}(e_1) \\ k_4\dot{e}_4 \\ k_3\dot{e}_3 \\ k_5\dot{e}_5 \end{bmatrix} \\
&= - \begin{bmatrix} u_1 \\ u_2 \\ u_3 \\ u_4 \end{bmatrix} + \begin{bmatrix} f_{v1} \\ f_{v2} \\ f_{r1} \\ f_{r2} \end{bmatrix} + \begin{bmatrix} (e_2 + p_m)\dot{\omega}_{\phi} + (v_r \cos\psi_r \sin e_4 \\ -e_1\omega_{\phi})\omega_{\phi} - \dot{e}_4v_r \cos\psi_r \sin e_4 \\ + k_1\dot{e}_1 + |\dot{e}_2|\text{sgn}(e_1) \\ k_4\dot{e}_4 \\ k_3\dot{e}_3 \\ k_5\dot{e}_5 \end{bmatrix} \quad (7.8)
\end{aligned}$$

Herein, a robust control law using sliding mode method can be chosen as the following:

$$\begin{aligned}
\begin{bmatrix} u_1 \\ u_2 \\ u_3 \\ u_4 \end{bmatrix} &= \begin{bmatrix} Q_1 S_1 \\ Q_2 S_2 \\ Q_3 S_3 \\ Q_4 S_4 \end{bmatrix} + \begin{bmatrix} P_1 \text{sgn}(S_1) \\ P_2 \text{sgn}(S_2) \\ P_3 \text{sgn}(S_3) \\ P_4 \text{sgn}(S_4) \end{bmatrix} + \begin{bmatrix} (e_2 + p_m)\dot{\omega}_{\phi} + (v_r \cos\psi_r \sin e_4 - \\ k_4\dot{e}_4 \\ k_3\dot{e}_3 \\ k_5\dot{e}_5 \\ e_1\omega_{\phi})\omega_{\phi} - \dot{e}_4v_r \cos\psi_r \sin e_4 + k_1\dot{e}_1 + |\dot{e}_2|\text{sgn}(e_1) \end{bmatrix} \quad (7.9)
\end{aligned}$$

where Q_i, P_i are constant positive values.

According to that control law, Eq. (7.8) can be re-expressed as:

$$\dot{S} = -QS - P \text{sgn}(S) + f \quad (7.10)$$

A positive definite Lyapunov candidate function is chosen as:

$$V = \frac{1}{2}S_1^2 + \frac{1}{2}S_2^2 + \frac{1}{2}S_3^2 + \frac{1}{2}S_4^2 = \frac{1}{2}\mathbf{S}^T\mathbf{S} \quad (7.11)$$

$$\begin{aligned} \Rightarrow \dot{V} &= S_1\dot{S}_1 + S_2\dot{S}_2 + S_3\dot{S}_3 + S_4\dot{S}_4 = \mathbf{S}^T\dot{\mathbf{S}} \\ &= \mathbf{S}^T(-\mathbf{QS} - \mathbf{P}\operatorname{sgn}(\mathbf{S}) + \mathbf{f}) \\ &= -\mathbf{S}^T\mathbf{QS} - (\mathbf{P}|\mathbf{S}| - \mathbf{fS}) \end{aligned} \quad (7.12)$$

Obviously, when P_i are greater than or equal to the bounded values of f_i , \dot{V} always satisfies negative, and the control law (7.9) will stabilize the sliding surface (7.4).

For proving that $\lim_{t \rightarrow \infty} [e_1 \ e_2 \ e_3 \ e_4 \ e_5]^T = 0$, at first, \mathbf{S} must be proved to satisfy $\lim_{t \rightarrow \infty} \mathbf{S} = 0$. Herein the Barbalat's lemma is used as following. As for first condition of the lemma, because $\dot{V} \leq 0$, so S_i are bounded. Furthermore, referring Eq. (7.11), when S_i are bounded, V has a finite limit as $t \rightarrow \infty$. As for second condition of the lemma, the value of the derivative of \dot{V} is calculated as:

$$\frac{d\dot{V}}{dt} = (\dot{S}_1^2 + S_1\ddot{S}_1) + (\dot{S}_2^2 + S_2\ddot{S}_2) + (\dot{S}_3^2 + S_3\ddot{S}_3) + (\dot{S}_4^2 + S_4\ddot{S}_4) \quad (7.13)$$

Easily, because S_i and their first and second derivatives are bounded, the derivative of \dot{V} is bounded too. Therefore \dot{V} satisfies the sufficient condition of a uniformly continuous function. According to two above-mentioned conditions, by Barbalat's lemma, the result is obtained as $\lim_{t \rightarrow \infty} \dot{V} = 0$.

Now, Eq. (7.12) can be re-written as follows:

$$0 = -\mathbf{S}^T\mathbf{QS} - (\mathbf{P}|\mathbf{S}| - \mathbf{fS}) \quad (7.14)$$

Eq. (7.14) implies that $\lim_{t \rightarrow 0} S_i = 0$, then the system's behavior comes on the sliding surface and Eq. (7.4) can be re-expressed as the following:

$$\begin{bmatrix} \dot{e}_1 \\ \dot{e}_4 \\ \dot{e}_3 \\ \dot{e}_5 \end{bmatrix} = \begin{bmatrix} -k_1 e_1 - |e_2| \text{sgn}(e_1) \\ -k_4 e_4 \\ -k_3 e_3 \\ -k_5 e_5 \end{bmatrix} \quad (7.15)$$

Equation (7.15) shows that the errors e_1, e_3, e_4, e_5 and their derivatives always have an opposite signs. Therefore, when the errors go out of the sliding surface, their derivatives make a trend that pulls them back to the sliding surface so the errors can converge to zero. In the first row of equation (7.15), $|e_2|$ is assumed to be bounded, so e_1 and its derivative also satisfy the condition mentioned above. Also based on this row of equation (7.15), it can be realized that after e_1 went to zero the error e_2 is too.

According to everything mentioned above, a conclusion can be inferred: the equilibrium point $e_i = 0$ is uniformly asymptotically stable.

In practice, the control law (7.9) cannot be used due to the so-called chattering phenomenon. It is a discontinuous function with the signum function, so it generates the chattering of the trajectories on the surface $S_i = 0$. In order to eliminate this phenomenon, the signum function is replaced by a saturation function, and the control law can be re-expressed as shown below:

$$\begin{bmatrix} u_1 \\ u_2 \\ u_3 \\ u_4 \end{bmatrix} = \begin{bmatrix} Q_1 S_1 \\ Q_2 S_2 \\ Q_3 S_3 \\ Q_4 S_4 \end{bmatrix} + \begin{bmatrix} P_1 \text{sat}(S_1, \Phi) \\ P_2 \text{sat}(S_2, \Phi) \\ P_3 \text{sat}(S_3, \Phi) \\ P_4 \text{sat}(S_4, \Phi) \end{bmatrix} + \begin{bmatrix} (e_2 + p_m) \dot{\omega}_\phi + (v_r \cos \psi_r \sin e_4 - k_4 \dot{e}_4) \\ k_3 \dot{e}_3 \\ k_5 \dot{e}_5 \end{bmatrix}$$

$$\left. e_l \omega_\phi) \omega_\phi - \dot{e}_4 v_r \cos \psi_r \sin e_4 + k_l \dot{e}_l + |\dot{e}_2| \text{sgn}(e_l) \right] \quad (7.16)$$

where $\begin{cases} \text{sat}(S, \Phi) = \frac{S}{\Phi} & \text{if } \left| \frac{S}{\Phi} \right| \leq 1 \\ \text{sat}(S, \Phi) = \text{sgn}\left(\frac{S}{\Phi}\right) & \text{otherwise} \end{cases}$, and Φ is boundary layer thickness.

Based on the dynamic relationship in Eq. (7.6), the control input of the system can be expressed as the following:

$$\boldsymbol{\tau} = \overline{\mathbf{M}} \dot{\mathbf{h}}_r + \overline{\mathbf{C}} \mathbf{h} + \overline{\mathbf{M}} \mathbf{u} \quad (7.17)$$

where $\boldsymbol{\tau} = [\boldsymbol{\tau}_v \quad \boldsymbol{\tau}_r]^T$ is the vector of applied torques on mobile platform's and manipulator's actuators, $\overline{\mathbf{M}} = \begin{bmatrix} \overline{\mathbf{M}}_{11} & 0 \\ 0 & \overline{\mathbf{M}}_{22} \end{bmatrix}$, $\mathbf{h}_r = [v_{xyr} \quad \omega_{\phi r} \quad v_{zr} \quad \omega_{\psi r}]^T$ is the vector of desired velocity, $\overline{\mathbf{C}} = \begin{bmatrix} \overline{\mathbf{C}}_{11} & 0 \\ 0 & \overline{\mathbf{C}}_{22} \end{bmatrix}$, $\mathbf{h} = [v_{xy} \quad \omega_\phi \quad v_z \quad \omega_\psi]^T$ is the vector of actual velocity, and \mathbf{u} is the control law.

7.3 Simulation and Experiment Results

In this chapter, the reference trajectory that is used in the simulation is the same with the previous chapters and can be referred in the Fig. 4.2. In this time, the initial errors are chosen with a little difference from the previous chapter, but they are still in the customary rate. The numerical values of the system's parameters are shown in Table 7.1. Therein, the parameters for dealing with the bounded external disturbances such as f_i are also listed.

Table 7.1 Numerical values of the system's parameters

Parameters	Description	Values	Units
r	Radius of the wheels	0.03	m
b	Half of the wheel-to-wheel distance	0.15	m
$l_1 = l_2 = l$	Length of the first and second link	0.222	m
$l_3 + l_4$	Length of the third + fourth link	0.172	m
p_m	Projection of the manipulator on Oxy	0.38	m
Δx_i	Initial position error in x direction	0.005	m
Δy_i	Initial position error in y direction	0.025	m
Δz_i	Initial position error in z direction	0.005	m
$\Delta \phi_i$	Initial orientation error in horizontal	20	deg
$\Delta \psi_i$	Initial orientation error in vertical	20	deg
k_1	Weight factor of the controller	1.5	
k_2	Weight factor of the controller	15	
k_3	Weight factor of the controller	1.5	
k_4	Weight factor of the controller	2.5	
k_5	Weight factor of the controller	1.2	
Q_1	Constant of the controller	1.5	
Q_{2-4}	Constant of the controller	1	
P_i	Constant of the controller	0.5	
f_i	Constant of the controller	0.5	N
m_c	Mass of the platform's body	4	Kg
m_w	Mass of the wheels	0.5	Kg

I_c	Inertia moment of the platform's body	0.31	Kgm ²
I_w	Inertia moment of the wheels	4.5×10^{-4}	Kgm ²
m_1	Mass of the first link	2	Kg
m_2	Mass of the second link	1.5	Kg
$m_{(3+4)}$	Mass of the set (third + fourth links)	0.8	Kg
I_1	Inertia moment of the first link	0.31	Kgm ²
I_2	Inertia moment of the second link	0.27	Kgm ²
I_{3+4}	Inertia moment of the set (3+4)	0.22	Kgm ²
$I_{4+torch}$	Inertia moment of fourth link + torch	0.013	Kgm ²
Φ	Boundary layer thickness	0.5	

In figure 7.1 the position tracking errors converge to zero after about nine seconds, especially, the error e_1 suddenly oscillate at the two junction points between the circular sectors. They can be explained by the so-called trade-off between tracking performance and the system modeling: more flexible modeling choice, more deteriorative tracking performance, and vice versa. However, in general, it also stables in throughout the simulation. The Figs. 7.3-10 are reserved for demonstrating the ability ameliorating the system's performance of the saturation function. The characteristic curves of the system in the sliding surface are intensively improved after the saturation function is applied and the chattering phenomenon is perfectly eliminated. Fig. 7.11 is used for comparing the system performance with the desired trajectory.

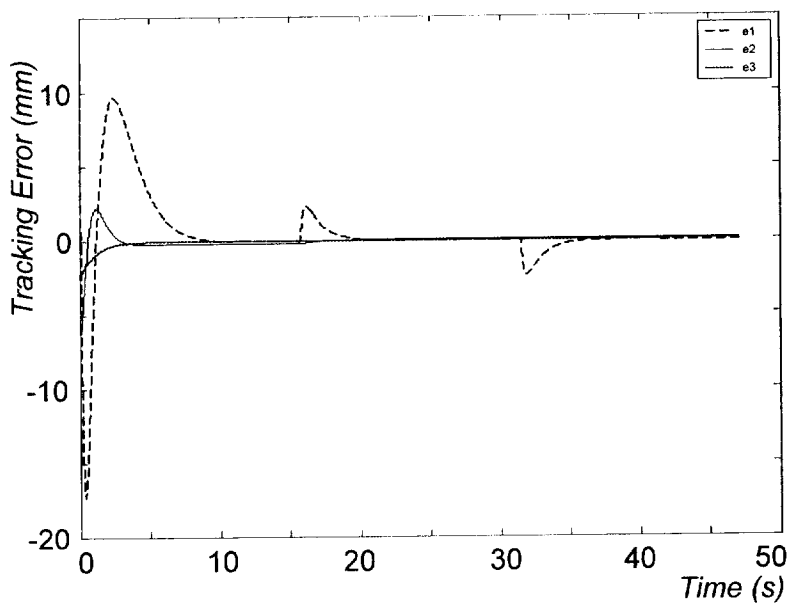


Fig. 7.1 Tracking errors e_1 , e_2 , and e_3

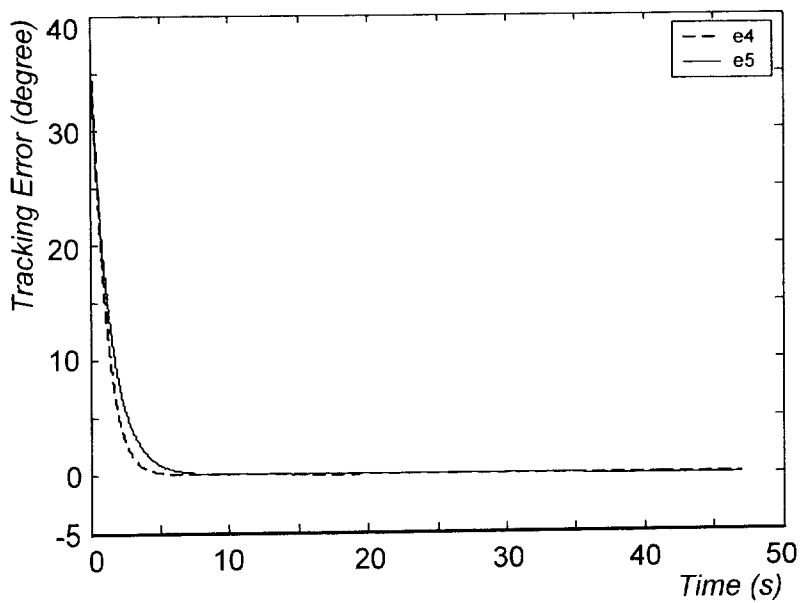


Fig. 7.2 Tracking errors e_4 , and e_5

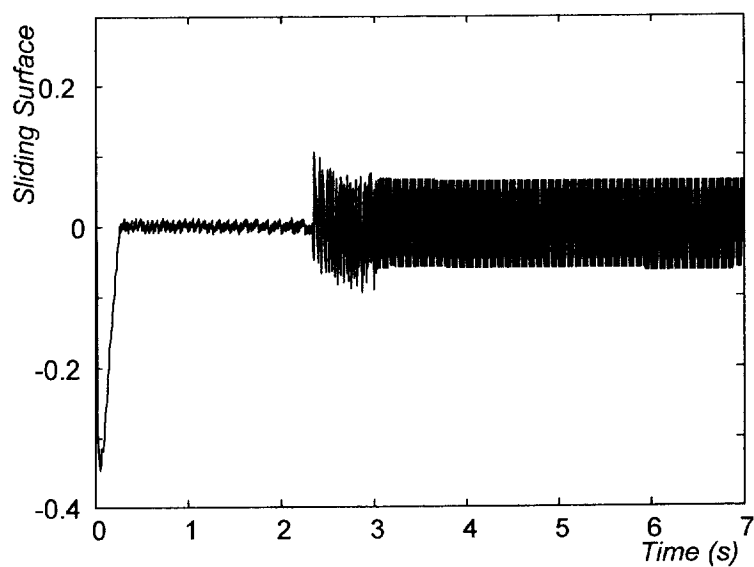


Fig. 7.3 Sliding surface component S_l without saturation function

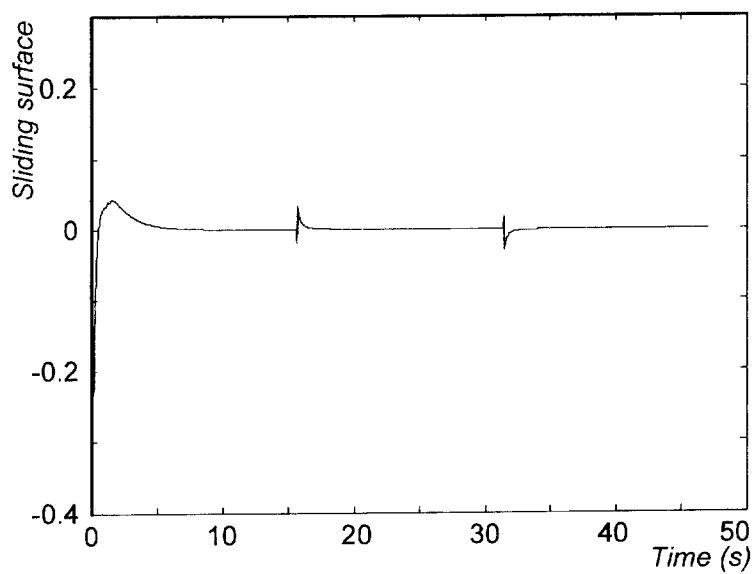


Fig. 7.4 Sliding surface component S_l with saturation function

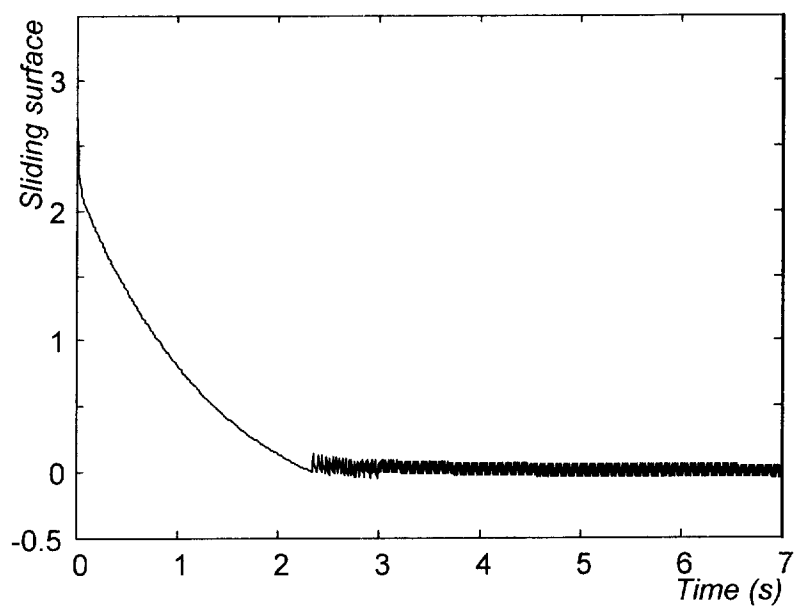


Fig. 7.5 Sliding surface component S_2 without saturation function

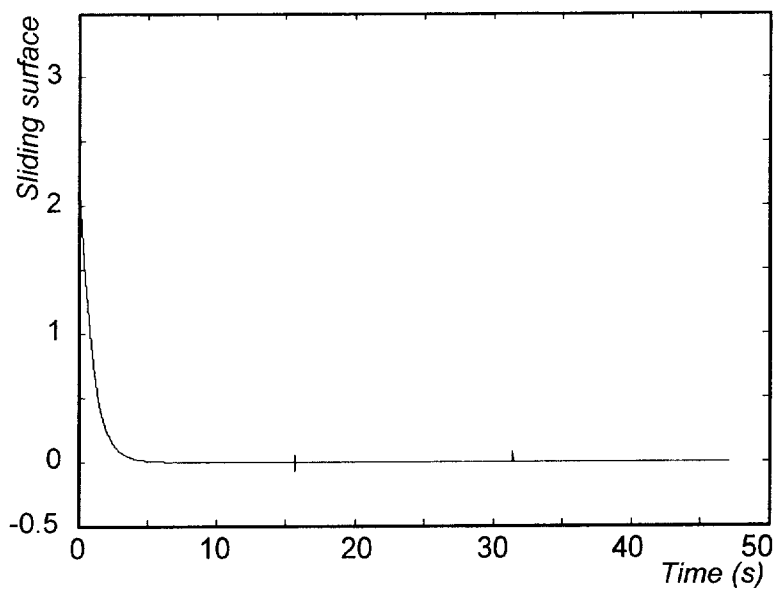


Fig. 7.6 Sliding surface component S_2 with saturation function

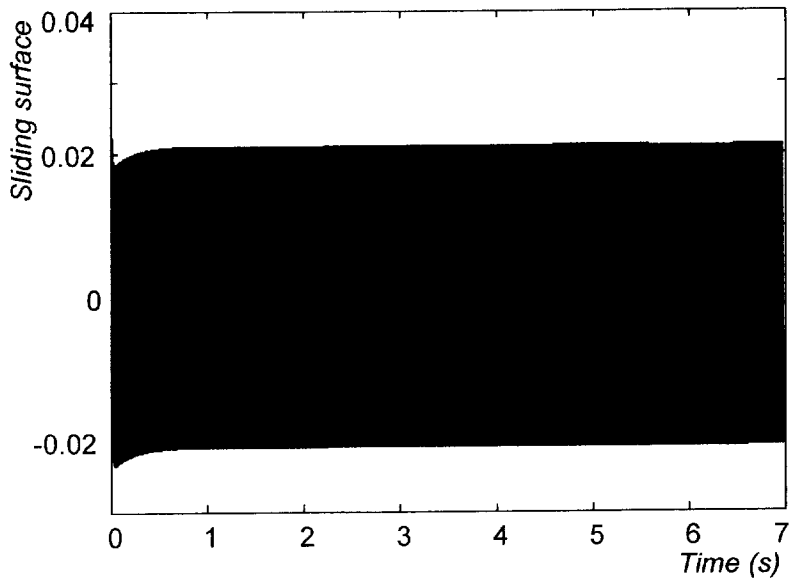


Fig. 7.7 Sliding surface component S_3 without saturation function

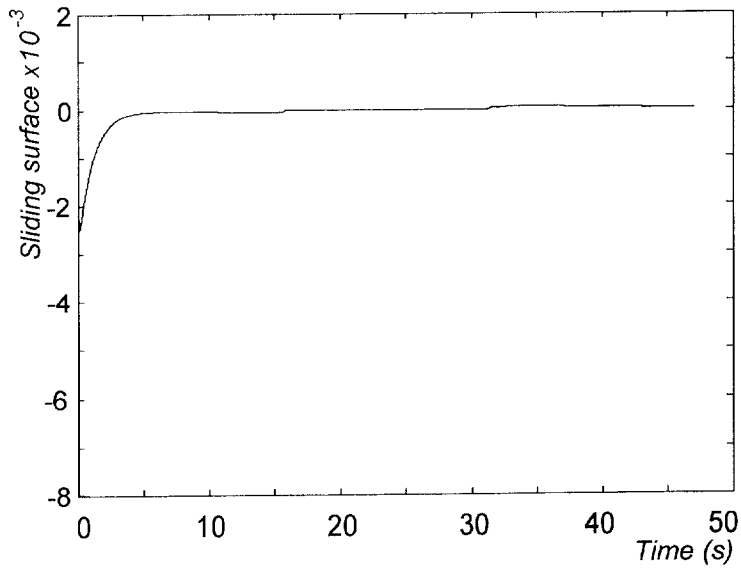


Fig. 7.8 Sliding surface component S_3 with saturation function

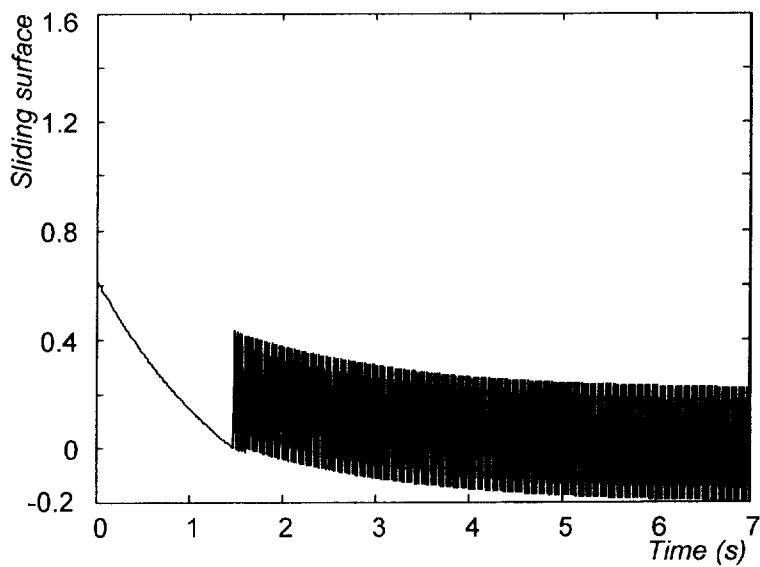


Fig. 7.9 Sliding surface component S_4 without saturation function

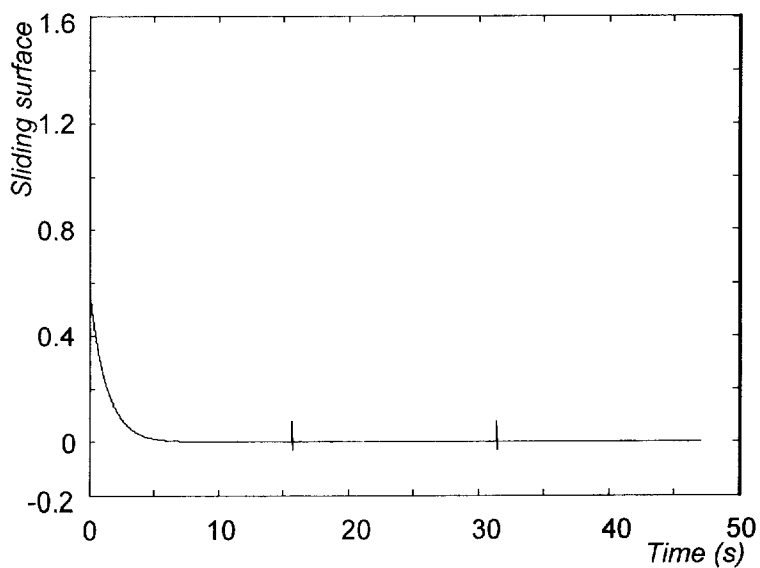


Fig. 7.10 Sliding surface component S_4 with saturation function

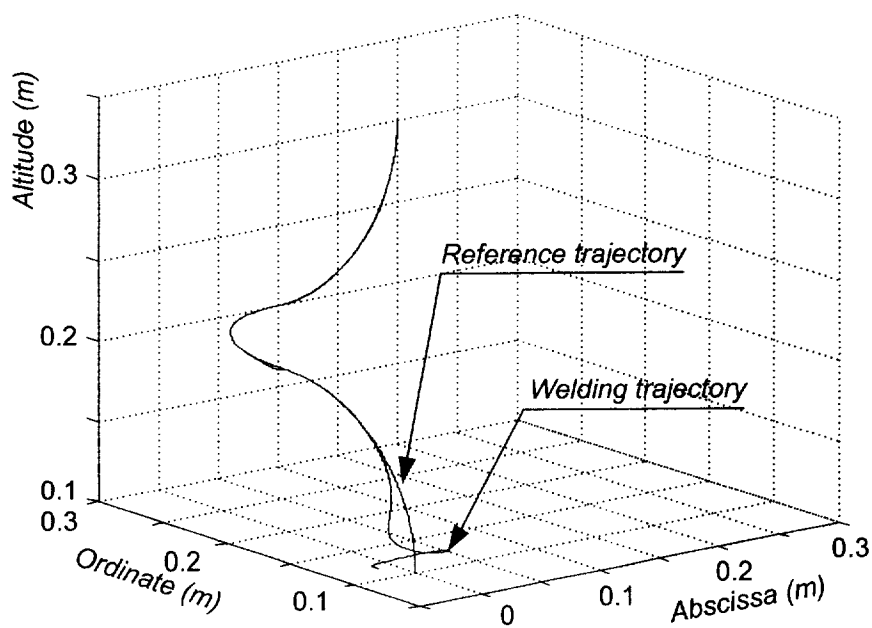


Fig. 7.11 Reference trajectory and welding trajectory

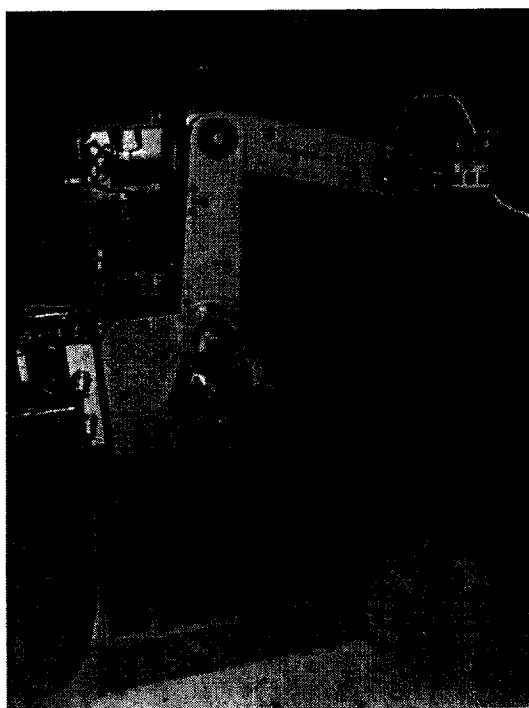


Fig. 7.12 Mobile manipulator in the tracking experiment

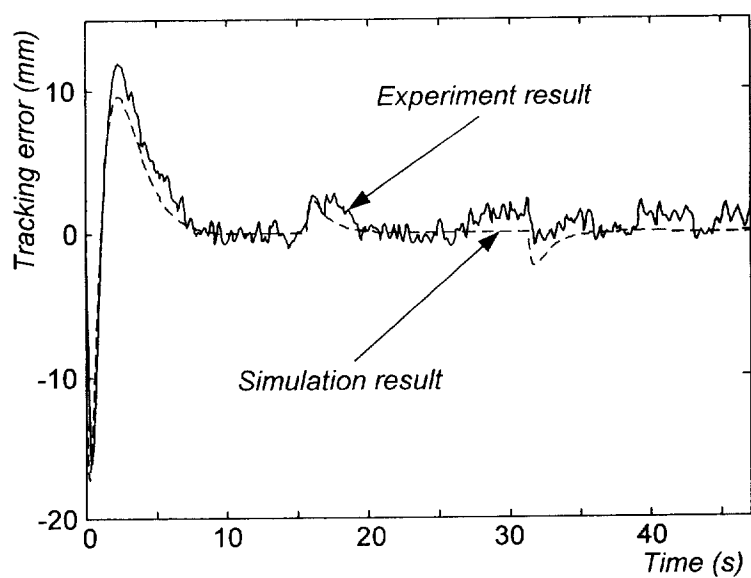


Fig. 7.13 Tracking error e_1

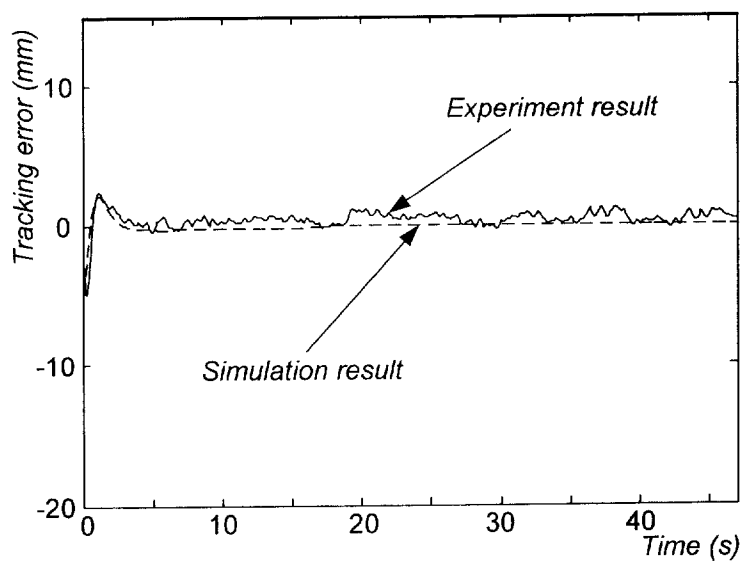


Fig. 7.14 Tracking error e_2

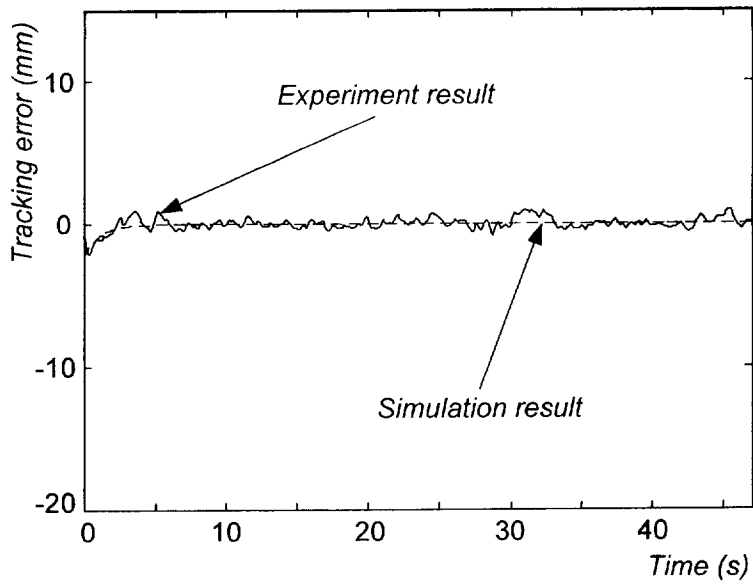


Fig. 7.15 Tracking error e_3

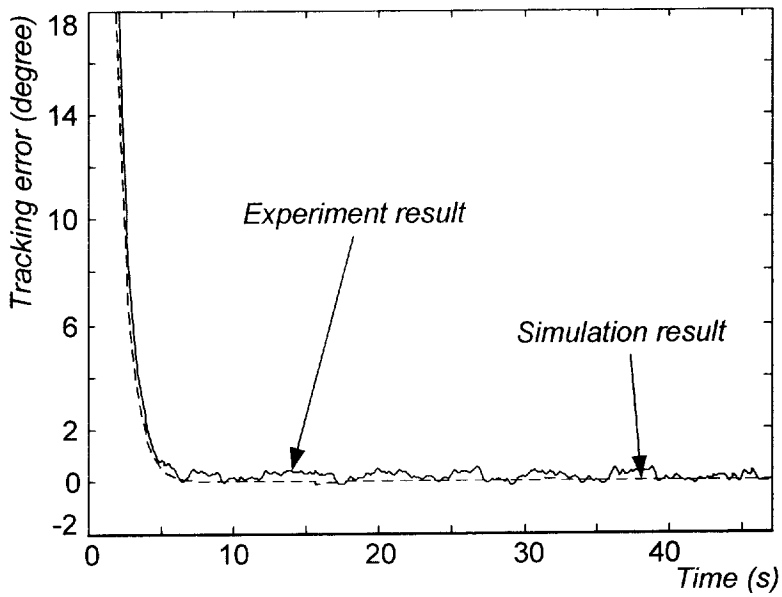


Fig. 7.16 Tracking error e_4

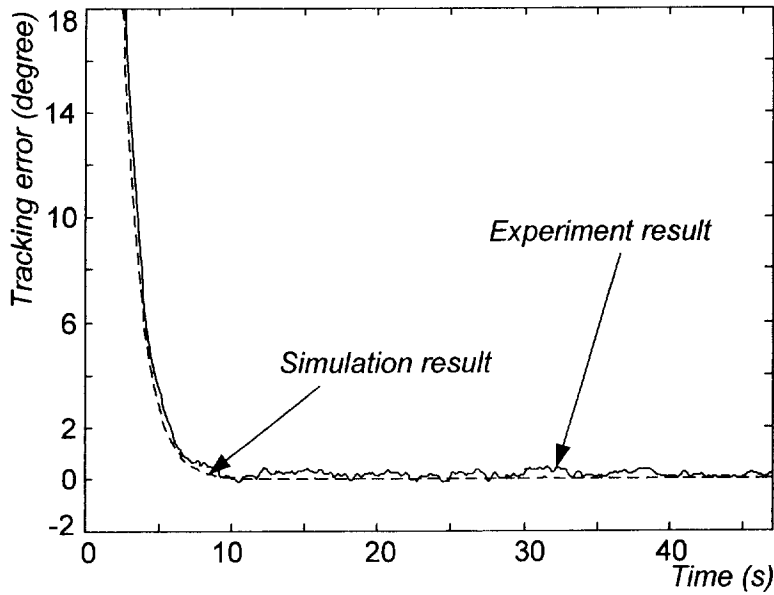


Fig. 7.17 Tracking error e_5

The implementation of the mobile manipulator in the experiment is depicted in Fig. 7.12. The successive Figs. 7.13-17 are reserved for showing the tracking errors. With the fluctuation of the results not exceeding 3mm in position deviation and 1deg in angular deviation, they prove the validity of the proposed controller.

7.4 Chapter Summary

A robust control algorithm based on the sliding mode technique is proposed and applied to a mobile manipulator in the 3D smooth curve welding process. The uniform asymptotical stability of the system and the simultaneous equality to zero at the equilibrium point of the tracking errors are proved by Lyapunov - like analysis using Barbalat's lemma. Also, in this chapter, the issue about how to eliminate the chattering phenomenon occurring in the sliding surface is considered. A saturation function is proposed for this issue and a better performance of system

is shown in the graphs after using the saturate function. They all introduce the usefulness of this algorithm in 3D welding process.

The contribution in this chapter:

- ❖ Showing the method for design of a robust controller using sliding mode technique with concerning the bounded external disturbance for a mobile manipulator performing the smooth 3D curved welding trajectory.
- ❖ Introducing how to use saturation function to eliminate the chattering phenomenon for enhancing the performance of the system.

Chapter 8

Conclusions

8.1 Controllers in Comparison

The destination of thesis is to design the tracking controllers for a mobile manipulator performing the smooth 3D curved welding tasks so the controllers will be compared based on this aspect. For easy to comment about the controllers, the following table with their main characteristics is established.

(Note: Controller 1, Controller 2, Controller 3 and Controller 4 stand for the controllers in chapter 4, chapter 5, chapter 6 and chapter 7, respectively)

Table 8.1 Controllers in comparison

Criterion	Controller 1	Controller 2	Controller 3	Controller 4
Kind of the model	Kinematic	Kinematic	Hybrid	Dynamic
Control input	Velocity	Velocity	Torques	Torques
Unknown parameter	No	Welding arc length	No	External disturbances
Experiment position deviation	$\leq 1\text{mm}$	$\leq 1\text{mm}$	$\leq 1\text{mm}$	$\leq 3\text{mm}$
Experiment angular deviation	$\leq 0.5\text{ deg}$	$\leq 1.5\text{ deg}$	$\leq 0.5\text{ deg}$	$\leq 1\text{ deg}$

Jerk when the parameters change state	No	No	No	Yes
---------------------------------------	----	----	----	-----

Based on Table 8.1, the following conclusions can be stated:

- ❖ For performing the welding task in the isolated environment, without the external disturbances, the controller 2 is a logical choice. It made the system an acceptable performance with only a relative simple control law. It also solved the unmeasured welding arc length - an inevitable problem in any arc-welding process. On the contrary, the controller 2 owns a weak point: It does not consider to the dynamic response of the system. Fortunately, as for a welding process with the very slow motion (velocity of the welding torch tip is only 0.0075m/s) the impact of the system's dynamic characteristics is trivial and can be dispensed.
- ❖ For the welding task requiring the fast motion such as the spot contact welding in the automobile industry, the effect of the system's dynamic characteristics is remarkable and the good choice is controller 3 or controller 4. In this case, according to whether the external disturbances occur or not, one can make a choice with controller 4 or controller 3.

However, the above remarks are relative, depending on the concrete conditions, according to what controller will be chosen. For example, if the arc welding tasks require the high accuracy, the effect of the dynamic characteristics cannot be dispensed (relevant to the small tolerance) and the choice is changed to the other controller concerning to the dynamic characteristics of the system.

8.2 Prospects of the Topic and the Future Works

Automation has been strongly developed resulting from the more and more social needs. Especially, in the heavy industry, there are many hard and harmful works that the worker's life can be endangered. Therein, welding is the special case because of its pollution environment effect. Un-suspiciously, in near future, welding industry will be developed both the quality and quantity. The system with the high level of accuracy and sophistication will be produced and the needs of the high class control systems are accompanied.

As for this thesis, the following future works are made as a necessary destination:

- ❖ Considering to the other kinds of adaptive control and robust control, continuously try to apply the new algorithms to find out the adequate one for introducing to the welding mobile manipulator.
- ❖ Concentrating to the hybrid algorithms established by the adaptive control and the robust control so that can make the new controller with the higher flexibility.
- ❖ With the mobile platform: Trying to use the special structure to make the mobile platform can operate under unexpected terrain environment. This will make the mobile manipulator an unlimited motion so it can remarkably enlarge the robot's application fields.
- ❖ With the manipulator: Trying to study about the control concerning to the interaction with surrounding environment such as force control. Therefore, the mobile manipulator can perform the diversified tasks, for example, home services, wash building windows or assembly.

References

- [1] G. F. Franklin, J. D. Powell, A. E. Naeini, *Feedback Control of Dynamic Systems*, Prentice Hall Publishing Company, New York, USA, 2002.
- [2] D. Neculescu, *Mechatronics*, Prentice Hall International, 2002.
- [3] S. B. Niku, *Introduction to Robotics Analysis, Systems, Application*, Prentice Hall Publishing Company, New York, USA, 2001.
- [4] S. Sastry, *Nonlinear Systems Analysis, Stability, and Control*, Springer Verlag, New York, USA, 1999.
- [5] M. Jamshidi and many authors, *Nonlinear Control of Robotic Systems for Environmental Waste and Restoration*, Prentice Hall Publishing Company, New Jersey, USA, 1995.
- [6] K. J. Astrom and B. Wittenmark, *Adaptive Control*, Addison Wesley Publishing Company, 1995.
- [7] R. M. Murray, Z. Li and S. S. Sastry, *A Mathematical Introduction to Robotic Manipulation*, CRC Press, New York, USA, 1994.
- [8] F. L. Lewis, C. T. Abdallah and D. M. Dawson, *Control of Robot Manipulators*, Macmillan Publishing Company, New York, USA, 1993.
- [9] F. Z. Yuan and many authors, *Recent Trends in Mobile Robot*, Word Scientific Publishing Co. Pte. Ltd., Singapore, 1993.
- [10] J. J. E. Soltine and W. Li, *Applied Nonlinear Control*, Prentice Hall International, 1991.

- [11] P. J. Mc Kerrow, *Introduction to Robotics*, Addison, Wesley Publishers, 1991.
- [12] J. J. Craig, *Introduction to Robotics Mechanics and Control*, Addison Wesley Publishing Company, 1989.
- [13] T. T. Phan, *Control of Mobile Manipulators for Tracking Horizontal Smooth Curved Welding Path*, Ph. D. Thesis, Department of Mechatronics Engineering, Pukyong National University, Korea, 2005.
- [14] T. H. Bui, *Control of Two-Wheeled Welding Mobile Robots for Tracking Smooth Curved Welding Path*, Ph. D. Thesis, Department of Mechatronic Engineering, Pukyong National University, Korea, 2004.
- [15] H. K. Kim, *Counting Algorithm of Microorganism and Control of Bioreactor System*, Ph. D. Thesis, Department of Mechatronic Engineering, Pukyong National University, Korea, 2002.
- [16] Y. Yamamoto, *Control and Coordination of Locomotion and Manipulation of a Wheeled Mobile Manipulator*, Ph. D. Thesis, Department of Computer and Information Science, University of Pennsylvania, USA, 1994.
- [17] N. A. N. Hootsmans, *The Motion Control of Manipulators on Mobile Vehicles*, Ph. D. Thesis, Department of Mechanical Engineering, Massachusetts Institute of Technology, USA, 1992.
- [18] E. Zergeroglu, D. D. Dawson, I. W. Walker, P. Setlur, "Nonlinear Tracking Control of Kinematically Redundant Robot Manipulators", *Transactions on IEEE/ASME Mechatronics*, Vol. 9 , pp. 129-132, 2004.
- [19] W. E. Dixon, M. S. de Queiroz, D. M. Dawson and T. J. Flynn,

- “Adaptive Tracking and Regulation of a Wheeled Mobile Robot With Controller/Update Law Modularity”, *IEEE Transactions on Control Systems Technology*, Vol. 12, No. 1, pp. 138-147, January 2004.
- [20] Tr. H. Bui, T. L. Chung, J. H. Suh and S. B. Kim, “Adaptive Control for Tracking Trajectory of a Two Wheeled Welding Mobile Robot with Unknown Parameters”, *Proceedings of the International Conference on Control, Automation and Systems*, pp. 191-196, 2003.
- [21] Tr. H. Bui, T. T. Nguyen, T. L. Chung and S. B. Kim, “A Simple Nonlinear Control of a Two-Wheeled Welding Mobile Robot”, *Transactions on International Journal of Control, Automation, and Systems (IJCAS)*, Vol. 1, No. 1, pp. 35-42, 2003.
- [22] M. P. Cheng and C. C. Tsai, “Dynamic Modeling and Tracking Control of a Non-holonomic Wheeled Mobile Manipulator with Two Robotic Arms”, *Proceedings of the IEEE Conference on Decision and Control*, Vol. 3, pp. 2932-2937, 2003 .
- [23] S. Furuno, M. Yamamoto and A. Mohri, “Trajectory planning of mobile manipulator with stability considerations” *Proceedings of the IEEE International Conference on Robotics and Automation*, Vol.3, pp. 3403-3408, 2003.
- [24] B. Bayle, I. Y. Fourquet, F. Lamiriaux and M. Renaud, “Kinematic Control of Wheeled Mobile Manipulators”, *Proceedings of the IEEE/RSJ International Conference on Intelligent Robots and Systems*, Vol. 2, pp 1572-1577, 2002.
- [25] Y. B. Jeon, B. O. Kam, S. S. Park, and S. B. Kim, “Modeling and Motion Control of Mobile Robot for Lattice Type Welding”, *Transactions on*

International Journal (KSME), Vol. 16, No 1, pp. 83-93, 2002.

- [26] K. Nagatani, T. Hirayama, A. Gofuku and Y. Tanaka, "Motion Planning for Mobile Manipulator with Keeping Manipulability" *Proceedings of the IEEE/RSJ International Conference on Intelligent Robots and System*, Vol. 2, pp. 1663 - 1668, 2002.
- [27] S. Lin and A. A. Goldenberg, "Robust Damping Control of Mobile Manipulators" *IEEE Transactions on System, Man and Cybernetics*, Vol. 32, No.1, pp. 126 - 132, 2002.
- [28] H. Xu and S. X. Yang, "Tracking Control of a Mobile Robot with Kinematic and Dynamic Constraints", *Proceedings of the IEEE International Symposium on Computational Intelligence in Robotics and Automation*, Canada, pp. 125-130, July 2001.
- [29] B. O. Kam, Y. B. Jeon, and S. B. Kim, "Motion Control of Two-Wheeled Welding Mobile Robot with Seam Tracking Sensor", *Proceedings of the IEEE International Symposium on Industrial Electronics*, Vol. 2, pp. 851-856, June 2001.
- [30] J. Tan, and N. Xi, "Unified Model Approach for Planning and Control of Mobile Manipulators", *Proceedings of the IEEE International Conference on Robotics and Automation*, Korea, pp. 3145-3152, May 2001.
- [31] E. Lefeber, J. Jakubiak, K. Tchon, and H. Nijimeijer, "Observer Based Kinematic Tracking Controllers for a Unicycle-type Mobile Robot", *Proceedings of the IEEE International Conference on Robotics and Automation*, Vol. 2, pp. 2084-2089, 2001.
- [32] W. Dong and W. L. Xu, "Adaptive Tracking of Uncertain Non-

- holonomic Dynamic System”, *IEEE Transactions on Automatic Control*, Vol. 46, No. 3, pp. 450-454, March 2001.
- [33] W. S. Yoo, J. D. Kim and S. J. Na “A study on a mobile platform-manipulator welding system for horizontal fillet joints” *Transactions on Mechatronics*, Vol. 11, pp 853-868, 2001.
 - [34] Y. B. Jeon, B. O. Kam, S. S. Park and S. B. Kim, “Seam Tracking and Welding Speed Control of Mobile Robot for Lattice Type Welding”, *Proceedings of the IEEE International Symposium on Industrial Electronics*, Vol. 2, pp. 857-862, June 2001.
 - [35] T. C. Lee, K. T. Song, C. H. Lee and C. C. Teng, “Tracking Control of Mobile Robots Using Saturation Feedback Controller”, *IEEE Transactions on Control Systems Technology*, Vol. 9, No.2, pp. 305-318, 2001.
 - [36] W. Dong, Y. Xu and Q. Wang, “On Tracking Control of Mobile Manipulators”, *Proceedings of the IEEE International Conference on Robotics and Automation*, Vol. 4, pp. 3455-3460, 2000.
 - [37] J. Tan, and N. Xi, “Hybrid System Design for Singularityless Task Level Robot Controllers”, *Proceedings of the IEEE International Conference on Robotics and Automation*, pp. 3007-3012, April 2000.
 - [38] T. Fukao, H. Nakagawa and N. Adachi, “Adaptive Tracking Control of a Non-holonomic Mobile Robot”, *Transactions on Robotics and Automation*, Vol. 16, No. 5, pp. 609-615, 2000.
 - [39] T. C. Lee, C. H. Lee and C. C. Teng, “Adaptive Tracking Control of Non-holonomic Mobile Robots by Computed Torque”, *Proceedings of the Conference on Decision and Control*, Vol. 2, pp. 1254-1259, 1999.

- [40] J. M. Yang, and J. H. Kim, "Sliding Mode Control for Trajectory Tracking of Nonholonomic Wheeled Mobile Robots", *IEEE Transactions on Robotics and Automation*, Vol. 15, No. 3, pp. 578-587, 1999.
- [41] H. Wang, T. Fukao and N. Adachi, "An Adaptive Tracking Control Approach for Non-holonomic Mobile Robot", *Proceedings of the IFAC World Congress*, pp. 609-615, 1999.
- [42] Y. Tang and G. Guerrero, "Decentralized Robust Control of Robot Manipulator", *Proceedings of the American Control Conference*, Pennsylvania, USA, pp. 922-926, June 1998.
- [43] G. Foulon, J. Y. Fourquet and M. Renaud, "Planning Point to Point Paths for Non-holonomic Mobile Manipulators", *Proceedings of the IEEE/RSJ International Conference on Intelligent Robots and Systems*, pp 374-379, 1998.
- [44] S. V. Gusev, I. A. Makarov, I. E. Paromtchik, V. A. Yakubovich and C. Laugier, "Adaptive Motion Control of a Non-holonomic Vehicle", *Proceedings of the IEEE International Conference on Robotics and Automation*, pp. 3285-3290, May 1998.
- [45] F. Cheng, T. Hour, Y. Sun, and T. H. Chen, "Study and Resolution of Singularities for a 6 DOF PUMA Manipulators", *IEEE Transactions on System, Man, and Cybernetics*, Vol. 27, No. 2, pp. 332-343, April 1997.
- [46] K. Tahboub, "Observer-based Control for Manipulators with Moving Bases", *Proceedings of the IEEE/RSJ International Conference Intelligent Robots and System*, pp. 1279-1284, 1997.
- [47] M. Tarokh, "A Decentralized Nonlinear Three-Term Controller for

- Manipulator Trajectory Tracking”, *Proceedings of the IEEE International Conference on Robotics and Automation*, Minnesota, pp.3683-3688, April 1996.
- [48] Y. C. Chang and B. S. Chen, “Adaptive Tracking Control Design of Non-holonomic Mechanical Systems”, *Proceedings of Conference on Decision and Control*, Kobe, Japan, pp. 4739-4744, December 1996.
 - [49] O. Khatib et al., “Vehicle/arm Cordination and Multiple Mobile Manipulator Decentralized Cooperation”, *Proceedings of the IEEE/RSJ International Conference Intelleigent Robots and System*, Vol. 3, pp. 546-553, 1996.
 - [50] Y. Yamamoto and X. Yun, “Effect of the Dynamics Interaction on Coordinated Control of Mobile Manipulator” *IEEE Transactions on Robotics and Automation*, Vol. 12, pp. 816-824, 1996.
 - [51] G. Campion, G. Bastin and B. d’Andrea Novel, “Structural Properties and Classification of Kinematic and Dynamic Models of Wheeled Mobile Robots”, *IEEE Transactions on Robotics and Automation*, Vol. 12, pp. 47-62, 1996.
 - [52] H. Seraji, “Configuration Control of Rover Mounted Manipulators”, *Proceedings of the IEEE International Conference on Robotics and Automation*, Vol. 3, pp. 2261-2266, 1995.
 - [53] R. Fierro and F. L. Lewis, “Control of a Non-holonomic Mobile Robot: Backstepping Kinematics into Dynamics”, *Proceedings of the IEEE Conference on Decision and Control*, Vol. 4, pp. 3805-3810, 1995.
 - [54] Y. Yamamoto and X. Yun, “Modeling and Compensation of the Dynamic Interaction of a Mobile Manipulator”, *Proceedings of the IEEE*

- International Conference on Robotics and Automation*, Vol. 3, pp. 2187-2192, May 1994.
- [55] Y. Kanayama, "Two Dimensional Wheeled Vehicle Kinematic", *Proceedings of the IEEE International Conference on Robotics and Automation*, Vol. 4, pp 3079-3084, 1994.
 - [56] Y. Yamamoto and X. Yun, "Coordinating Locomotion and Manipulation of a Mobile Manipulator", *IEEE Transactions on Automatic Control*, Vol. 39, pp. 1326-1332, 1994.
 - [57] H. Seraji, "Motion control of mobile manipulators" *Proceedings of the IEEE International Conference on Intelligent Robots and Systems*, Vol. 3, pp. 2056-2063, 1993.
 - [58] J. Lloyd and V. Hayward, "Singularity Control of Robot manipulator using Closed form Kinematic Solutions", *Proceedings of the Conference on Electrical and Computer Engineering*, Vol.2, pp. 1065-1068, 1993.
 - [59] N. Sarkar, X. Yun and V. Kumar, "Dynamic Path Following: A New Control Algorithm for Mobile Robots", *Proceedings of the Conference on Decision and Control*, Texas, USA, pp. 2670-2675, December 1993.
 - [60] R. Colbaugh, H. Seraji and K. Glass, "A New Approach to Adaptive Manipulator Control", *Proceedings of the IEEE International Conference on Robotics and Automation*, Vol. 1, pp.604-611, May 1993.
 - [61] Z. Deng and M. Brady, "Dynamic Tracking of a Wheeled Mobile Robot", *Proceedings of the IEEE/RSJ International Conference on Intelligent Robots and Systems*, Yokohama, Japan, pp. 1295-1298, July 1993.
 - [62] T. Burke and H. F. Durrant-Whyte, "Kinematic for Modular Wheeled

- Mobile Robots”, *Proceedings of the IEEE/RSJ International Conference on Intelligent Robots and Systems*, pp 1279-1286, 1993.
- [63] X. Yun and Y. Yamamoto, “Internal Dynamics of a Wheeled Mobile Robot”, *Proceedings of the IEEE/RSJ International Conference on Intelligent Robots and Systems*, Japan, pp. 1288-1294, July 1993.
 - [64] T. Isobe, K. Nagasaka and S. Yamamoto, “A New Approach to Kinematic Control of Simple Manipulators”, *IEEE Transactions on Systems, Man and Cybernetics*, Vol. 22, pp. 1116-1124, 1992.
 - [65] N. A. M. Hootsmans and S. Dubowsky, “The Experimental Performance of a Mobile Manipulator Control Algorithm” *Proceedings of the IEEE International Conference on Robotics and Automation*, pp.1948-1954, 1992.
 - [66] A. Khoukhi and Y. Hamam, “Mobile Robot Kinematic, Dynamic, and Mobility”, *Proceedings of the ICAR International Conference on Advanced Robotics*, Vol. 2, pp. 1111-1117, 1991.
 - [67] B. d’Andrea-Novet, G. Bastin and G. Campion, “Modeling and Control of Non-holonomic Wheeled Mobile Robots”, *Proceedings of the IEEE International Conference on Robotics and Automation*, California, pp. 1130-1135, April 1991.
 - [68] C. Abdallah, D. M. Dawson, P. Dorato and M. Jamshidi, “Survey of Robust Control for Rigid Robots” *IEEE Transactions on Control Systems Magazine*, Vol. 11, pp. 24-30, 1991.
 - [69] N. A. M. Hootsmans and S. Dubowsky, “Large Motion Control of Mobile Manipulator Including Vehicle Suspension Characteristics” *Proceedings of the IEEE International Conference on Robotics and*

Automation, pp.2336-2341, 1991.

- [70] Y. Kanayama, Y. Kimura, F. Miyazaki and T. Noguchi, "A Stable Tracking Control Method for a Non-holonomic Mobile Robot", *Proceedings of the IEEE/RSJ International Workshop on Intelligent Robots and Systems*, Japan, Vol. 3, pp. 1236-1241, 1991.
- [71] K. Liu and F. L. Lewis "Decentralized Continuous Robust Controller for Mobile Robots", *Proceedings of the IEEE International Conference on Robotics and Automation*, pp. 1822-1827, 1990.
- [72] W. F. Carriker, P. K. Khosla and B. H. Krogh, "The Use of Simulated Annealing to Solve The Mobile Manipulator Path Planning Problem", *Proceedings of the IEEE International Conference on Robotics and Automation*, pp. 204-209, 1990.
- [73] G. L. Wiens, "Effect of Dynamic Coupling in Mobile Robotics Systems" *Proceedings of the SME International Conference on Robotics Research*, pp. 43-57, 1989.
- [74] H. Seraji, "An Adaptive Cartesian Control Scheme for Manipulators", *Proceedings of the IEEE International Conference on Robotics and Automation*, Vol. 4, pp. 157-164, 1987.
- [75] J. J. Craig, P. Hsu and S. S. Sastry, "Adaptive Control of Mechanical Manipulators", *Proceedings of the IEEE International Conference on Robotics and Automation*, Vol. 2, pp. 190-195, 1986.
- [76] R. G. Morgan and U. Ozguner, "A Decentralized Variable Structure Control Algorithm for Robotic manipulator", *IEEE Transactions on Journal of Robotic and Automation*, pp. 57-65, March 1985.

Publications and Conferences

A. Publications

- [1] Thien Phuc Tran, Tan Lam Chung, Hak Kyeong Kim, Sang Bong Kim and Myung Suk Oh, “3D Smooth Seam Tracking for a Mobile Manipulator Using Adaptive Control with Unknown Parameter”, ICASE International Journal, submitted (March, 2005).
- [2] Thien Phuc Tran, Tan Lam Chung, Sang Bong Kim and Myung Suk Oh, “3D Smooth Seam Tracking for Mobile Manipulator Using Sliding Mode Control”, KSPE International Journal, submitted (March, 2005).
- [3] Thien Phuc Tran, Tan Lam Chung, Sang Bong Kim and Myung Suk Oh, “Nonlinear Feedback Tracking Control of the Mobile Manipulator for Smooth 3D Curved Welding Task”, KSOE International Journal, submitted (April, 2005).
- [4] Thien Phuc Tran, Tan Lam Chung, Hak Kyeong Kim, Sang Bong Kim and Myung Suk Oh, “Tracking Control of the Mobile Manipulator for Smooth 3D Curved Welding Task”, KSPSE Journal, submitted (March, 2005).

B. Proceedings

- [1] Thien Phuc Tran, Tan Lam Chung, Hak Kyeong Kim, Sang Bong Kim, and Myung Suk Oh, “Trajectory Tracking of Mobile Manipulator for Welding Task Using Sliding Mode Control,” *Proceedings of The 30th Annual Conference of The IEEE Industrial Electronics Society (IECON*

2004), Paradise Hotel, Pusan, Korea, CD-style Proceedings, November 2-6, 2004.

- [2] Thien Phuc Tran, Tan Lam Chung, Hak Kyeong Kim, Sang Bong Kim, and Myung Suk Oh, "Tracking Control of Mobile Manipulator For Vertical Welding Task," *Proceedings of 2004 International Conference on Dynamics, Instrument and Control CDIC'04*, Hilton Hotel, Nanjing, China, pp. 1-10, August 18-20, 2004.
- [3] Tan Tung Phan, Thien Phuc Tran, Trong Hieu Bui, and Sang Bong Kim, "Decentralized Control Method for a Welding Mobile Manipulator", *Proceedings of 2004 International Conference on Dynamics, Instrument and Control CDIC'04*, Hilton Hotel, Nanjing, China, pp. 1-10, August 18-20, 2004.
- [4] Thien Phuc Tran, Tan Lam Chung, Hak Kyeong Kim, Sang Bong Kim, and Myung Suck Oh, "Control of Mobile Manipulator for Tracking Vertical Smooth Welding Trajectory," *Proceedings of KSPSE 2004 Spring Conference*, Mokpo Maritime University, Korea, pp. 237-243, May 28-29, 2004.
- [5] Thien Phuc Tran, Tan Lam Chung, Manh Dung Ngo, and Sang Bong Kim, "Tracking Control For Mobile Manipulator Performing 3D-Smooth Seam," *Proceeding of The International Symposium on Advanced Science and Engineering (ISASE)*, HCMC University of Technology, HoChiMinh City, Vietnam, pp. 301-308, May 20-21, 2004.
- [6] Trong Hieu Bui, Tan Tien Nguyen, Tan Lam Chung, Thien Phuc Tran, and Sang Bong Kim, "Adaptive Controller for Trajectory Tracking of Welding Mobile Robot," *Proceeding of The International Symposium on Advanced Science and Engineering (ISASE)*, HCMC University of

Technology, HoChiMinh City, Vietnam, pp. 225-231, May 20-21, 2004.

- [7] Thien Phuc Tran, Tan Tung Phan, Tan Lam Chung, and Sang Bong Kim, "A Study on Torque Adaptive Control for Welding Mobile Manipulator," *Proceedings of ICASE Joint Conference*, Pusan National University, Korea, pp. 265-270, December 12-13, 2003.
- [8] Tan Tung Phan, Soung Jea Park, Thien Phuc Tran, and Sang Bong Kim, "Adaptive Tracking Control of Smooth Curved Seam for Mobile Manipulator", *Proceedings of ICASE Joint Conference*, Pusan National University, Korea, pp. 153-158, December 12-13, 2003.
- [9] Thien Phuc Tran, Tan Tung Phan, Tan Lam Chung and Sang Bong Kim, "Control of the Welding Mobile Manipulator for Tracking Space Smooth Seam," *Proceedings of The Korean Society for Power System Engineering*, Pusan, Korea, pp. 154-159, November 28-29, 2003.
- [10] Tan Tung Phan, Thien Phuc Tran, Trong Hieu Bui, and Sang Bong Kim, "Decentralized Control for Welding Mobile Manipulator Robot", *Proceedings of The Korean Society for Power System Engineering*, Pusan, Korea, pp. 147-153, November 28-29, 2003.
- [11] Thien Phuc Tran, Tan Tung Phan, Tan Lam Chung, and Sang Bong Kim, "Adaptive Control for Welding Mobile Manipulator," *Proceedings of the International Symposium on Advanced Engineering*, Pusan, Korea, pp. 240-244, November 13-15, 2003.
- [12] Tan Tung Phan, Tan Tien Nguyen, Thien Phuc Tran, and Sang Bong Kim, "Adaptive Control for a Mobile Manipulator with Unknown Parameters", *Proceedings of the International Symposium on Advanced Engineering*, Pusan, Korea, pp.206-210, November 13-15, 2003.

- [13] Thien Phuc Tran, Tan Tung Phan, Tan Tien Nguyen, and Sang Bong Kim, "Control of a Mobile Manipulator for Tracking Welding Path in Vertical", *Proceedings of the International Symposium on Mechatronics*, HCM City, Vietnam, pp.31-36, September 13-16, 2003.
- [14] Trong Hieu Bui, Tan Lam Chung, Thien Phuc Tran, and Sang Bong Kim, "H_∞ and Adaptive Robust Controls of Active Suspension System," *Proceedings of the International Symposium on Mechatronics*, HCM City, Vietnam, pp. 104 -109, September 13, 2003.
- [15] Tan Tung Phan, Thien Phuc Tran, Tan Lam Chung, and Sang Bong Kim, "A Nonlinear Control of a Welding Mobile Manipulator", *Proceedings of the International Symposium on Mechatronics*, HCM City, Vietnam, pp.13-18, September 13-16, 2003.
- [16] Tan Tien Nguyen, Trong Hieu Bui, Thien Phuc Tran, and Sang Bong Kim, "A Hybrid Control of Active Suspension System Using H_∞ and Nonlinear Adaptive Controls", *Proceedings of the ISIE 2001-IEEE International Symposium on Industrial Electronics*, pp. 839-844, vol. 2, June 12-16, 2001.
- [17] Thien Phuc Tran, Song Cau Bui, "Studying an Algorithm of Determining the Path of Mobile Robots used for CIM systems", *Proceedings of the VICA Symposium on Automation*, Hanoi, Vietnam, April 9-11, 1998.

Appendix

A1. Proof of the forming Eq. (4.2)

Herein, the tracking errors equation (Eq. (4.2)) is re-written as the following:

$$\begin{bmatrix} e_1 \\ e_2 \\ e_3 \\ e_4 \\ e_5 \end{bmatrix} = \begin{bmatrix} \cos \phi_w & \sin \phi_w & 0 & 0 & 0 \\ -\sin \phi_w & \cos \phi_w & 0 & 0 & 0 \\ 0 & 0 & 1 & 0 & 0 \\ 0 & 0 & 0 & 1 & 0 \\ 0 & 0 & 0 & 0 & 1 \end{bmatrix} \begin{bmatrix} x_r - x_w \\ y_r - y_w \\ z_r - z_w \\ \phi_r - \phi_w \\ \psi_r - \psi_w \end{bmatrix} \quad (\text{A1.1})$$

Taking the first derivative of Eq. (A1.1) yields

$$\begin{bmatrix} \dot{e}_1 \\ \dot{e}_2 \\ \dot{e}_3 \\ \dot{e}_4 \\ \dot{e}_5 \end{bmatrix} = \begin{bmatrix} -\dot{\phi}_w \sin \phi_w & \dot{\phi}_w \cos \phi_w & 0 & 0 & 0 \\ -\dot{\phi}_w \cos \phi_w & -\dot{\phi}_w \sin \phi_w & 0 & 0 & 0 \\ 0 & 0 & 0 & 0 & 0 \\ 0 & 0 & 0 & 0 & 0 \\ 0 & 0 & 0 & 0 & 0 \end{bmatrix} \begin{bmatrix} x_r - x_w \\ y_r - y_w \\ z_r - z_w \\ \phi_r - \phi_w \\ \psi_r - \psi_w \end{bmatrix} +$$

$$\begin{bmatrix} \cos \phi_w & \sin \phi_w & 0 & 0 & 0 \\ -\sin \phi_w & \cos \phi_w & 0 & 0 & 0 \\ 0 & 0 & 1 & 0 & 0 \\ 0 & 0 & 0 & 1 & 0 \\ 0 & 0 & 0 & 0 & 1 \end{bmatrix} \begin{bmatrix} \dot{x}_r - \dot{x}_w \\ \dot{y}_r - \dot{y}_w \\ \dot{z}_r - \dot{z}_w \\ \dot{\phi}_r - \dot{\phi}_w \\ \dot{\psi}_r - \dot{\psi}_w \end{bmatrix} \quad (\text{A1.2})$$

Expanding the right hand side of Eq. (A1.2), with referring Eq. (2.9) obtains

$$\begin{aligned}
\begin{bmatrix} \dot{e}_1 \\ \dot{e}_2 \\ \dot{e}_3 \\ \dot{e}_4 \\ \dot{e}_5 \end{bmatrix} &= \dot{\phi}_w \begin{bmatrix} -\sin \phi_w & \cos \phi_w & 0 & 0 & 0 \\ -\cos \phi_w & -\sin \phi_w & 0 & 0 & 0 \\ 0 & 0 & 0 & 0 & 0 \\ 0 & 0 & 0 & 0 & 0 \\ 0 & 0 & 0 & 0 & 0 \end{bmatrix} \begin{bmatrix} x_r - x_w \\ y_r - y_w \\ z_r - z_w \\ \phi_r - \phi_w \\ \psi_r - \psi_w \end{bmatrix} + \\
&\begin{bmatrix} \cos \phi_w & \sin \phi_w & 0 & 0 & 0 \\ -\sin \phi_w & \cos \phi_w & 0 & 0 & 0 \\ 0 & 0 & 1 & 0 & 0 \\ 0 & 0 & 0 & 1 & 0 \\ 0 & 0 & 0 & 0 & 1 \end{bmatrix} \begin{bmatrix} v_r \cos \psi_r \cos \phi_r - v_{xyw} \cos \phi_w + p_m \omega_{\phi w} \cos \phi_w \\ v_r \cos \psi_r \sin \phi_r - v_{xyw} \sin \phi_w + p_m \omega_{\phi w} \sin \phi_w \\ v_r \sin \psi_r - v_{zw} \\ \omega_{\phi r} - \omega_{\phi w} \\ \omega_{\psi r} - \omega_{\psi w} \end{bmatrix} \\
\Leftrightarrow \begin{bmatrix} \dot{e}_1 \\ \dot{e}_2 \\ \dot{e}_3 \\ \dot{e}_4 \\ \dot{e}_5 \end{bmatrix} &= \omega_{\phi w} \begin{bmatrix} -\sin \phi_w & \cos \phi_w & 0 & 0 & 0 \\ -\cos \phi_w & -\sin \phi_w & 0 & 0 & 0 \\ 0 & 0 & 0 & 0 & 0 \\ 0 & 0 & 0 & 0 & 0 \\ 0 & 0 & 0 & 0 & 0 \end{bmatrix} \begin{bmatrix} x_r - x_w \\ y_r - y_w \\ z_r - z_w \\ \phi_r - \phi_w \\ \psi_r - \psi_w \end{bmatrix} + \\
&\begin{bmatrix} v_r \cos \psi_r (\cos \phi_r \cos \phi_w + \sin \phi_r \sin \phi_w) - (v_{xyw} - p_m \omega_{\phi w}) (\cos^2 \phi_w + \sin^2 \phi_w) \\ v_r \cos \psi_r (-\cos \phi_w \sin \phi_r + \sin \phi_w \cos \phi_r) \\ v_r \sin \psi_r - v_{zw} \\ \omega_{\phi r} - \omega_{\phi w} \\ \omega_{\psi r} - \omega_{\psi w} \end{bmatrix}
\end{aligned}$$

Referring Eq. (A1.1), now, a simplifying is made for obtaining the following:

$$\begin{bmatrix} \dot{e}_1 \\ \dot{e}_2 \\ \dot{e}_3 \\ \dot{e}_4 \\ \dot{e}_5 \end{bmatrix} = \omega_{\phi w} \begin{bmatrix} e_2 \\ -e_1 \\ 0 \\ 0 \\ 0 \end{bmatrix} + \begin{bmatrix} v_r \cos \psi_r \cos(\phi_r - \phi_w) - v_{xyw} + p_m \omega_{\phi w} \\ v_r \cos \psi_r \sin(\phi_r - \phi_w) \\ v_r \sin \psi_r - v_{zw} \\ \omega_{\phi r} - \omega_{\phi w} \\ \omega_{\psi r} - \omega_{\psi w} \end{bmatrix}$$

$$\Leftrightarrow \begin{bmatrix} \dot{e}_1 \\ \dot{e}_2 \\ \dot{e}_3 \\ \dot{e}_4 \\ \dot{e}_5 \end{bmatrix} = \begin{bmatrix} v_r \cos \psi_r \cos e_4 - v_{xyw} + (e_2 + p_m) \omega_{\phi w} \\ v_r \cos \psi_r \sin e_4 - \omega_{\phi w} e_1 \\ v_r \sin \psi_r - v_{zw} \\ \omega_{\phi r} - \omega_{\phi w} \\ \omega_{\psi r} - \omega_{\psi w} \end{bmatrix}$$

$$\Leftrightarrow \begin{bmatrix} \dot{e}_1 \\ \dot{e}_2 \\ \dot{e}_3 \\ \dot{e}_4 \\ \dot{e}_5 \end{bmatrix} = \begin{bmatrix} v_r \cos \psi_r \cos e_4 \\ v_r \cos \psi_r \sin e_4 \\ v_r \sin \psi_r \\ \omega_{\phi r} \\ \omega_{\psi r} \end{bmatrix} + \begin{bmatrix} -v_{xyw} + (e_2 + p_m) \omega_{\phi w} \\ -\omega_{\phi w} e_1 \\ -v_{zw} \\ -\omega_{\phi w} \\ -\omega_{\psi w} \end{bmatrix}$$

At last, the first order derivative of tracking error can be expressed as the following:

$$\begin{bmatrix} \dot{e}_1 \\ \dot{e}_2 \\ \dot{e}_3 \\ \dot{e}_4 \\ \dot{e}_5 \end{bmatrix} = \begin{bmatrix} v_r \cos \psi_r \cos e_4 \\ v_r \cos \psi_r \sin e_4 \\ v_r \sin \psi_r \\ \omega_{\phi r} \\ \omega_{\psi r} \end{bmatrix} + \begin{bmatrix} -1 & e_2 + p_m & 0 & 0 \\ 0 & e_1 & 0 & 0 \\ 0 & 0 & -1 & 0 \\ 0 & -1 & 0 & 0 \\ 0 & 0 & 0 & -1 \end{bmatrix} \begin{bmatrix} v_{xyw} \\ \omega_{\phi w} \\ v_{zw} \\ \omega_{\psi w} \end{bmatrix}$$

A2. Determination of the matrices in Eqs. (2.26) and (2.29) [16]

❖ The motion equation of a mobile platform is expressed as in Eq. (2.26):

$$\overline{M_{11}}\dot{v} + \overline{C_{11}}v + \overline{\tau_{d1}} = \tau_v \quad (\text{A2.1})$$

Therein, the matrix terms are defined as:

$$M_{11} = \begin{bmatrix} m & 0 & -m_c c d \sin \phi & m_c c d \sin \phi \\ 0 & m & m_c c d \cos \phi & -m_c c d \cos \phi \\ -m_c c d \sin \phi & m_c c d \cos \phi & I_c^2 + I_w & -I_c^2 \\ m_c c d \sin \phi & -m_c c d \cos \phi & -I_c^2 & I_c^2 + I_w \end{bmatrix}$$

$$C_{11} = \begin{bmatrix} -m_c d \dot{\phi}^2 \cos \phi \\ -m_c d \dot{\phi}^2 \sin \phi \\ 0 \\ 0 \end{bmatrix}$$

$$\tau_v = \begin{bmatrix} \tau_l \\ \tau_r \end{bmatrix}$$

$$S = \begin{bmatrix} cb \cos \phi & cb \cos \phi \\ cb \sin \phi & cb \sin \phi \\ 1 & 0 \\ 0 & 1 \end{bmatrix}$$

where d is the distance from the center of the mobile platform to the base of the manipulator, $m = m_c + 2m_w$, $I = I_c + 2m_w b^2 + 2I_m$, and $c = \frac{r}{2b}$.

❖ The motion equation of a manipulator is expressed as in Eq. (2.29):

$$\overline{M_{22}}\ddot{q}_r + \overline{C_{22}}\dot{q}_r + \overline{\tau_{d2}} = \tau_r \quad (\text{A2.2})$$

Therein, the terms are defined as:

$$M_{22} = [M_{i,j}]$$

$$C_{22} = [C_{i(j,k)}]$$

$$F_2 = G_2 = [G_i]$$

$$M_{i,j} = \sum_{k=\max(i,j)}^n \text{trace} \left[\frac{\partial T_k}{\partial q_i} J_k \frac{\partial T_k^T}{\partial q_j} \right]$$

$$C_{i(j,k)} = \sum_{h=\max(i,j,k)}^n \text{trace} \left[\frac{\partial T_h}{\partial q_i} J_h \frac{\partial^2 T_h^T}{\partial q_j \partial q_k} \right]$$

$$G_i = \sum_{k=i}^n m_k g^T \frac{\partial T_k}{\partial q_i} \bar{r}^{(i)}$$

where T_i is the transform matrix, J_i is the pseudo-inertia matrix of the link i , m_i is the mass of the link i , g is the gravitational acceleration vector, and $\bar{r}^{(i)}$ is the vector pointing from the origin of frame i to the mass center of the link with respect to the frame i .